THE ROLE OF THE DORSAL PREMOTOR AND SUPERIOR PARIETAL CORTICES IN DECOUPLED VISUOMOTOR TRANSFORMATIONS

Patricia F. Sayegh

A dissertation submitted to the Faculty of Graduate Studies in partial fulfillment of the requirements for the degree of

Doctor of Philosophy

Graduate Program in Kinesiology and Health Science
York University
Toronto, Ontario
May, 2014

ABSTRACT

In order to successfully interact with objects located within our environment, the brain must be capable of combining visual information with the appropriate felt limb position (i.e. proprioception) in order compute an appropriate coordinated muscle plan for accurate motor control. Eye-hand coordination is essential to our independence as a species and relies heavily on the reciprocally-connected regions of the parieto-frontal reach network. The dorsal premotor cortex (PMd) and the superior parietal lobule (SPL) remain prime candidates within this network for controlling the transformations required during visually-guided reaching movements. Our brains are primed to reach directly towards a viewed object, a situation that has been termed a "standard" or coupled reach. Such direct eye-hand coordination is common across species and is crucial for basic survival. Humans, however, have developed the capacity for tool-use and thus have learned to interact indirectly with an object. In such "non-standard" or decoupled situations, the directions of gaze and arm movement have been spatially decoupled and rely on both the implementation of a cognitive rule and on online feedback of the decoupled limb.

The studies included within this dissertation were designed to further characterize the role of PMd and SPL during situations in which when a reach requires a spatial transformation between the actions of the eyes and the hand. More specifically, we were interested in examining whether regions within PMd (PMdr, PMdc) and SPL (PEc, MIP) responded differently during coupled versus decoupled visuomotor transformations. To

address the relative contribution of these various cortical regions during decoupled reaching movements, we trained two female rhesus macaques on both coupled and decoupled visually-guided reaching tasks. We recorded the neural activity (single units and local field potentials) within each region while the animals performed each condition. We found that two separate networks emerged each contributing in a distinct ways to the performance of coupled versus decoupled eye-hand reaches. While PMdr and PEc showed enhanced activity during decoupled reach conditions, PMdc and MIP were more enhanced during coupled reaches. Taken together, these data presented here provide further evidence for the existence of alternate task-dependent neural pathways for visuomotor integration.

To my father-in-law, Fred Granek. Although your physical presence in my life was too short, your influence on me will last my entire lifetime. You have quietly taught me strength, confidence, patience and have given me the unconditional love that usually only comes from a parent. You welcomed this Catholic girl, who you first encountered after landing your son in the hospital, into your Jewish home. You taught me, guided me, and welcomed me into a world I knew nothing about, opening my eyes to a wonderful family and culture. Your love of life and devotion to your family is something I will always admire and strive to obtain. I am so blessed to have met you and to have had the pleasure to be changed by your life. Your spirit lives on in your children and in my children Jaden and little Bean. Although it saddens me that she/he will never know you, your influence on this family and therefore on her/him will help lessen that pain. I will always miss you…

ACKNOWLEDGEMENTS

I would like to acknowledge my parents. Mom and Dad, who knew this skipping school, sneaking out, always grounded, barely passing high school student would end up with a doctorate degree. Faced with many challenges the confidence and trust I received from both of you pushed me to expect great things of myself. Despite all my struggles you both never gave up on me and for that I am extremely grateful. Mom and Dad, I admire the relationship you have today which has taught me that there will never be a problem too great to separate a family. The friendship you both now share is more meaningful to me then you likely realize. To my second mom Debbie, thank you for your unconditional love and support. Your arms have always been open to me and I cherish you for it. I do not know if I would have made it through graduate school without our weekly dinners, which always nourished and grounded me. To my sister Adri, I miss those lazy days when we would invent crazy thing to keep busy with, always resulting in hysterical memories that I cherish so much. You have influenced me in more ways than you realize.

To my husband and children, Joshua the words we spoke at our wedding remain strong for me. You have always inspired me to reach my full potential both professionally and spiritually. We have had some tough moments, two PhD candidates with a sleepless baby, but through it all you have taught me some amazing life lessons. Although we have many more to learn I am glad they will be together. I would not be as confident, successful or proud of myself if it were not for the things you have taught me. Jaden and little Bean, my light, you both have filled my heart with so much love it may explode. Being a mother is the greatest gift I have ever received, thank you Josh. I am so grateful that you have both picked me to be your mother and your guide through this world. I love my life!

I would also like to thank Dr. Lauren Sergio for her mentorship over these past years. The projects you assigned me were the hardest and best things that I will likely ever experience professionally. It taught me to be resourceful and confident in myself along with the many life lessons I will need as a researcher. I would also like to thank my lab-mates, past and present. The shenanigans, coffee breaks, lunch breaks, inside jokes, venting sessions, travel buddies, and knowledge sessions were priceless, it really does take a village. To Dr. Kari Hoffman, thank you for your suggestions and invaluable input. You have been a vital mentor for me and I thank you for always having your door open to my numerous questions. Finally, to the vivarium staff, Julie, Natasha, Veronica, Janet and Taiwo, none of this work would be possible without your help, knowledge and quick thinking.

TABLE OF CONTENTS

LIST OF FIGURES

Glossary of Abbreviations

Abbreviation	Non-Abbreviated Term
AD	Alzheimer's Disease
AIP	Anterior intraparietal sulcus
BG	Basal ganglia
BOLD	Blood oxygenated level dependent
CUE	Cue period
DLPFC	Dorsal lateral prefrontal cortex
EEG	Electroencephalogram
fMRI	Functional magnetic resonance imaging
IDP	Instructed delay period
IPL	Inferior parietal lobule
IPS	Intraparietal sulcus
ITC	Inferotemporal cortex
LIP	Lateral intraparietal sulcus
LFP	Local field potentials
M1	Primary motor cortex
MCI	Mild cognitive impariments
MIP (mIPS)	Medial intraparietal sulcus
MT	Movement time
NS	Decoupled condition (Non-standard)
OA	Optic ataxia
PCG	Postcentral gyrus
PE	Superficial region of SPL, area 5
PEc	Superficial- caudal region of SPL, area 5
PEm	Superficial-medial region of SPL, area 5
PD	Preferred direction of a cell
PF	Inferior parietal lobule, area 7
PG	Inferior-caudal arietal lobule, area 7
PMd	Dorsal premotor region
PMdc	Caudal dorsal premotor region
PMdr	Rostral dorsal premotor region
PMv	Ventral premotor region
POJ	Parieto-occipital junction
POS (PO)	Parieto-occipital sulcus
PPC	Posterior parietal cortex
S	Coupled condition (Standard)
SC	Spinal cord
SFC	Spike-field coherency

SPL	Superior parietal lobule
SPOC	Superior parietal occipital cortex
V6A	Macaque homolog of PO
VIP	Ventral intraparietal sulcus

Chapter One

General Introduction

Imagine for a moment that you lost the ability to reach towards or grasp an object. Imagine that every time you tried to pick up an object you reached in the wrong direction or were unable to scale your finger-opening to match the object's size. Eye-hand coordination is an important aspect of our ability to interact with the world around us. Our brain is an expert at coupling visual signals with manual motor behaviours to allow for a variety of visually-guided reaching movements. Most of the time, a visual stimulus and its required motor action are in alignment. If your phone on the table in front of you rings, your natural reaction would be to reach towards it and pick it up. These types of reaches are referred to as a *standard* "coupled" reaches because the visual object guiding the movement is the target of the action itself (Wise et al. 1996). However, the demand for planning and executing visually-guided reaching movements has become more complex as primates have evolved to use tools. Often, our interactions with objects in our environment demand more intricate eye-hand coordination and rely on a different set of visuomotor transformations from those of coupled reaches. Many of these transformations innvolve situations in which the correspondence between vision and action is indirect such that the association between stimulus and response must be learned and calibrated (Wise et al. 1996; Murray et al. 2000; Sergio et al. 2009). These movements differ markedly in the sense that they require a "decoupling" between gaze direction and hand orientation to successfully reach towards the object of interest. During our daily life, many of us become extremely familiar with the spatial transformations necessary for decoupled reaches. Most of us can use a computer quite successfully and understand that a forward displacement of the mouse on a horizontal table will move a cursor vertically on a computer screen. Such movements have also been referred to in the literature as *non-standard* reaching movements and have been suggested to rely on the integration of specific rules and spatial algorithms relating the visual stimulus to the direction of

movement (Wise et al. 1996; Murray et al. 2000). The main difference between coupled, standard movements and decoupled, non-standard movements is the congruency between the action of the eyes to the hand (Wise et al. 1996; Sergio et al. 2009).

It is well established that reaching movements rely on a network of brain regions located within the parieto-frontal reach network (Kalaska et al. 1998; Battaglia-Mayer et al. 2001; Caminiti et al. 1999). What has yet to be fully understood is how activity within this network can be modulated during reaching movement when there is a decoupling between the actions of the eyes and hand. Recent research supports a hypothesis that decoupled reaching movements alter the regions within the reaching network from those involved during coupled reaching (Prado et al. 2005; Clavagnier et al. 2007). More support for this idea comes from the observation that decoupled eye-hand coordination develops only later in childhood (Bo et al. 2006), and that patients with neurological disorders show impaired decoupled reaching while standard reaching is largely unaffected (Tippett et al. 2012; Tippett and Sergio 2006; Granek et al. 2012; Salek et al. 2011). Specifically, recent work in our laboratory revealed that although coupled reaching movements were not impaired in early Alzheimer's disease (eAD) and adults with Mild Cognitive Impairment (MCI), performance significantly declined as soon as an element of eye-hand decoupling was introduced. Taken collectively, evidence suggests that these different types of reaching movements may be sub-served by altered cortical networks. Imaging studies have proposed that within the parieto-frontal reach network, changes in the recruitment of the sub-regions of premotor and parietal cortices occur during different types of eye-hand coupling (Prado et al. 2005; Clavagnier et al. 2007; Granek et al. 2010; Gorbet et al. 2004; Picard and Strick 2001; Gorbet and Sergio 2007). What has yet to be established is how the specific regions wihtin this network are altered and how the local computations within each region shift to handle

the different types of visually-guided reaches performed by primates. As such, the goal of my doctoral work has been to gain an understanding of how regions within the parieto-frontal reach network are altered during decoupled relative to coupled visually-guided reaching movements. This work has consisted of three separate projects, which are discussed in detail in the following chapters. The remainder of the introduction is divided into sections that will provide a background of information with which one can understand the following studies. I begin by giving a brief overview of the behavioural profile of a visually-guided reach and the types of transformations that must occur. Then, I will discuss the cortical network and key brain regions that are critical to these types of transformations. I will also discuss how decoupled reaches affect our reach profile and why these types of reaches are thought to depend on altered cortical activity from more natural coupled reaches. Because the majority of the analyses were performed on the local field potentials (LFP) activity recorded within each cortical region examined, I will finish by giving an overview of what LFP recordings reflect and why they are important.

1.1. Visually guided reaching and visuomotor transformations.

In the early 19th century the pioneering work of Jackson (1873), Fritsch and Hitzig (1870) and Ferrier (1873) motivated researchers to question how the brain plans and execute movement. From early on in recorded medical history, observations of motor dysfunction following head injuries lead to the idea that motor control was somehow tied to the brain (Taylor and Gross 2003). John Hughlings Jackson made some stunning observation by watching the spread of convulsions during epileptic seizures, many of which came from his wife. He inferred that different muscle groups were controlled by different parts of the cortex organized in a similar fashion to the organization of the body (Hughlings Jackson 1873). With the advancements in surgical and anaesthetic techniques, researchers were finally able to perform

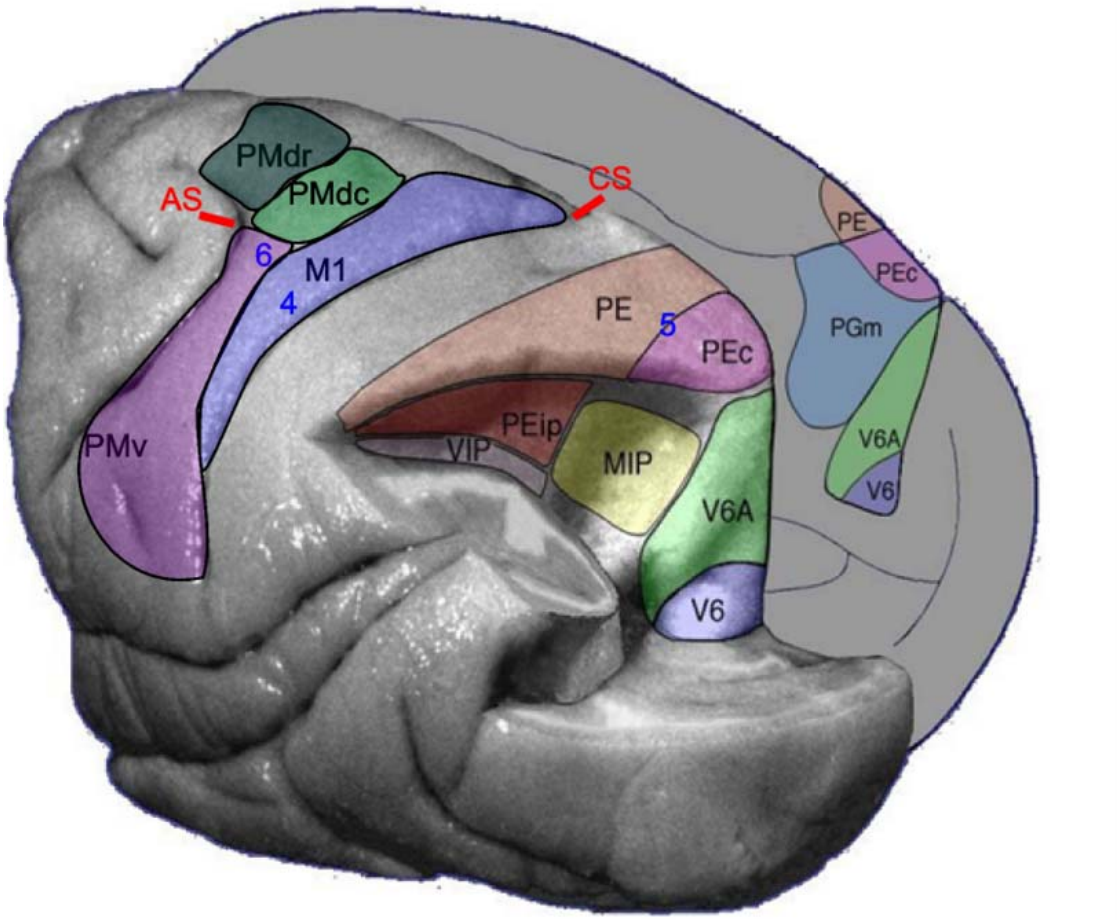

Figure 1.1. Anatomical locations of macaque reach related regions that are involved in visuomotor transformations. Posterlateral view of a macaque brain. The occipital pole and inferior parietal lobule of the right hemisphere were partially removed to show the cortical areas located in the medial bank of the intraparietal sulcus and the anterior bank of the parieto-occipital sulcus. Premotor region were added. Blue numbers denotes Brodmann regions, Red labels denotes sulcus location, CS: Central sulcus, AS: Arcuate sulcus. Figure and text adapted from (Galletti et al. 1999).

invasive experiments on animals that allowed researchers to begin to explore the idea of motor control. One of the most important studies in the history of neuroscience was the initial work of Gustav Fritsch and Eduard Hitzig (1870) which was followed by the work of David Ferrier (1873). These pioneers were among the first to witness how electrical stimulation of the cerebral cortex produced movements of the body. Their conclusions about the function of the cerebral cortex and observation of a topographical representation of the body within the cortex came at a time when several controversies existed about the importance of the brain (Taylor and Gross 2003; Fritsch and Hitzig 1870; Ferrier 1873). These researchers made three very important observations that still remain influential: First, electrical stimulation evoked contralateral movements. Second, stimulation to different parts of the cortex activated different muscle groups.Third, the excitable sites formed a topographical map of movements of the body. In the century following these first electrical stimulation studies on the motor cortex, in conjunction with the advancements in surgical and recording techniques, scientists have advanced, and continue to advance, the understanding of motor control.

As the study of neuroscience progressed, researchers began to understand how movements could be internally generated, which are made without the guidance of vision, or externally generated, which are triggered by external cues (Roland et al. 1980; Halsband et al. 1994). We have also identified that visually-guided reaches follow a specific characteristic. Before a reach commences, a saccade towards the target of interest occurs follow by a hand movement towards the direction of gaze (Gielen et al. 1984; Prablanc et al. 1979). Although the signal that drives these two effectors arrives to the spinal cord at the same time, the difference in inertia between them causes the eye to align with the target slightly before the hand (Sergio et al. 2009; Prablanc et al. 1979). We have also learned that the movement of the eyes and the hand share an

extremely close relationship (Prablanc et al. 1979; Henriques et al. 1998; Neggers and Bekkering 2000). This tight coupling suggests that our natural behaviour is to move the eyes and the hand towards the object we are interacting with. Such a linkage may very well be an efficient way for the brain to handle the programming of an overwhelming amount of coupled reaches that we perform in our daily lives (*for discussion, see section 1.3*). This observation has been one of the most important motivations for our work. As previously discussed, our capabilities to perform decoupled reaches have become a critical part of our daily tasks. Thus, an important question that emerges here is: will breaking the tight linkage between these effectors change the neural computations required from those computed during natural reaching behaviour? Although an important matter, this has been something that has not received much attention over the years and will be discussed further in later sections.

Just as John Hughlings Jackson suggested so long ago, the cortex must be involved in some form of neural interaction that links sensory and motor functions and this idea has advanced research regarding visuomotor transformations. In order to reach towards a visual target the available sensory or visual information regarding the location of the hand and the target must somehow be converted into a motor signal that will guide the hand to the appropriate location. The sensory signal that specifies the position of the target is known to be initially coded in fixation- or eye-centered reference frames (Batista et al. 1999; Soechting and Flanders 1992) while the location of the hand can be coded in either eye-, body- or head-centered reference frames (Buneo et al. 2002; Shadmehr and Wise 2005). Numerous research studies suggest that when a reach is performed under visually reliable situations, the brain will code the target location in visual coordinates but the limb can be coded in either visual or proprioceptive coordinates (Prablanc et al. 1979; Buneo et al. 2002; Graziano et al. 2000; Crawford et al. 2004)

with a preference for visual, or eye-centered coordinates (Sober and Sabes 2005; Buneo and Andersen 2006; Vesia and Crawford 2012). However, when visual information is unreliable, a limb-centered posture-defined coordinate system must be used to control the reach (Batista et al. 1999; Buneo and Andersen 2006; Rushworth et al. 1997a; Jackson et al. 2000; Pellijeff et al. 2006; Jackson et al. 2009). Thus before a motor command can be generated, the reference frames between these effectors must be integrated to generate a difference vector regarding the displacement of the target relative to the hand (Shadmehr and Wise 2005). This is specifically important during situations in which the visual signal about the arm or target is unreliable or missing. Once the vector describing the difference between the current hand location and the desired target location has been computed, a spatial or visuomotor transformation must occur to map the sensory information into a motor command (Sober and Sabes 2005; Sabes 2000). The cortical control of visually-guided movements has been described as a model of coordinate system transformations which describes how the cell activity in different cortical areas relate to sensory and motor events during reaching movements (Sergio et al. 2009; Kalaska et al. 1997). This visuomotor-transformation occurs throughout various regions of the parietofrontal reach network (Figure 1.1) and is discussed in detail in the following section.

1.2. The parieto-frontal network and visuomotor transformations.

In order to reach accurately to an object, one must transform a sensory signal into a complex pattern of muscle activity. Reviewing the literature, it has been shown consistently that reaching movements rely on a network of brain regions including the dorsal premotor (PMd) and superior parietal lobule (SPL, Figure 1.2), regions located within the dorsomedial parieto-frontal network (Sergio et al. 2009; Kalaska et al. 1998; Battaglia-Mayer et al. 2001; Caminiti et al. 1999; Gorbet et al. 2004; Buneo and Andersen 2006; Kalaska et al. 1997; Granek et al. 2007;

Wise et al. 1997; Tanne-Gariepy et al. 2002). Evidence of strong, reciprocal association fibres between these regions (Tanne-Gariepy et al. 2002; Marconi et al. 2001) have been thought to play a significant role in the preparation and guidance of visually-guided arm movements. However, the neurological processes underling this seemingly straightforward transformation is not yet completely understood. Direct interactions with an object, where the action of the eyes and the hand are coupled, have been suggested to be controlled by a "default visuomotor network" (Gorbet et al. 2004). This default visuomotor network involves the combined activation of the contralateral primary motor cortex (M1), medial motor areas, lateral premotor areas, and the posterior partial cortex (PPC) which are all activated during the preparatory stages of a coupled visuomotor transformation (Figure 1.1). Less is known about the control of decoupled eye and hand reaches and specifically how the default network is affected. What is known about the role of PMd and SPL to visuomotor transformations will be discussed in their respective sections.

Prior to our knowledge of the parieto-frontal reach network, scientists did not have a clear understanding about the functional dichotomies regarding the visual system. Schneider (1969) proposed the influential 'two visual system' hypothesis. He argued that while retinal projections to the superior colliculus process the localization of stimulus, the geniculostriate system processes stimulus identity. When thinking about these separate streams most people think of the work of Ungerleider and Mishkin (1982) and their suggestion of a ventral 'what' stream for processing object qualities and a dorsal 'where' stream for object localization. This is because their work came with a very critical distinction: they suggested that this division in visual processing occurred within the cerebral cortex (Ungerleider and Haxby 1994; Ungerleider and Mishkin 1982). Now, this functional dichotomy, initially referred to as the 'what' and

'where' streams, are mapped on to two diverging streams originating from the striate cortex and progressing either ventrally to the inferotemporal cortex (ITC) or dorsally to the PPC (Ungerleider and Mishkin 1982). A decade or so after this discovery, Goodale and Milner re-examined the literature and advanced this putative proposal of the ventral and dorsal stream by suggesting a more perceptual function for the ventral stream and more visuomotor control function for the dorsal stream (Goodale and Milner 1992; Goodale 1993; Milner and Goodale 1995). In their famous 1992 paper they coined the phrase 'vision for perception' and 'vision for action' for these two streams. The remainder of this review will focus on the function of the dorsal stream.

From the dorsal stream there arise two major parieto-frontal networks connecting parietal and premotor cortices. The *dorsolateral* parieto-frontal pathway connects the inferior parietal lobule (IPL) to the ventral premotor cortex (PMv) (Tanne-Gariepy et al. 2002; Tomassini et al. 2007). This pathway is more specific to the online control of grasping (Grol et al. 2007) and will not be discussed further within this paper. The *dorsomedial*, parieto-frontal pathway connects the SPL to PMd (Tanne-Gariepy et al. 2002; Tomassini et al. 2007; Gamberini et al. 2009; Passarelli et al. 2011). This network originates from the caudal portion of SPL, the human homologue of V6A (Fattori et al. 2004; Galletti et al. 2003), and has been suggested to have a primary role in calculating the appropriate reach vector goal (Fattori et al. 2004; Galletti et al. 2003). The function of this network is important here because intact parietal inputs into this network are necessary for the guidance of a limb using peripheral vision (Prado et al. 2005; Battaglia-Mayer et al. 2012; Hwang et al. 2012; Battaglini et al. 2003), during the integration of cognitive visuo-perceptual skills with complex visuomotor skills (Pisella et al. 2013), and during decoupled reaching in darkness (Marzocchi et al. 2008).

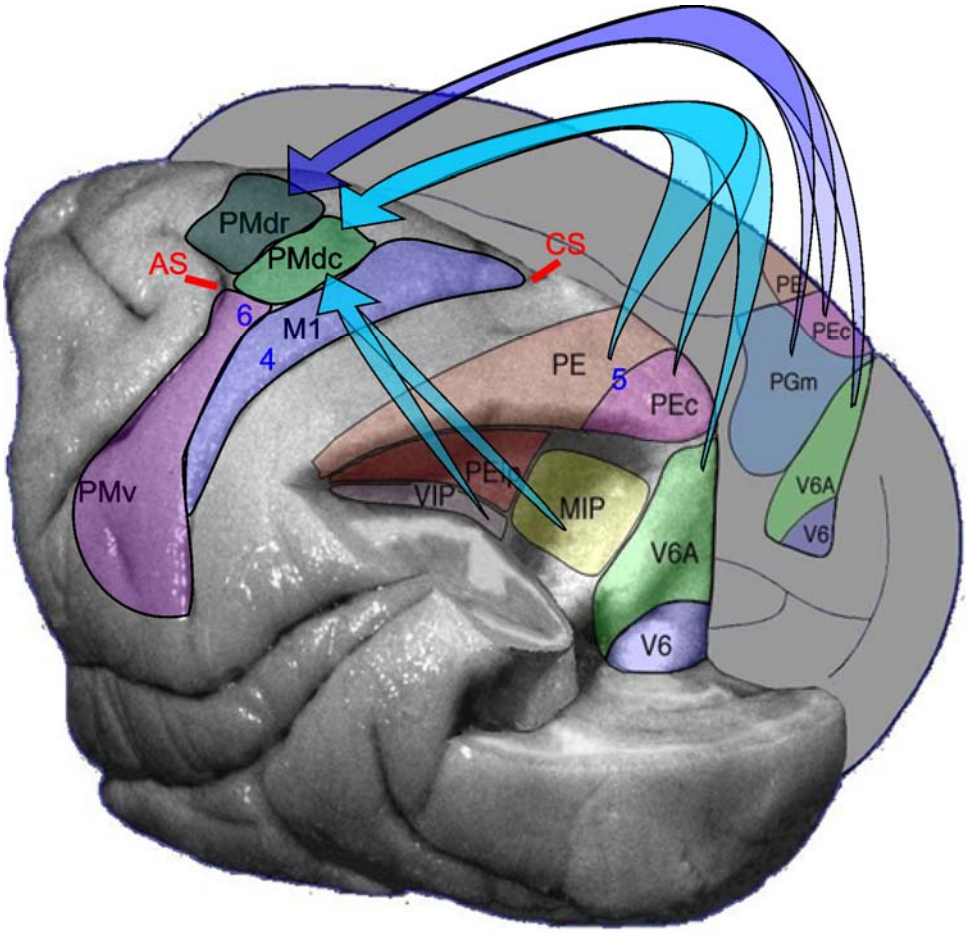

Figure 1.2. Cortico-cortico connections of region located within the parietofrontal reach network that are involved in visuomotor transformations. Posterlateral view of a macaque brain, same as in Figure 1.1. Figure and text adapted from (Galletti et al. 1999).

The connections between parietal and frontal reach regions are extremely important for the control of visually-guided reaches. The connections between these two structures are known to follow a neuroanatomical gradient (Marconi et al. 2001; Matelli et al. 1998). Areas located more posterior within SPL (e.g. V6A or PO) have a strong connection to PMdr (Marconi et al. 2001) while more anterior regions within SPL (e.g. area 5 or PEc) are linked more to caudal frontal regions (e.g. M1 or PMdc) (Marconi et al. 2001; Gamberini et al. 2009; Bakola et al. 2010). Understanding the roles of each of these regions and how they are affected by different types of visually-guided reaches will provide insight into how these networks change during complex visuomotor transformations. In the last 20 or so years, analyses on the coding of reaching movements have led to the conclusion that motor, premotor, and SPL (area 5) regions combine visual information about the target location with somatic information about the limb in space (Caminiti et al. 1990; Caminiti et al. 1991). What remains to be determined is how the weight of each region is affected when the action of the eyes and hand are decoupled. In the following sections we will explore how the frames of reference and flexibility in the weight placed on proprioceptive versus visual control may adapt to task demands associated with decoupled visually-guided movement control.

1.2.1. Role of PMd in visuomotor transformations.

PMd is located on the dorsal aspect of the premotor area (Wise et al. 1996; Shadmehr and Wise 2005; Barbas and Pandya 1987; Matelli et al. 1985) and is the anatomical interface between parietal and primary motor regions (Marconi et al. 2001; Matelli et al. 1998; Johnson et al. 1996). The role of PMd in motor preparation was initially proposed based on the observation of set-related activity, defined as neuronal activity that starts following an instructional cue about an upcoming movement (Wise and Mauritz 1985). By examining this set-related activity,

researchers suggested that it reflected the motor significance of the cue, based largely on the representation of this activity to movement parameters, such as direction, amplitude and speed of a limb movement (di Pellegrino and Wise 1993; Kurata 1993; O'Leary and Hatsopoulos 2006b). For instance, Churchland and colleagues (2007) applied subthreshold intracortical microstimulation to disrupt this set-related preparatory activity while monkeys performed a visually guided reaching task. They observed a highly specific increase in reaction times principally when microstimulation was applied around the time of the go cue, with no deficits to the movement itself. No deficits in reaction times were seen in saccadic eye movements or when microstimulation was applied to other nearby motor regions. Similar results were also observed when TMS was applied to the dorsal premotor region of human subjects, although there were sex-related differences (Gorbet and Staines 2010). Research into set-related activity also discovered that these reach parameters, such as movement direction, are coded as a vector within PMd (Caminiti et al. 1990; Caminiti et al. 1991; Kurata 1993; Weinrich and Wise 1982; Weinrich et al. 1984). This is largely based on the observation that neural activity varies with movement direction demonstrating maximal response for a preferred direction (Georgopoulos and Massey 1988). Studies also support a role for PMd in the execution of movements, specifically in the online control of a reach (Lee and van Donkelaar 2006; Archambault et al. 2011; Clower et al. 1996). Using a combined TMS and prism adaption paradigm, (Lee and van Donkelaar 2006) observed that TMS applied to humans, while they pointed to targets using prism goggles, slowed down their rate of adaption and on-line corrections when vision of the hand was available. When vision of the hand was not available, no alterations in adaption were observed. They concluded that PMd contributed to the generation of visually based on-line error corrections to help remap the position of the arm. Recently, Archambault and colleagues (2011)

used a target jump paradigm that supported these findings but concluded that PMd has more of a high-order role in commanding or signalling the correction of a motor intention.

The neural activity within PMd has also been shown to be affected by the direction of gaze (Boussaoud 1995; Pesaran et al. 2006; Pesaran et al. 2010). More recently, Pesaran et al., (2006) examined this phenomenon using a paradigm that cleverly dissociated the location of the target, the start position of the eyes, and the start position of the hand. Pesaran and colleagues (2006) were able to demonstrate that these gaze effects in fact reflected the changes in the relative position between these three variables. If any of them were to shift, like gaze, than the underlying neural activity within PMd would also shift. These results suggest that the cells within PMd can simultaneously encode multiple vectors (Pesaran et al. 2006). This seems practical for PMd because in order to accurately plan and execute reaching movements, information regarding the start position of the hand and eye, and the location of the target must be integrated somehow (Hoshi and Tanji 2000; Kurata 1994; Rizzolatti et al. 1998; Lloyd et al. 2003). Such a system also allows some form of flexibility within PMd if the weight of any of these signals were altered. In an elegant study by Hoshi and Tanji (2000), monkeys were trained to reach towards a target. They gave monkeys two sets of instructions, one regarding which target to reach for and one regarding which limb to use. Importantly, these instructions were given in two steps so that second instruction represented the combination of the target location and limb position. Most cells, as expected represented the first instructed component (for example which target to reach towards). What was striking was that many of these same cells represented the integrated component of the two signals following the second instruction. This remarkable observation suggests that PMd has some role in the integration of the signals important for visually-guided reaches.

As shown, the role of PMd in planning and executing the kinematics of an intended movement is unequivocal (Wise et al. 1996; Shadmehr and Wise 2005; Caminiti et al. 1990; Raos et al. 2004; Cisek and Kalaska 2002a; Boussaoud and Wise 1993a; Boussaoud 2001). However, over the years various studies have begun to report that the role of PMd to reach planning depended also on the behavioural context of the upcoming reach (Picard and Strick 2001; di Pellegrino and Wise 1993; Archambault et al. 2011; Boussaoud and Wise 1993a; Boussaoud and Wise 1993b; Wise et al. 1996; Crammond and Kalaska 1994; Kurata and Hoffman 1994; Halsband and Passingham 1985; Passingham 1988; Grafton et al. 1998; Petrides 1985). Many of these observations were largely based on lesion or cooling studies. For instance, muscimol injections into the PMd of primates led to an increase in directional errors during visually-guided reaches that required a conditional forelimb movement (Kurata and Hoffman 1994). Similarly, ablation studies in primates (Halsband and Passingham 1985; Halsband and Passingham 1982) and lesion studies in humans (Halsband and Freund 1990) showed that damage to PMd caused impairments in re-learning a task that required the selection of a movement when the choice was based on sensory instructions. These results were not based on purely motor deficits since visually-guided reaching movements remained intact (Halsband and Passingham 1985; Halsband and Passingham 1982; Halsband and Freund 1990). The consensus in the literature is that PMd neurons rely on sensory information to select the appropriate behaviour to execute (Weinrich and Wise 1982; Crammond and Kalaska 1994; Godschalk et al. 1981; Cisek and Kalaska 2005). Thus, neurons within PMd are involved in conditional visuomotor transformations because the movement selection will be based on some sort of learned association. Neurophysiological results also support this observation (di Pellegrino and Wise 1993; Kurata 1993; Weinrich and Wise 1982; Weinrich et al. 1984; Crammond and

Kalaska 1994). A classic study by Crammond and Kalaska (1994) explored the activity of individual cells within PMd while a monkey performed an instructed, delayed reaching task. During each trial a CUE appeared instructing the animal whether they were to move towards or away from the target. Shortly following cue onset the majority of PMd cells responded in a typical manner, with maximal response when the CUE was in their preferred direction (PD). This activity is suggested by the authors to possibly reflect an initial plan to reach towards the sensory cue, thus suggesting a more 'motor' rather than sensory response. However, the important observation was that by late reach planning PMd activity shifted into reflecting the direction of the intended movement, regardless of where the CUE location appeared (Figure 1.3). This rapidly occurring re-direction of neural response may reflect recognition and the re-coding of the motor response in order to represent the correct associative rule. The authors concluded that PMd activity likely contributes to the selection process when similar motor responses have different associative rules (Crammond and Kalaska 1994), and provides evidence for the existence of a multiple parameter representation in a given population of neurons that change over the course of a planned behaviour. In fact, work by Cisek and colleagues have demonstrated how the activity of PMd simultaneously represent two possible reach plans until the decision regarding the selection of a reach target has been made (Cisek and Kalaska 2005; Cisek and Kalaska 2002b). Archambault (2011) also reported that PMd activity simultaneously represent two motor plans during a target jump paradigm. This strongly implicated PMd in mediating the visuomotor transformation required during delayed reaching (Crammond and Kalaska 1994; Shen and Alexander 1997b; Hocherman and Wise 1991; Shen and Alexander 1997a) but also implicated PMd in decoupled visuomotor transformation which require the incorporation of a rule into the

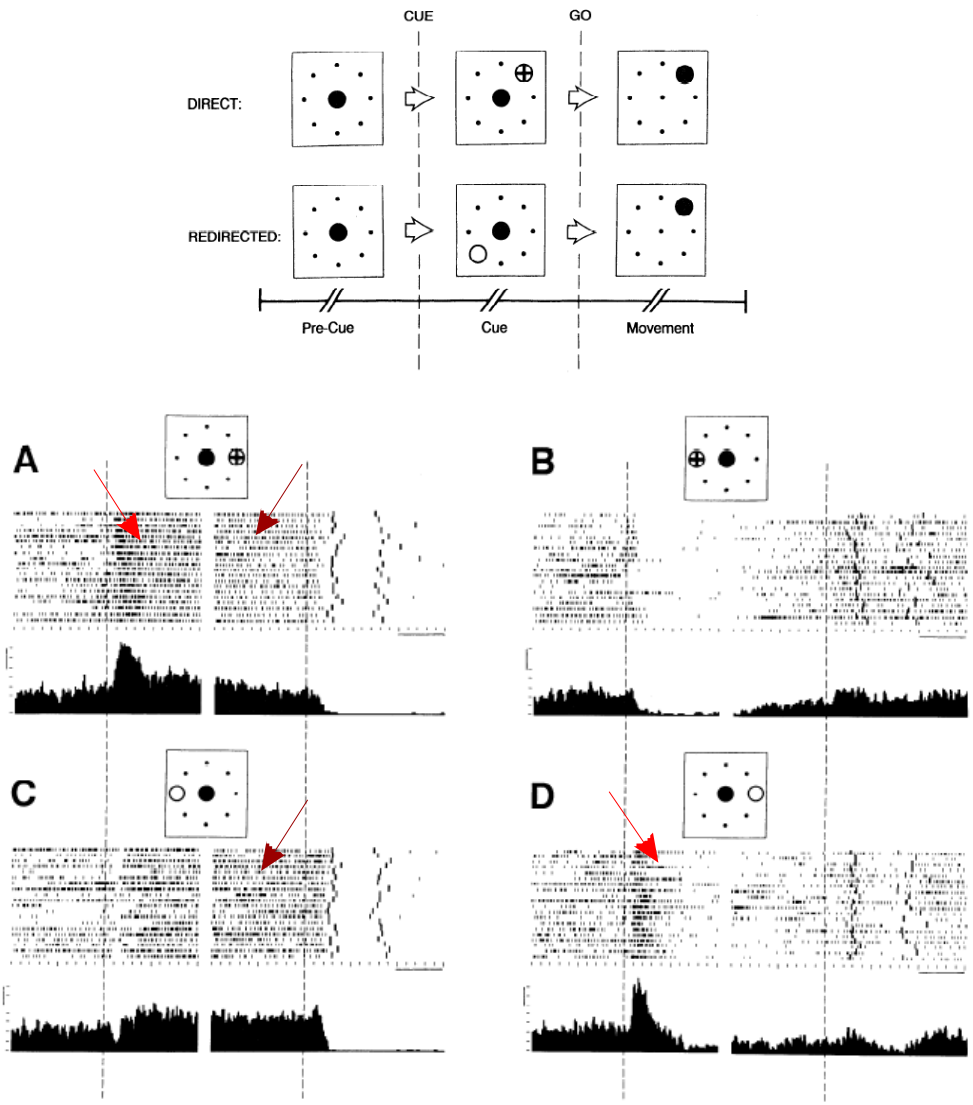

Figure. 1.3 Response of PMd cell during both early and late planning. Top panel: Monkeys were trained to perform an instructed delay task in which a CUE stimulus could appear in one of two locations and corresponded to either the preferred or opposite direction. The CUE instructed movements wither towards or away from the stiumulus. Bottom panel: Neural response from a PMd cell during direct (A and B) or redirect (C and D) conditions. Vertical dashed lines indicates CUE onset (right) or movement onset (left). Early in trail the CUE evoked strong activity when it was presented at 0 degrees (the cells PD, red arrow) regardless of condition. By late within the trail maximal activity was observed when the intended movement was towards the cells PD regardless of the CUE location (mahogany arrow). Figure and text adapted from (Crammond and Kalaska 1994)

motor plan. Visuomotor transformation will depend on a cascade of events from purely sensory processing to context-dependant or associative processing and finally to purely motor processing (Shen and Alexander 1997a). Taken collectively, these studies have established a concrete role for PMd not only in movement planning and selection, but in particular when the movement is dependent on some contextual-association. These observations are important in the context of the current projects because they influenced our exploration of the role of PMd during different types of visually-guided reaching movements, where the mapping between stimulus and limb movements are altered based on a rule that must be incorporated into the visuomtor transformation.

1.2.2. Topographical divisions in PMd and their separate functions in visuomotor control.

The story of reach movement control becomes more complicated when one takes into account the different sub-divisions of PMd. Although not normally addressed, PMd can be divided into rostral (PMdr) and caudal (PMdc) sub-regions. This division was initially based on physiological and anatomical differences (Picard and Strick 2001; Barbas and Pandya 1987; Matelli et al. 1985; Kurata 1991; Fujii et al. 2000). However more recently, researchers began to report clear functional differences as well (Prado et al. 2005; Clavagnier et al. 2007); Grafton et al. 1998; (Hanakawa et al. 2006); (Picard and Strick 2001; Grafton et al. 1998). In the seminal work of Picard and Strick (2001), they re-examined the current literature on PMd to reveal that the activity within PMdr has a stronger role in context-based associations, while cells within PMdc demonstrate mostly movement-related activity (Picard and Strick 2001; Grafton et al. 1998). The authors suggested that the term “Pre-PMd” be used to describe PMdr, reflecting its role in planning reaching movement that relies on arbitrary or contextual associations (Wise et al. 1996; Boussaoud 2001; Grafton et al. 1998). Anatomical studies also support these functional

differences between PMdr and PMdc. PMdc shares connections with parietal-dependent motor area and has direct connections with the primary motor area (M1) and the spinal cord (Matelli et al. 1985; Fujii et al. 2000; Matelli and Luppino 2001). These connections support PMdc in preferentially coding limb movement parameters (Cisek et al. 2003; Alexander and Crutcher 1990; Kurata 1989) primarily when arm movements are controlled by visual or somatosensory information (Luppino et al. 2003; Abe and Hanakawa 2009). PMdr, a fronto-dependent motor area, receives major connections from the prefrontal and cingulate cortex (Matelli et al. 1985; Fujii et al. 2000; Matelli and Luppino 2001; Lu et al. 1994; Lu et al. 1994; Tachibana et al. 2004)with no direct connections to M1 (Barbas and Pandya 1987; Kurata 1991; Tachibana et al. 2004; Luppino and Rizzolatti 2000). These prefrontal connections will allow PMdr to have a more cognitive or top-down role in visually-guided reaching. For instance, PMdr and the dorso-lateral prefrontal cortex (DLPFC) become functionally coupled when a motor behaviour is guided by a rule (Murray et al. 2000; Luppino et al. 2003; Abe and Hanakawa 2009; White and Wise 1999). Although not primary, PMdr does share some connection to mesial and caudal portions of the parietal cortex (Marconi et al. 2001; Matelli et al. 1998; Luppino and Rizzolatti 2000; Geyer et al. 2000). The functional difference between PMdr and PMdc, and their separate anatomical connections to areas within the SPL, suggest that they play separate but interconnecting roles in visuomotor transformations. While PMdc may be more active during the computations of coupled reaches (Prado et al. 2005; Picard and Strick 2001; Lee and van Donkelaar 2006; Sayegh et al. 2013; Gail et al. 2009), PMdr is likely more active when a rule is required during decoupled reaches (Prado et al. 2005; Picard and Strick 2001; Grafton et al. 1998).

It must be noted here that although separate functions are ascribed to these sub-regions,

activity can be observed throughout PMd for the various tasks previously mentioned. As proposed by Abe and colleagues (2009), the weight of each of these sub-regions will change depending on the type of visuomotor transformation at hand. During more complex rule based reaches, the influence of PMdr, and its pre-frontal connections, may be more dominant than during more natural standard types of reaches where activity within PMdc may dominate. The studies presented here examine this idea that the weight of each of these regions shifts between different types of visually-guided reaching movements.

1.2.3. Role of the parietal cortex in visuomotor transformations.

The posterior parietal cortex (PPC, Figure 1.1) is located between the visual cortex in the occipital lobe and the somatosensory cortex in the postcentral gyrus (PCG) and is dorsally bordered by the Sylvian fissure (Rizzolatti and Matelli 2003; Rizzolatti et al. 1997). In all primates, the PPC is divided by the intraparietal sulcus into the superior parietal lobule (SPL), housing Brodmann areas 5, PE, PEc and PEm and the inferior parietal lobule (IPL), housing Brodmann area 7, PG and PF (Lynch 1980; Cavada and Goldman-Rakic 1989; Luppino 2005). Situated between sensory and motor cortices, SPL was traditionally viewed as a somatosensory or somatomotor region known for its role in the spatial representations of action (Wise et al. 1997; Mountcastle et al. 1975; Kalaska et al. 1983; Kalaska et al. 1990; Sakata et al. 1973). However, based on the influential work by Mountcastle and colleagues (1975), the parietal lobe was proposed as a central node within a distributed network suitable for supplying the frontal motor regions with a representation of visuomotor information (Caminiti et al. 1996). This proposal emerged from the existence of neurons within area 5 and 7 which were active when reaching to visual targets and were modulated by visual fixation, visual tracking, saccade generation (Mountcastle et al. 1975; Lynch et al. 1977; MacKay 1992), and coding of target

location in eye-centered or craniocentric reference frames (Andersen et al. 1985; Mazzoni et al. 1991). These observations in conjunction with the deficits observed by researchers in patients with PPC damage substantiated the notion that the parietal lobe was, among other things, important for providing the motor regions with the visual signals needed for accurate motor behavior (Bates and Ettlinger 1960; Denny-Brown and Chambers 1958; Perenin and Vighetto 1988). Both human patient (Granek et al. 2012; Battaglia-Mayer et al. 2012; Blangero et al. 2007; Rossetti et al. 2005; Pisella et al. 2009; Pisella et al. 2000; Grea et al. 2002; Granek and Sergio 2014; Hawkins et al. 2013), and animals studies (Battaglia-Mayer et al. 2012; Battaglia-Mayer and Caminiti 2002) show that damage within SPL (Blangero et al. 2009; Karnath and Perenin 2005; Luppino et al. 2005), resulting in optic ataxia (OA), often produces misreaching and misgrasping deficits to extra-foveal targets.

However, the idea that the parietal cortex in some way feeds forward the necessary visuomotor signals to the frontal cortex was tempered by an anatomical problem. Since early on, neuroanatomists understood that there were no direct projections between V1 and SPL (Johnson et al. 1996), nor between V1 and the frontal motor regions (Jones and Powell 1970; Pandya and Kuypers 1969). In an effort to explain how exactly the motor regions received the necessary visual information, researchers began looking within the IPL as a possible intermediate link. However, anatomical studies quickly revealed otherwise (Jones and Powell 1970; Pandya and Kuypers 1969), instead showing that it was the SPL, specifically area 5, that was the major parietal projections to the premotor regions and not IPL (Jones and Powell 1970; Pandya and Kuypers 1969). This observation provided no additional insight into the problem because area 5 was already known to be void of visual inputs (Jones and Powell 1970; Pandya and Kuypers 1969). It was not until the early part of the 1990's that anatomical studies identified a new visual

area located within the rostral bank of the parieto-occipital sulcus (POs) known as PO in humans or V6A in monkeys (Galletti et al. 1991). These studies concluded that PO not only projected to region within SPL - some even reciprocal connected - but it also carried rich visual information (Passarelli et al. 2011; Cavada and Goldman-Rakic 1989; Caminiti et al. 1996; Galletti et al. 2001; Colby et al. 1988; Blatt et al. 1990). The functional properties of PO, specifically in motion-sensitivity, gaze angle, encoding target location in spatial coordinates, and its emphasis on the periphery, suggest that this region would be suitable for the types of visual analysis needed for spatial localization of a visual target (Galletti et al. 2003; Galletti et al. 1991; Galletti et al. 1993; Galletti et al. 1997). Most importantly, PO has strong projections to the frontal cortex (Matelli et al., 1998; Gamerini et al., 2009), and acute lesions to this area produced the misreaching and misgrasping deficits observed with OA patients (Battaglini et al., 2002). In fact recent studies show that OA patients often have damage to regions usually restricted within the anterior bank of the POS (Blangero et al. 2009; Karnath and Perenin 2005; Luppino et al. 2005). Researchers had now found an avenue by which visual signals could reach the premotor regions (Caminiti et al. 1996; Galletti et al. 2001; Shipp et al. 1998) (Figure 1.4) and since then various studies have shown the crucial role for the parietal cortex in visually guided reaching, specifically in visuomotor transformations (Caminiti et al. 1999; Kalaska et al. 1997; Goodale and Milner 1992; Caminiti et al. 1996; Mountcastle 1995; Colby and Goldberg 1999; Battaglia-Mayer et al. 2006; Culham et al. 2006; Culham and Valyear 2006; Culham and Kanwisher 2001).

The discovery that cells within regions of SPL receives somatosensory and now visual information (Cavada and Goldman-Rakic 1989; Andersen and Buneo 2002) makes this region a prime location for the integration of senses for motor output. This idea has propelled research

and our current understanding of the role of SPL in visuomotor transformations. We now understand that SPL integrates eye and hand signals in order to successfully calculate the reach vector under sensory guidance (Graziano et al. 2000; Vesia and Crawford 2012; Rushworth et al. 1997a; Battaglia-Mayer and Caminiti 2002; Vesia et al. 2010; Grefkes et al. 2004; Andersen et al. 1987). For instance, neurons within SPL have been shown to discharge in response to both sensation and movement, and are thus considered crucial in the transformation of visual information needed for motor behaviours (Goodale 1993; Blangero et al. 2009; Milner and Harvey 2006; Kalaska 1996). A set of seminal studies completed by Battaglia-Mayer and colleagues looked at the visual and motor properties of SPL in an effort to examine if and how these signals are combined (Battaglia-Mayer et al. 2001; Battaglia-Mayer and Caminiti 2002). By using a multi-task approach they manipulated the eye and hand during center-out reaching tasks to reveal that these eye and hand-related signals often coexisted within the same cell. The critical observation was that when the preferred direction was obtained from all the epochs for all the conditions and represented on a unit circle, the orientation of the preferred direction of movement for the different effectors represented in the same cell clustered within a limited space. This remarkable directional feature is what they refer to as a global tuning field (Battaglia-Mayer et al. 2001; Battaglia-Mayer and Caminiti 2002; Battaglia-Mayer et al. 2000; Battaglia-Mayer et al. 2003). Observations such as these suggest that the combination of eye and hand signals occurs early on in the visuomotor processing stage (Johnson et al. 1996). The multimodal properties of neurons located within PMd and now SPL and their high degree of reciprocal connectivity (Battaglia-Mayer et al. 2001; Matelli et al. 1998; Matelli et al. 1998; Luppino and Rizzolatti 2000; Geyer et al. 2000; Galletti et al. 1991; Colby et al. 1988; Colby and Duhamel 1991; Petrides and Pandya 1984) enables the different sensory and motor signals that arise

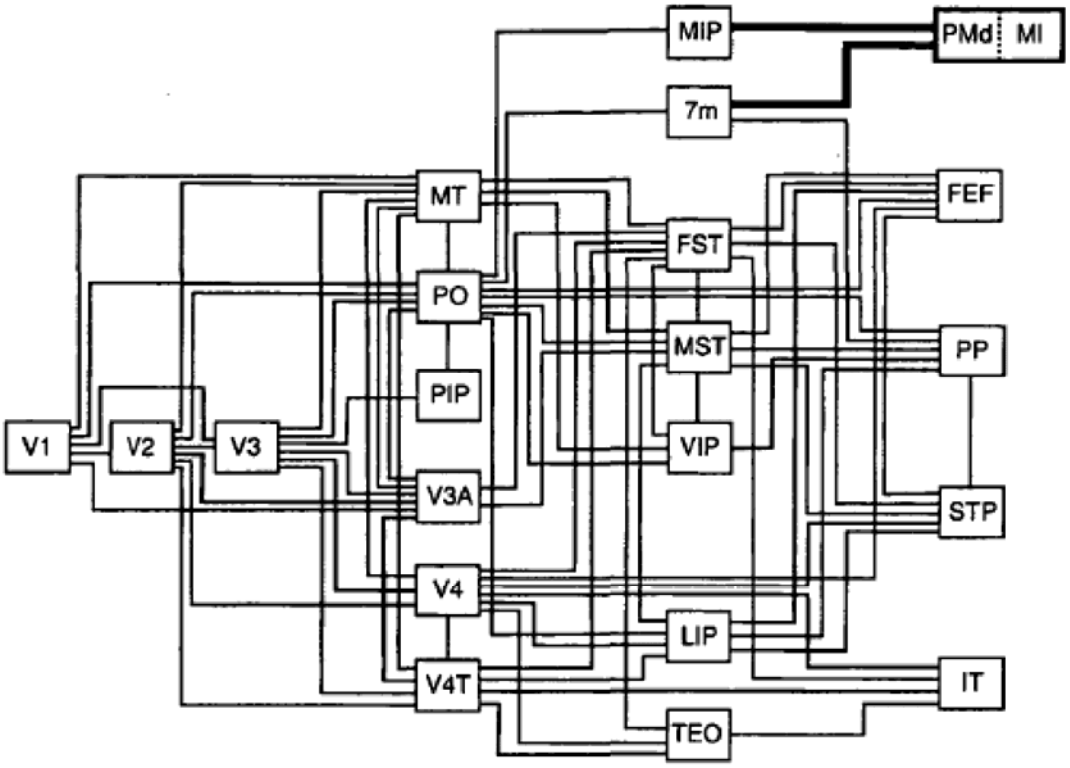

Figure 1.4. Diagram of (Colby and Duhamel 1991) connection of the visual areas. This diagram is suggested to illustrate how premotor and motor region receive the nesecary visual information required for visually-guided reaching movements. Adapted from (Johnson et al. 1996)

during reaching movements to be combined and transformed into the appropriate motor commands (Caminiti et al. 1996; Caminiti et al. 1998). Specifically, these studies suggested that the SPL could supply proprioceptive, and importantly visual information to frontal motor regions (Johnson et al. 1993). The reciprocal communication between them will then allow for the motor command to progress which will be particularly important during motor execution. Indeed it has been suggested that the parietal cortex is involved in the transformation of the initial visual information into a motor plan, and also in using visual feedback to guide an ongoing movement (Vesia and Crawford 2012; Crawford et al. 2011; Iacoboni 2006). Understanding the role of SPL to visuomotor transformations and its communication with PMd is important because we want to understand how the computations within these regions are affected during different levels of visuomotor compatability. Although some studies have examined how SPL responds during extrafoveal reaching (Battaglia-Mayer et al. 2001; Prado et al. 2005; Clavagnier et al. 2007; Gail et al. 2009; Andersen et al. 1997) which can be considered a type of decoupled reaching, to date there are no studies that have directly compared the activity of SPL during coupled reaching to one that involved dissociation between the eyes and the hand to a foveated target. Numerous research studies have, however, concluded that when a reach is performed under visually reliable situations, the brain favours eye-centered or visual coordinates (Sober and Sabes 2005; Buneo and Andersen 2006; Vesia and Crawford 2012). When visual information is unreliable, the reliance on proprioceptive control will be favoured (Batista et al. 1999; Buneo and Andersen 2006; Rushworth et al. 1997a; Jackson et al. 2000; Pellijeff et al. 2006; Jackson et al. 2009). During decoupled eye-hand reaching, no visual information is available regarding the position of the hand. Thus the weight of proprioceptive information along with the spatial transformation will need to be incorporated into the computations of the reach. The question that

arises here is what is the role of SPL in this computation?

Within SPL the frames of references used to plan and control reaching movements are highly flexible and task specific (Buneo et al. 2002; Battaglia-Mayer and Caminiti 2002; Battaglia-Mayer and Caminiti 2002; Newport et al. 2006). SPL receives information to maintain an updated representation about the relative position between the hand and the reach goal in eye-centered coordinates (Buneo and Andersen 2006; Rushworth et al. 1997a; Jackson et al. 2009; Wolpert et al. 1998). The rapid online updating about limb position relies on forward model predictions that combine efference copy motor commands, sensory feedback (visual and proprioceptive), and an internal model regarding the dynamics of the arm as the movement unfolds (Buneo and Andersen 2006; Vesia and Crawford 2012; Battaglia-Mayer et al. 2012; Wolpert et al. 1998; Desmurget and Grafton 2000; Desmurget et al. 1999). This updating function depends heavily on the integrity of PPC. For instance, Filimon (2009) compared visible and non-visible reaching movements to eye movements to identify reach-related areas and specifically regions modulated by visual feedback of the hand. They showed that regions located within the superior end of the PO were more active for visual than for non-visual reaches. They concluded that this region may process visual feedback of the hand or the visual distance between the effector and target (Filimon et al. 2009). Vesia and colleagues' (2010) recent work suggests that it is the spatial goal of the movement that is encoded within this region. Using transcranial magnetic stimulation (TMS), Vesia and colleagues applied short trains of stimulation to the superior parietal occipital cortex (SPOC) and regions within the medial IPS (mIPS) while subjects performed various reaching tasks. They observed that visual feedback of the hand did not correct errors induced by TMS over SPOC but it did correct errors induced by TMS over mIPS. They proposed that PO codes the spatial goal of a reach while mIPS is more specific to

using visual and somatosensory signals to calculate the reach vector. Over the years, Buneo and colleagues have conducted numerous studies seeking to identify the representation of the different coordinated frames within SPL (Batista et al. 1999; Buneo et al. 2002; Buneo et al. 2003). They reasoned that if a region encodes a particular frame of reference (e.g. eye-centered), than varying the frame of reference in one variable while holding the suggested frame constant should not modulate the activity of that region (Buneo and Andersen 2006). What they, along with others observed was evidence of a difference in the functional properties of neurons within SPL as a function of depth from inseparable to separable reference frames (Buneo et al. 2002; Caminiti et al. 1996; Kalaska 1996; Colby and Duhamel 1991; Kalaska and Crammond 1995a). Specifically, neurons located within the dorsal exposed part of area 5 (like PEc) are more somatosensory in nature, coding the difference between the target and hand position. While deeper cells located within the bank of the IPS (like MIP) are more separable and tend to be more aligned either to motor or visual functions (Caminiti et al. 1996; Colby and Duhamel 1991; Crammond and Kalaska 1989; Burbaud et al. 1991). These data suggest that under visually unreliable situations, regions located more superficially within SPL may have a stronger role in providing the necessary proprioceptive inputs to guide the limb. This notion is discussed in greater detail below.

1.2.4. How PMd and SPL may contribute to different visuomotor transformations.

As previously mentioned the connections between the parietal and frontal reach regions are important for visuomotor transformation. The neuroanatomical gradient of cortical connections between these two structures serves to connect functionally similar regions (Johnson et al. 1996; Caminiti et al. 1996) and provides evidence for a division in the roles in which these regions play in the computations required during visually-guided reaching (Figure 1.2). Area PEc

is modulated by somatosensory inputs but also responds to the position of the hand in space and the direction of movement (Caminiti et al. 1991; Mountcastle et al. 1975; Breveglieri et al. 2006). In addition, its main source of cortio-cortical projection is to PMdc (Marconi et al. 2001; Matelli et al. 1998) which is a region known not only for its role in movement kinematics (Prado et al. 2005; Picard and Strick 2001; Grafton et al. 1998), but also in the online error corrections that underlie the remapping of the felt position of the arm (Lee and van Donkelaar 2006). PMdc also receives inputs for area V6A and MIP (Marconi et al. 2001; Matelli et al. 1998). The work completed by Galletti and colleagues reveal that cells within V6A encode the spatial coordinates of a visual target and are sensitive to the direction and orientation of a moving stimulus (Galletti et al. 1999; Fattori et al. 2004; Galletti et al. 2003; Galletti et al. 2001; Galletti et al. 1997; Battaglini et al. 2002). More importantly, cells within this area are modulated by somatosensory information about arm movements regardless of the visual information (Galletti et al. 1997). Area MIP transforms visual target information into a common eye-centered reference frame that can be used by the motor system (Cohen and Andersen 2002). MIP neurons have also been shown to be directionally selective to the direction of hand movements (Eskandar and Assad 1999) and as such are also implicated in visuomotor transformations (Grefkes et al. 2004). The reciprocal communication between these regions likely plays a role in encoding the kinematics needed to perform simple reaches.

PMdr, on the other hand, receives parietal inputs mainly from mesial and caudal portions of the parietal cortex (Marconi et al. 2001; Matelli et al. 1998; Luppino and Rizzolatti 2000; Geyer et al. 2000). Cells within this region respond to a diverse set of reach-related activity (Pandya & Seltzer 1982) like eye-position, oculomotor information (Pandya & Seltzer, 1982) and target localization (Matelli & Luppino, 2001; Pandya & Seltzer, 1982). These different

neuroanatomical connections within the parieto-frontal reach network may very well serve the different types of visuomotor transformations that are required during visually-guided reaching.

In order to perform reaching tasks that rely on arbitrary associations or require novel rules to be learned about how to move the eyes and hand towards a visual target (such as the situation of using a computer mouse or a new track pad), the parieto-frontal network must be able to change or adapt to these new demands. Thus it seems logical that the contribution of these cortical regions to the necessary visuomotor transformations must be altered to reflect this extra processing (Wise et al., 1997). The main goal of these next chapters, each representing a distinct research study, was to examine specifically how the neural activity within different parietal and premotor regions were altered between coupled and decoupled reaches, in an effort to advance our understanding of how these brain networks contribute to the control of skilled visually-guided movement.

1.3. The different types of decoupled reaches.

In the literature, decoupled visuomotor transformations are referred to as either "arbitrary" or "transformational" (Wise et al. 1996). Arbitrary mappings occur when there is an arbitrary association between a visual stimulus and a corresponding motor behaviour. A common example is the motor behaviour that occurs when a driver comes to a traffic light. A green light primes the driver to apply force to the gas pedal whereas a red light will prime the driver to remove force from the gas pedal. The stimulus (traffic light color) that triggers this motor response is completely arbitrary and has no relevance to that action, and as a consequence must be learned. Transformational mappings, like arbitrary mappings, also require a dissociated visual stimulus to guide the motor response. However during transformational mappings, a spatial algorithm and the integration of cognitive rules are incorporated into the motor plan (Wise et al.

1996; Murray et al. 2000), A common example of this type of transformation is the use of a computer. Typically, a horizontally placed keyboard or mouse is used to control a cursor displayed on a vertical screen. One must learn the spatial rule that moving the cursor "upward" on the screen requires the hand to move the mouse "forward" on the desk. Both types of non-standard visuomotor mappings need to be learned, however arbitrary mappings depend on the stimulus features, while transformational mapping depends on the stimuli's location (Shadmehr and Wise 2005).

Decoupled transformational mappings (as opposed to arbitrary mappings) can take two forms: *sensorimotor recalibration and strategic control.* Sensorimotor recalibration occurs when one must adapt to a change in the physical location of the visual stimulus relative to the plane of the limb movement (e.g. those where the hand moves in a different location relative to the visual target). Such a recalibration requires a coordinated remapping between different sensory modalities such as vision and proprioception (Bedford 1993; Clower and Boussaoud 2000; Lackner and Dizio 1994). Strategic control occurs when one must adapt to situations where a cue signals a movement in some direction (often opposite) to the cued target location (Bock 2005; Redding et al. 2005; Redding and Wallace 1996). Strategic control can include having to integrate various rules for correctly acquiring a new skill (Wise et al. 1996; Murray et al. 2000; Sergio et al. 2009). In both of these cases, gaze and hand locations must be decoupled for successful performance.

Although previous human and animal studies have found that performing decoupled reaches alters the activity of regions located within the parieto-frontal reach network (Battaglia-Mayer et al. 2001; Prado et al. 2005; Granek et al. 2010; Gorbet et al. 2004; Sayegh et al. 2013; Gail et al. 2009; Gail et al. 2009; Andersen et al. 1987; Andersen et al. 1997; Grafton et al. 1996;

Connolly et al. 2000; Hawkins et al. 2012), many of these studies focused only on foveated, eyes foveate the taget, versus extra-foveated reaching, such as anti-pointing or central fixation paradigms (Battaglia-Mayer et al. 2001; Prado et al. 2005; Clavagnier et al. 2007; Gail et al. 2009; Andersen et al. 1997; Connolly et al. 2000). Many of these paradigms require one to maintain fixation at a central target while reaching to an extra-foveal target. Anti-pointing tasks rely more heavily on strategic control as opposed to sensorimotor recalibration. Thus our current understanding regarding the cortical control of a reaching movement which relies heavily on sensorimotor recalibration is lacking.

1.3.1 Evidence for a difference in the cortical control between coupled and decoupled visuomotor transformations.

There is a large body of evidence to suggest that the action of the eye and hand are tightly linked (Gielen et al. 1984; Prablanc et al. 1979; Henriques et al. 1998; Neggers and Bekkering 2000; Gail et al. 2009; Gauthier and Mussa Ivaldi 1988; Gauthier and Hofferer 1976; Morasso 1981; Sergio and Scott 1998; Vercher et al. 1994; Gorbet and Sergio 2009; Terao et al. 2002). One of the most persuasive pieces of evidence in support of this linkage is the observation of what Neggers and Bekkering refer to as gaze anchoring (Neggers and Bekkering 2000), which is the inability to saccade to a second target until the reach to the first target is complete. Gaze anchoring is thought to be driven by internally generated mechanism such as proprioceptive control based on the observation that it remains even in the absence of visual signals (Neggers and Bekkering 2001). Henriques et al. (1998) observed that when reaching to a previously foveated targets without visual feedback of the hand, reaching errors occur in the direction opposite the current gaze position (Henriques et al. 1998). The strong relationship between the eyes and the hand are further exemplified by behavioural studies that show significant changes in

the reach profile when the action of the eyes are decoupled from the action of the hand. Recently, Gorbet and Sergio (2009) had subjects perform coordinated eye and hand reach from a central towards a peripheral target. Using a digitizing tablet, subjects either performed a standard task, where both the eyes and hand moved towards the peripheral target, or a dissociated task where an algorithm was used so that the subjects hand movements were rotated 180 degrees. Thus to reach towards a target on the right the subject had to move their eyes towards the right while moving their hand towards the left. During these dissociated trials, the researchers observed a significant change in the kinematic profile of both the eyes and the hand when compared to standard reaches. This included the latency and peak velocity of eye and hand movements and the curvature of hand-path trajectories (Figure 1.5A and B). Messier and Kalaska (1997) also observed similar results when they asked subjects to reach to 25 targets located on a horizontal screen while either viewing the targets directly, or while viewing them on a vertical monitor. Similar to Gorbet and Sergio (2009), they also observed an increase in movement amplitude errors along with an increase in number of errors when the movement was non-standard (Figure 1.5A and B). Researchers have also shown that performance improves during visual tracking of a moving target when the individual simultaneously tracks the target with the hand (Koken and Erkelens, 1992). This tight coupling between the actions of the eyes and the hand suggests that our natural behaviour is to move them together towards the object we are interacting with, and is exemplified by the observation that decoupling the eye from the hand affects movement profile as well as accuracy of the upcoming reach (Clavagnier et al. 2007; Prablanc et al. 1979; Henriques et al. 1998; Gorbet and Sergio 2009; Terao et al. 2002; Messier and Kalaska 1997; Gordon et al. 1994; Goodbody and Wolpert 1999). Consequently, during decoupled reaching movements, a specific set of transformations – involving inhibition at some stage - must occur in

order to break this tight linkage (Sergio et al. 2009). As a result, decoupled reaches likely depend on neural circuitry that is different but albeit interconnected with the neural circuitry important for controlling natural coupled reaching movements (Sergio et al. 2009; Prado et al. 2005; Clavagnier et al. 2007; Gail et al. 2009). An easy way to address this idea is to look at the performance of young children. Bo and colleagues (2006) looked at the performance of children aged 4, 6, 8 and adults while they performed three different types of visuomotor transformations. They performed a center-out drawing task in coupled or decoupled conditions. In the decoupled conditions the target and line path were either displayed on a horizontal screen above their arm, or on a vertical screen in front of them. They observed that the younger children had significantly greater movement times and movement variability during the decoupled conditions when compared to both the adults and or during the coupled conditions across all ages. These results suggest that these types of decoupled mappings are not innate and must be learned (Sergio et al. 2009; Bo et al. 2006; Piaget 1965). Because these mappings seem to develop later in childhood, it seems logical to believe that they rely on separate circuits formed later than those used by the default standard mappings, circuits that rely at least partly on communication with inhibitory frontal lobe structures not fully formed early in life.

Recently, advances in imaging techniques have facilitated research aimed specifically at identifying the neural circuits involved in different types of reaching conditions. Various studies have compared the cortical activation between coupled and decoupled reaching movements and found differences in the cortical areas recruited during each type of reaching movement (Prado et al. 2005; Clavagnier et al. 2007; Gorbet et al. 2004; Grafton et al. 1998; Hanakawa et al. 2006; Grafton et al. 1996; Connolly et al. 2000). In an elegant study using functional magnetic resonance imaging (fMRI), Prado and colleagues (2005) revealed two distinct patterns of

activation for foveal (i.e. coupled) and extra-foveal (i.e. decoupled) reaching. Specifically, coupled reaching activated a restricted network mainly within the mIPS and PMdc. This network has been observed by others and is sometimes referred to in the literature as the 'default reach network' (Wise et al. 1996; Sergio et al. 2009; Gorbet et al. 2004; Gail et al. 2009). Decoupled reaching activated a similar circuit with additional activation in POJ and PMdr. In fact, a few studies have implicated a role for POJ in decoupled reaching (Jackson et al. 2009; Culham et al. 2006). The additional activation of these areas appears to be crucial for in the ability to perform decoupled visuomotor transformations. Based on the abovementioned functions of these key regions (the sub-divisions of PMd and SPL) to visuomotor transformations these observations are not surprising, and are supported by the few neurophysiological studies that have examined specifically how these regions are altered during decoupled compared to coupled reaches. Recently, Gail and colleagues (2009) demonstrated that single unit activity within PMd increases during performance of extra-foveal reaching conditions when compared to coupled foveated reaching conditions. On the contrary, parietal regions, like MIP, showed enhanced directional tuning during coupled versus decouple reaches. Unfortunately, Gail et al., (2009) did not distinguish between PMdr and PMdc, and in general a great majority of studies that investigate the functional aspects of PMd have neglected to separate PMd into its PMdr-PMdc sub-divisions.

Some of the best evidence for the different contributions that each subregion of PMd and SPL provide during different types of visuomotor compatibilities is shown by looking at function via dysfunction. Various patients with neurological disorders, such as Alzheimer's disease (AD), or mild cognitive impairments (MCI) demonstrate deteriorated reaching performance on decoupled reaching tasks while leaving reaching performance on coupled reaching tasks virtually

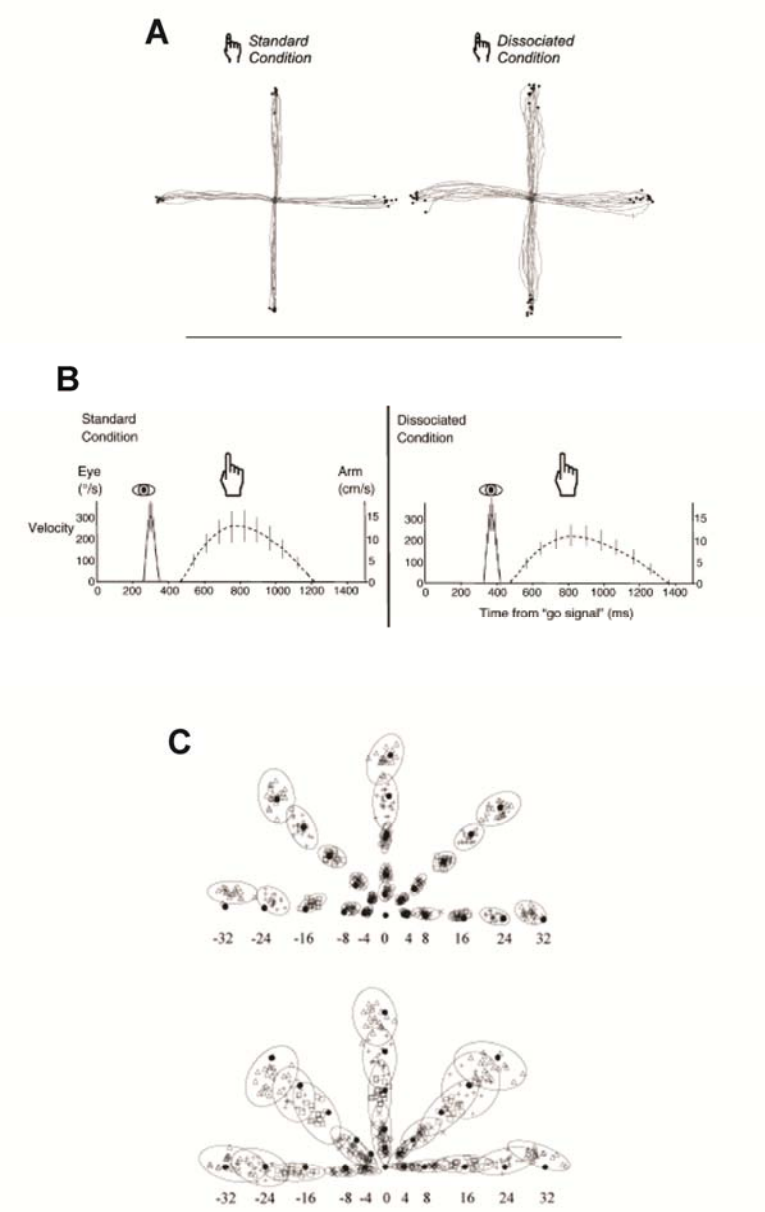

Figure 1.5: Differences in the kinematics of hand and eye paths during decoupled reaching. A) Sample hand-path trajectories for one subject in single blocks of the Standard condition (left) and Dissociated condition (right). B) Mean velocity profiles (solid line for the eye and dashed line for the arm) for group data from both conditions. Error bars represent standard deviation. C) Endpoint distributions for movements directed to targets located in five different directions and five different distances by one subject performing coupled (top) versus decoupled tasks (bottom). Figure and text adapted from (Gorbet and Sergio 2009; Messier and Kalaska 1999)

unaffected (Tippett and Sergio 2006; Salek et al. 2011; Pisella et al. 2009; Karnath and Perenin 2005; Karnath and Perenin 2005; Battaglini et al. 2002; Ghilardi et al. 1999; Tippett et al. 2007; Granek et al. 2013). Lesions to PMd, for instance, cause deficits in the visuomotor transformations that require the integration of a rule into the motor plan, a requirement of certain non-standard reaching movements (Halsband and Passingham 1985; Passingham 1988; Halsband and Freund 1990). Likewise, lesions centered around PO produce misreaching and misgrasping deficits to extra-foveal targets (Battaglini et al. 2003; Battaglini et al. 2002; Gaveau et al. 2008). Most strikingly is that the ability of all these patients to reach to foveated, coupled targets, remains for the most part unaffected (Karnath and Perenin 2005). These deficits likely arise from a breakdown in the sensorimotor transformations that allow reach direction and gaze direction to be decoupled (Jackson et al., 2005). This is an important finding because, like Alzheimer's patients, if decoupled and coupled types of visually guided reaches relied on the same circuit, then one would expect to find that these patients exhibit similar performance deteriorations during both types of reaching.

Aside from some patient data and limited imaging studies, we have not fully characterized how parietal and premotor areas contribute to eye-limb coordination under conditions requiring decoupled reaching movements. While it is well known that higher cognitive functions are related to activity in the frontal areas (Lu et al. 1994; Lamar and Resnick 2004; Mesulam et al. 2001; Mesulam 1990; Moscovitch et al. 1995; Petrides 1997), the contribution to the control of complex skill is less well formulated. Many studies have examined the degree to which cell activity in different frontal lobe regions co-varies with attributes of the sensory input, the motor output, and their various integrated combinations. As previously stated, although PMd was traditionally viewed as a region responsible for planning an intended

movement's kinematics, recent findings suggest that PMdr and PMdc have separate roles in the visuomotor transformation needed to plan an upcoming visually-guided reach (Wise et al. 1996Wise et al. 1996; Prado et al. 2005; Picard and Strick 2001; Gail et al. 2009). Strengthened by anatomical studies, PMdr is thought to have a more cognitive role in the context-dependent selection and planning of movements in conditions that involve decoupled mappings (Wise et al. 1996Wise et al. 1996; Prado et al. 2005; Picard and Strick 2001; Grafton et al. 1998; Lu et al. 1994; Gail et al. 2009). PMdc, and its strong connections to the primary motor cortex and the spinal cord (Barbas and Pandya 1987; Luppino et al. 1990) however, is thought to be more involved in coding limb movement parameters (Boussaoud 2001; Cisek et al. 2003; Alexander and Crutcher 1990). Research into the SPL has demonstrated its importance in the representation of posture and movement of the body and eyes and for visuomotor transformations (Battaglia-Mayer et al. 2001; Buneo and Andersen 2006; Kalaska et al. 1997; Battaglia-Mayer et al. 2006; Kalaska 1996; Caminiti et al. 1998; Andersen et al. 1997; Buneo et al. 2003; Breveglieri et al. 2006)**.** What is lacking is a clear understanding of how this region responds to situations where there is a spatial decoupling between the visual stimulus and motor behaviour towards a foveated stimulus. Our ability to break the tight eye-hand coupling requires additional processing beyond those regions needed to program and execute a natural coupled reach (Sergio et al. 2009). Thus it seems reasonable to expect that decoupled reaches will rely on changes to the 'default reach network' to allow for these additional processes. Decoupled reaches will not only require inhibition of the natural tendency to link the eye and the hand but also the incorporation of the spatial algorithms and cognitive rules that are needed to successfully perform a decoupling the eyes from the hand (Sergio et al. 2009; Gorbet and Sergio 2009).

1.4. LFPs, coherency, and single unit activity as measures of brain function.

Historically, neurophysiological recordings began with the recording of a mass action potential in the form of electroencephalogram (EEG) (Buzsaki 2006; Berger 1929). Considered one of the most influential researchers within the EEG field, Hans Berger (1929-1933) was one of the first scientists to ever report brain waves and is best known as the inventor of EEG. Berger published a series of papers regarding an electric effect which he detected in human subjects by applying electrodes to the head. This discovery began with a controversial idea Berger had that brains could communicate thru telepathy. Telepathy suggests that one can communicate thoughts, feeling, emotions, and so on with extrasensory channels without physical means. Motivated by this thought Berger set out to conducted experiments, as telepathy was regarded as 'occult' he conducted most of them in secret on himself and his son. Although his theory on telepathy was never proven he made the remarkable discovery of rhythmic oscillations coming from the brain. These oscillations had a frequency of around 10 cycles per second, termed the alpha wave, and were most evident from around the occipital part of the cortex when subjects were quiet with their eyes closed and were replaced by the smaller and faster "beta" wave when the eyes remained open (Buzsaki 2006; Berger 1929; Adrian and Matthews 1934b). Although it took some time for the importance of Berger's work to be recognized, his discoveries of the alpha, or "Berger" wave and the techniques of EEG helped to propel neuroscience (Wiedemann 1994). In the decade to follow many researchers attempted to make sense of the meaning of these waves mostly by looking at the clinical population, such as how frontal lobotomies affected brain waves (Davis 1941), and then by looking at the more fundamental relationships between brainwaves and behaviour (Bullock 1945; Marshall et al. 1937; Galambos 1941). As the technology advanced, the ability to record neural activity advanced with it. Technology eventally allowed researchers to record the activity of individual cells within the brain, known as the

spiking activity. The ease in which spiking activity could be interpreted and the relationship between spiking activity and behavior shifted the study of neurophysiologists towards relying on single unit recordings to listen in on the brain. However, largely owing to the huge advancements in equipment, analysis software, and the observation that oscillatory activity is closely tied to hemodynamic (Logothetis et al. 2001; Goense and Logothetis 2008; Nir et al. 2007), and EEG signals (Mitzdorf 1985; Schroeder et al. 1991), there has been a recent shift back towards understanding and recording mass action, or local field potentials (LFP) (Buzsaki 2006; Mitzdorf 1985).

Because of the initial shift away from the study of the cortical oscillatory activity, questions still remain about what brain waves, or more specifically what field potentials represent. Traditionally, LFPs have been viewed as the field potentials that arise locally as a result of both supra- and sub-threshold voltage fluctuations and ion channels that create a flow of currents across the membrane (Buzsaki 2006; Malmivuo and Plonsey 1995). The consensus is that LFPs represent the summed postsynaptic potentials from a population of neurons surrounding the microelectrode tip (Buzsaki 2006; Mitzdorf 1985; O'Leary and Hatsopoulos 2006). The microelectrode will pick up this lower-frequency (<300 Hz) electrical activity by spatially summating the field potentials surrounding the microelectrode, usually with a radius of a few millimetres (Buzsaki 2006; Mitzdorf 1985; O'Leary and Hatsopoulos 2006). Recently however, debate about the 'local' or the spatial radius of LFP recordings has been reported. While some researchers argue a more local nature (~250 microns) (Katzner et al. 2009; Engel et al. 1990) others suggest that LFP activity can spread to sites over a centimetre away from its origin, challenging the view that LFP activity represent local features (Logothetis et al. 2001; Mitzdorf 1985; Kajikawa and Schroeder 2011). Synaptic potentials can either have local origins

due to recurrent collaterals or they can reflect inputs from other regions (Pesaran et al., 2009). More research into this topic must be conducted to address these discrepancies.

In contrast to LFP activity, spiking activity is known to reflect supra-threshold inputs or outputs from pyramidal cells. The recorded activity will represent the action potentials that are being generated by the individual neuron that is being recorded (Brink et al. 1946; Moore et al. 1966). These observations suggest that LFP activity probably represent the inputs into the area, whereas spike activity most likely represents the outputs (Mitzdorf 1985; Scherberger et al. 2005). Based on the dichotomy of what LFPs and spiking activity represent, many researchers have concluded that spike and LFP recordings each carry a different set of information and can therefore be complementary tools for brain analysis (Buzsaki 2006; Mitzdorf 1985; Pesaran et al. 2002; Sanes and Donoghue 1993). Thus it seems reasonable to assume that in order to fully characterize the contribution of a region to a particular behaviour, analyzing both the single units and oscillatory activity will provide a richer repertoire of information than one technique alone. As research into LFP activity accumulates, various reports are emerging about the precision to which LFP activity measures neuronal processes such as attention, memory, action, and perception (O'Leary and Hatsopoulos 2006; Pesaran et al. 2002; Baker et al. 1999; Brovelli et al. 2005; Cooper et al. 2003; Donoghue et al. 1998; Jensen et al. 2007; Pesaran et al. 2008). In fact, some researchers have concluded that LFP is a better predictor of certain behavioural states compared to the activity of single units alone (Mitzdorf 1985; Scherberger et al. 2005; Pesaran et al. 2002; Engel and Fries 2010). In addition LFP activity has been successfully used to control neural prosthetics with amazing accuracy (Scherberger et al. 2005; Pesaran et al. 2002; Mehring et al. 2003; Rickert et al. 2005; Tillery and Taylor 2004). An attractive component of recording and analyzing LFP activity is that it shares a strong relationship with the blood-oxygen-level

dependent (BOLD) fMRI signal (Goense and Logothetis 2008; Nir et al. 2007), more so than single unit activity (Fries et al. 2001). For example, in the auditory cortex, gamma LFP activity was highly correlated with BOLD activity, whereas the relationship between BOLD and spike activity was variable (Nir et al. 2007). Researchers have also looked at the relationship between LFPs and spikes, the results of which have provided mixed results within the literature. While some research suggest that a strong relationship exists (Fries et al. 2001; Ray and Maunsell 2011; Zanos et al. 2012; Zanos et al. 2011), others suggest a difference between spiking and LFP activity (Pesaran et al. 2002; Flint et al. 2012). Despite these discrepancies, the relationship between LFP, spike, and BOLD activity can be used to benefit research as it helps bridge the gap between neurophysiological data in animals and fMRI recording in humans.

Analyzing LFP activity can provide information about locally generated oscillations and coherency between electrode sites (Sanes and Donoghue 1993). Currently, there are two overall ways to analyze LFP activity and its relationship to behaviour. The first is to analyze the evoked potential (EP) that arises from presentation of a stimulus (sensory or motor) (Rickert et al. 2005; Asher et al. 2007). The second approach is to look at the spectral analysis, or frequency domain of the signal, which just simply reveals how much of the signal falls within each specified frequency range (Scherberger et al. 2005; Pesaran et al. 2002). Using this latter approach, researchers can observe task dependent changes that may occur at specific frequency ranges or in certain phases of an oscillatory cycle (Scherberger et al. 2005; Pesaran et al. 2002). Regardless, both of these approaches allow oscillatory activity to be analyzed and interpreted. The projects presented here focus on the second approach of examining the spectral profile of the recorded LFP activity. In this way we can characterize the spectral profile during a reaching movement and its progression throughout the trial. More importantly, we can examine if and how this

profile changes during different types of visually-guided reaching behaviours.

Fluctuations in the extracellular potentials recorded as LFP activity reflects the rhythmic current flow across the cell membrane in local ensembles (Buzsaki 2006; Buzsaki and Draguhn 2004). Importantly, oscillatory LFP can alter the excitability of cells across different spatiotemporal scales, thought to occur because of feedback interactions between the neuronal activity and the endogenous extracellular field (Frohlich and McCormick 2010; Lakatos et al. 2005; Lampl et al. 1999). The oscillatory fluctuations in the extracellular potentials will provide a short period of enhanced rhythmic excitability (Traub et al. 2004; Womelsdorf and Fries 2006). Precise temporal control in neural networks will thus be critical because spikes arriving at the peak of this excitability will have the greatest effect on information transfer (Chrobak and Buzsaki 1998; Csicsvari et al. 2003). Such a relationship could serve as a mechanism for synaptic gain control, or could influence spike-timing-dependant plasticity (Harris et al. 2003; Zeitler et al. 2008). Additionally, synchrony between the spikes and LFPs could also serve as an additional way for information to be transmitted because the temporal pattern of spiking could change without a shift in firing rates being altered (Riehle et al. 1997).

This converging understanding of the meaning behind the different types of neurophysiological signals leads us to an emerging view within the field that neuronal coherency is essential to selecting and transmitting information required to integrate sensory information for motor performance (Pesaran et al. 2008; Womelsdorf and Fries 2006; Fries 2005). Neuronal coherency establishes effective communication between neuronal groups that are processing task-related information (Womelsdorf and Fries 2006). By effectively coupling the activity of spikes and LFPs (Womelsdorf and Fries 2006), communication through coherency (CTC) (Womelsdorf and Fries 2006; Fries 2005; Roberts et al. 2013) enables inputs that are arriving to

that local population to have a greater impact. This makes neuronal coherency an attractive mechanism by which the information can be selected and transmitted (Womelsdorf and Fries 2006; Fries 2005) by increasing the effectiveness of the connections between brain areas and enhance the representation of an attended stimuli (Fries et al. 2001; Fries 2005; Aertsen et al. 1989). In summary coherency serves as an effective way for functional cell assemblies to quickly form and disband to meet task demands (Koralek et al. 2013). By examining the change in coherency we can examine how the communication and representation of a reach plan is affected during different types of reaching movements.

1.4.1 The different frequency bands.

The results obtained from LFP analysis can help us identify how the different frequency ranges vary with and between tasks. Researchers over the years have suggested that the oscillations that occur within a gamma range (25-100 Hz) reflect local integration (Hughes 2008; von Stein and Sarnthein 2000), which is important for neuronal communication. Oscillations in the gamma frequency have the correct time frame to allow for temporal integration between neurons (Jensen et al. 2007) and may reflect the local interactions needed to enhance the representation of a stimulus that will be passed forward (Buschman 2007). Others have suggested that gamma band activity has an important role in attention and memory (Brovelli et al. 2005; Jensen et al. 2007; Sauve 1999). It has been suggested that beta band signals (12-18 Hz) are involved in multimodal processing (von Stein and Sarnthein 2000), while alpha band (8-12 Hz) activity, although originally thought to represent cortical idling (Cooper et al. 2003; Adrian and Matthews 1934a), more recently has been linked to working memory retention, mental imagery (von Stein and Sarnthein 2000; Jensen et al. 2002), or active inhibition of sensory information during internally driven attention (Cooper et al. 2003). Recently, an emerging view

has reshaped what oscillatory activity within a specific frequency range may represent. The view is largely based on the observation of distinct laminar differences within the frequency domain, suggested to be dependent on the microcircuitry within cortical and subcortical structures (Maier et al. 2010). Seminal work by Buffalo and colleagues (2011) confirmed a preference for synchronous LFP activity among the lower frequencies within the infragranular layers of a region, while supragranular cortical layers preferred gamma band synchrony (Maier et al. 2010; Bosman et al. 2012; Bastos et al. 2012; Roopun et al. 2006; Buffalo et al. 2011). Similar results have also been observed during single cell recording within V1, demonstrating differences in the spontaneous neural firing rate as a function of laminar layer (Snodderly and Gur 1995). This significant finding allowed researchers to take an extra glimpse into what LFP activity within these different frequency band represent within the brain. This proposal becomes more appealing with the observation that feed-forward connections originate from supragranular pyramidal cells from early cortical areas, and target the deeper layers of higher cortical regions (Bastos et al. 2012; Felleman and Van Essen 1991). Feedback connections originate largely from the deep pyramidal cells of higher cortical regions to terminate within the supragranular layers of earlier cortical regions (Bastos et al. 2012; Felleman and Van Essen 1991).

Taken collectively, LFP synchrony and coherency observed within the lower frequency bands are proposed to reflect feedback projections from distant signals involved in 'top down' neural processing (Maier et al. 2010; Bosman et al. 2012; Bastos et al. 2012). In contrast neuronal synchrony and spike-field coherence in the gamma range which are observed in the superficial and granular cortical layers of a region and thus proposed to reflect 'bottom up' processing (Engel and Fries 2010; Bastos et al. 2012; Donner and Siegel 2011; Siegel et al. 2012; Brovelli et al. 2004; Buschman et al. 2012). This idea was elegantly demonstrated by Buschman

and Miller (2007) with simultaneously recorded activity from the prefrontal and parietal regions. Macaques performed a visual detection task under 'pop-out' and 'search' conditions. These conditions depended on the degree to which distracters affected the detection of the target, with the pop-out condition having a very salient target and the search trials requiring more cognitive control. What they observed was that during search trials, which relied more heavily on top-down attention processes, prefrontal neurons reflected the location of the target prior to parietal neurons. On the contrary, during pop-out trials, parietal neurons reflected the target first. The most significant observation these researchers reported however, was that during top-down attention there was stronger synchrony between these regions within the lower frequencies (22-34 Hz) while high frequency (35-55 Hz), synchronization was enhanced during bottom-up attention (Figure 1.6). This idea is further supported by recent work into the functional role of beta oscillations by Engel and Fries (2010). They suggest that beta oscillations signal the current behavioural state, or the 'status quo', by promoting preferential or top-down processing of that state (such as the motor plan) (Scherberger et al. 2005; Pesaran et al. 2002; Engel and Fries 2010). In addition, past research has also suggested that feedback connections are largely inhibitory in nature while feedforward connections are excitatory (Bastos et al. 2012; Olsen et al. 2012; Knight et al. 1989; Murray et al. 2002; Alink et al. 2010; Zeki 1978). As suggested above, feedback connections tend to terminate within the first cortical layer which is made up almost entirely of strongly interconnected inhibitory cells that can provide strong monosynaptic inhibitory influence over deeper cortical layers (Chu et al., 2003; Meyer et al., 2011). This inhibitory drive from feedback connections may be one way top-down control can modulate cortical regions.

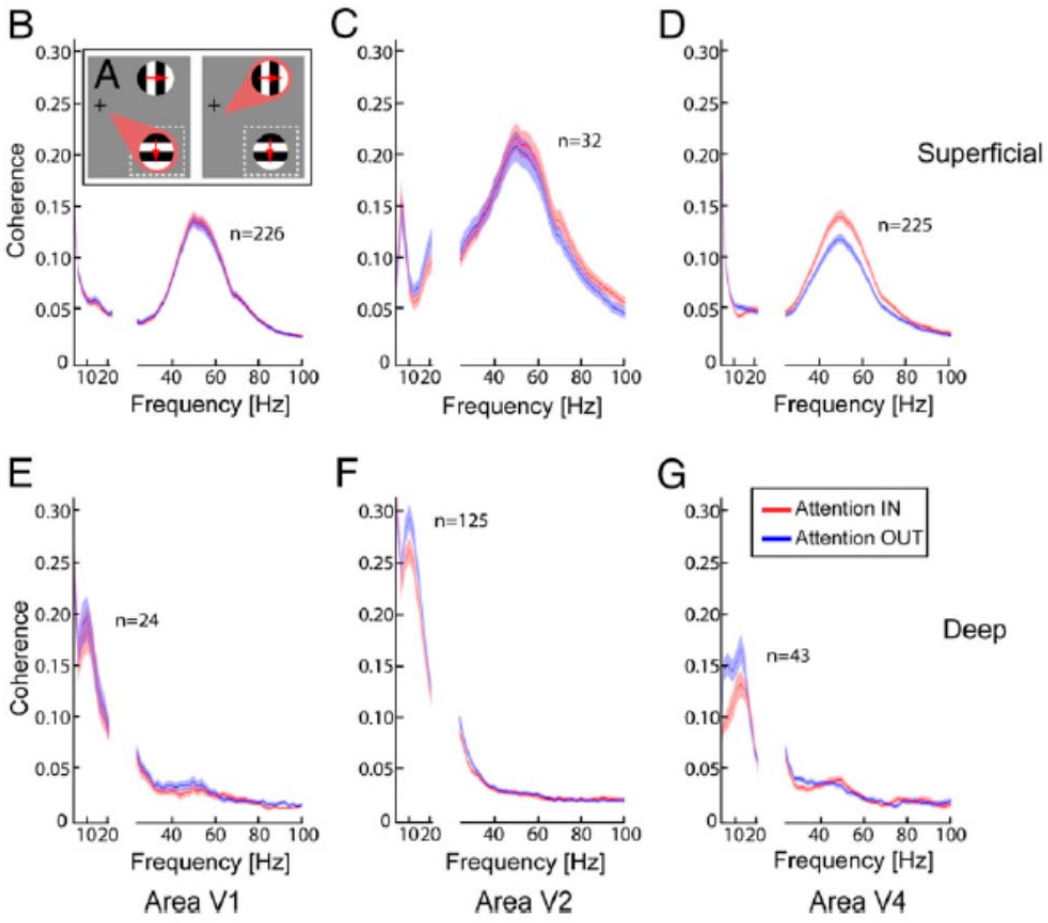

Figure 1.6 Laminar differences in the frequency range of LFP activity. Figure shows the attentional modulation of spike-field coherency (SFC) in areas V1, V2, and V4. A) On alternating blocks of trials, monkeys were cued to attend to a moving grating either inside (top) or outside (bottom) of the recorded neuron's RF. Red traces represent SFC in each area, with attention directed INTO the neuron's RF. Blue traces represent SFC with attention directed OUT of the RF. The magnitude of coherence as a function of frequency is shown for superficial recordings (B–D) and deep recordings (E–G) for areas V1 (B and E), V2 (C and E), and V4 (E and G). Shaded areas represent SEM. Figure and Text taken from Buffalo et al., (2011).

1.5. A brief overview of the three projects described in this dissertation.

Substantial evidence has accumulated to suggest that PMd and SPL play a critical role invisuomotor transformation. However what is less understood is how the computations required to perform a visually-guided reach is altered when there is a spatial transformation which must be incorporated into an upcoming reach. To date, no studies have directly compared the neural activity within PMd and SPL during coupled versus decoupled reaches. This is important because our ability to perform decoupled reaches is critical to our daily interaction with the world around us, and deteriorates under condition of mild brain dysfunction. Therefore the current goal of my dissertation is to address this knowledge gap in the motor control neuroscience literature. These studies will categorize how the neural activity within SPL and PMd are affected under different visuomotor mappings, and characterize the contribution that each region plays to the underlying neural control of decoupled reaching movements. Our research will contribute to our fundamental understanding of how the brain controls movement and utilizes spatial attention to improve visual detection and enhances visual processing to reachable objects.

For my first study (Chapter 2), I examined the single unit and LFP activity of PMd while two female rhesus macaques performed coupled and decoupled centre-out reaching tasks. The purpose of this first experiment was to investigate the the role of the neural activity within PMd during reaches that require a spatial decoupling between the action of the eyes and the hand. Based on previous research (Prado et al. 2005; Clavagnier et al. 2007; Picard and Strick 2001; Grafton et al. 1998) that showed topographical differences in the neural activity between PMdr and PMdc, we also investigated the topographical changes in the neural activity between rostral and caudal portions of PMd during performance on decoupled reaches.

In chapter 3, I examined the role of the SPL during decoupled visually-guided reaches in order to understand how this region responds during cognitive-rule integration. Similar to the first study, the oscillatory activity from two female rhesus macaques was examined while they perform coupled versus decoupled centre-out reaching task. The goal of this study was to understand how the neural activity within SPL is affected by performing reaching movements when the hand has been spatially decoupled from gaze direction.

For my final study (Chapter 4) we were interested in the relationship between the spiking activity and LFP. This was based largely on the idea that the relationship or coherency between these measures reflects effective communication to efficiently processing task-related information (Womelsdorf and Fries 2006). As such we wanted to take advantage of this observation by examining how the spike-field coherency is altered during different types of reaching movements. Using the previously recorded activity from projects one and two we analyzed the coherency within each region between the spikes and LFP.

Chapter Two

Differences in spectral profiles between rostral and caudal premotor cortex when hand-eye actions are decoupled.

Patricia F. Sayegh , Kara M. Hawkins, Kari L. Hoffman and Lauren E. Sergio

Reprinted with permission from Journal of Neurophysiology: P. F. Sayegh, K. L. Hawkins, K. Hoffman, L. E. Sergio. (2013) Differences in spectral profiles between rostral and caudal premotor cortex when eye-hand actions are decoupled. Journal of Neurophysiology , 10(4), 952-963.

ABSTRACT

The aim of this research was to understand how the brain controls voluntary movement when not directly interacting with the object of interest. Here we examined the role of premotor cortex in this behaviour. The goal of this study was to characterize the oscillatory activity within the caudal and rostral subdivisions of PMd (PMdc and PMdr) when going from the most basic reaching movement to one that involves a simple dissociation between the actions of the eyes and hand. We were specifically interested in how PMdr and PMdc respond when the eyes and hand are decoupled by moving along different spatial planes. We recorded single unit activity and local field potentials within PMdr and PMdc from two rhesus macaques during performance of two types of visually-guided reaches. During the standard condition, a visually guided reach was performed whereby the visual stimulus guiding the movement was the target of the reach itself. During the non-standard condition, the visual stimulus provided information about the direction of the required movement, but was not the target of the motor output. We observed distinct task-related and topographical differences between PMdr and PMdc. Our results support functional differences between PMdr and PMdc during visually-guided reaching. PMdr activity appears more involved in integrating the rule-based aspects of a visually-guided reach, while PMdc is more involved in the online updating of the decoupled reach. More broadly, our results highlight the necessity of accounting for the non-standard nature of a motor task when interpreting movement control research data.

Keywords: cognitive motor integration; local field potentials; neurophysiology; nonstandard reaching; premotor cortex

INTRODUCTION

Reaching movements rely on a network of brain regions including the dorsal premotor cortex (PMd) and superior parietal lobule (SPL) (Kalaska et al. 1998; Battaglia-Mayer et al. 2001; Caminiti et al. 1999). It is not well understood how activity within this network is modulated during a reaching movement when there is a dissociation between the actions of the eyes and hand, termed a "non-standard" movement (Wise et al. 1996Wise et al. 1996). There is strong evidence that the actions of the eyes and hand are tightly linked (Gielen et al. 1984; Prablanc et al. 1979; Henriques et al. 1998; Neggers and Bekkering 2000; Gauthier and Mussa Ivaldi 1988; Morasso 1981; Sergio and Scott 1998; Sergio and Scott 1998; Vercher et al. 1994; Gorbet and Sergio 2009; Terao et al. 2002), hence the brain must employ specific mechanisms to break this link during non-standard movements (Wise et al. 1996; Murray et al. 2000; Sergio et al. 2009). Inhibition of this linkage likely depends on neural circuitry that is different but interconnected with the circuitry important for controlling natural reaching movements (Sergio et al. 2009; Clavagnier et al. 2007; Gail et al. 2009). Support for this idea comes from the observation that decoupled eye-hand coordination develops only later in childhood (Sergio et al. 2009; Bo et al. 2006; Piaget 1965), that movements slow and accuracy declines when eye and hand movements are decoupled (Henriques et al. 1998; Terao et al. 2002; Messier and Kalaska 1997; Gordon et al. 1994; Goodbody and Wolpert 1999; Epelboim et al. 1997), and that patients with neurological disorders show impaired non-standard reaching, while standard reaching is largely unaffected (Tippett and Sergio 2006; Halsband and Passingham 1985; Halsband and Passingham 1982; Karnath and Perenin 2005; Ghilardi et al. 1999; Tippett et al. 2007; Jackson et al. 2005).

Cell activity in PMd is modulated by gaze direction, wrist orientation, hand direction, and

intended movement kinematics (Caminiti et al. 1990; Raos et al. 2004; Cisek and Kalaska 2002a; Boussaoud and Wise 1993a; Boussaoud 2001; Boussaoud and Wise 1993b; Boussaoud et al. 1998). Recent findings suggest that the rostral and caudal subdivisions of PMd (PMdr and PMdc) have separate roles in the visuomotor transformation needed to plan an upcoming visually-guided reach (Raos et al. 2004). These results are strengthened by anatomical studies, which demonstrate that PMdr and PMdc have separate cortical connections. PMdr has strong reciprocal connections with prefrontal regions (Lu et al. 1994) whereas PMdc has strong connections to the primary motor cortex and the spinal cord (Barbas and Pandya 1987; Geyer et al. 2000; Luppino et al. 1990), therefore, PMdc may be involved in coding limb movement parameters (Cisek et al. 2003; Alexander and Crutcher 1990). In contrast, PMdr may have a role in the context-dependent selection and planning of movements in conditions that involve non-standard mappings (Raos et al. 2004; Boussaoud 2001; Cisek and Kalaska 2005), though this remains to be tested directly.

Oscillatory activity (local field potential, LFP) has been used to measure many neuronal processes such as attention, memory, action and perception (O'Leary and Hatsopoulos 2006O'Leary and Hatsopoulos 2006; Baker et al. 1999; Brovelli et al. 2005; Cooper et al. 2003; Donoghue et al. 1998; Jensen et al. 2007). LFPs represent the activity within local cell assemblies (Scherberger et al. 2005) and are believed to represent the input into an area (Scherberger et al. 2005). Since spiking activity reflects supra-threshold inputs or outputs from pyramidal cells, it is very likely that spike and LFP recordings carry a different set of information and can therefore be complementary tools for brain analysis (Pesaran et al. 2002; Sanes and Donoghue 1993). In fact, some researchers have concluded that LFP activity is more accurate then spike activity when decoding certain behavioural states (Mitzdorf 1985). Another

benefit to LFP analysis is its strong relationship with BOLD fMRI activity in humans (Goense and Logothetis 2008) (Nir et al. 2007) and with spike activity in non-human primates (Fries et al. 2001). The relationship between LFP, spike, and BOLD activity can be used to bridge the gap between neurophysiological data in animals (single cell recording) and human fMRI recordings.

Here, we examine how oscillatory and spike activity within PMd are modulated when gaze and hand motions are spatially incongruent, relative to more natural spatially congruent reaches. In addition to overall changes in the spectral profile as a consequence of non-standard reaching, we predict that the rostral subdivision of PMd will show greater modulation, relative to the caudal subdivision, particularly during the planning phases of the task.

METHODS

Apparatus and Behavioural Task

Two rhesus monkeys (female *Macaca mulatta*, body weights: monkey A= 5.2 kg, monkey B = 5.2 kg) were trained to perform visually instructed, delayed reaching tasks in standard and non-standard conditions. All surgical and animal handling procedures were in accordance with *Canadian Council on Animal Care* guidelines on the use of laboratory animals and pre-approved by the *York University Animal Care Committee*.

During the experiment, the monkey was seated in a custom-built primate chair 40 cm in front of a 38.1 cm vertical screen, which was set at monkey eye level and centered with her midline. An additional 38.1 cm horizontal touch sensitive screen (Touch Controls Inc, San Diego CA) was set in front of the animal, between the animal's waist and xyphoid process, so that she could reach over the entire surface of the screen comfortably (Fig. 2.1). The horizontal touch screen was designed to detect spatial displacements as small as 3 mm using infrared beams, at a

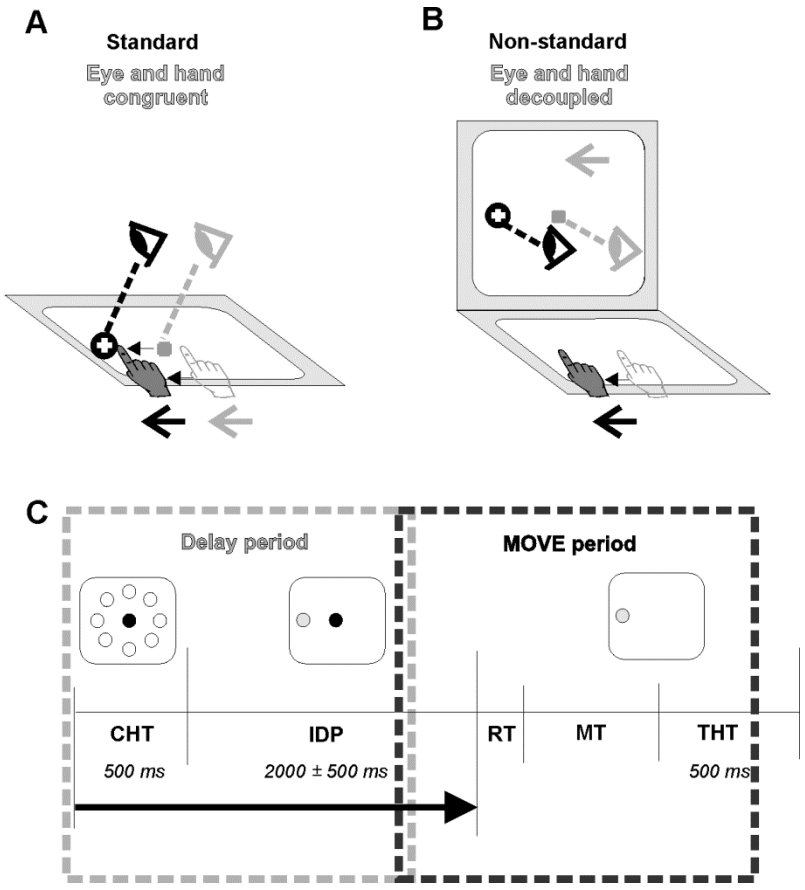

Figure 2.1. Experimental setup and trial timing. **A,** Schematic of the standard condition. **B,** Schematic of non-standard condition. During each trial, one of eight equally spaced (45°) peripheral targets were presented on either a touch-sensitive screen placed over the animal's lap (A) or on a monitor positioned vertically 40 cm away from the animal's frontal plane (B). Arm movements were always made over the horizontal touch screen. Light grey circles represent the eight possible target locations (not illuminated before cue). Epochs - CHT: centre hold time, IDP: instructed delay period, RT: reaction time, MT: movement time, THT: target hold time. The animal's head was fixed throughout the experiment.

sampling rate of 100 Hz. Continuous tracking of the eye was monitored using the ISCAN-ETL 200 Eye Tracking System (ISCAN Inc, Burlington MA) at a sampling rate of 60 Hz. Performance in both conditions required the animals to reach towards one of eight peripherally cued targets on the horizontal touch screen. The animals were trained to perform similar movements during both conditions and the biomechanical features of the reach movements were monitored to ensure that the movement profiles were similar between conditions. Additionally, to minimize any interference from the non-reaching limb, the animals were trained to maintain their non-reaching hand on a metal lever just beyond the lower corner of the horizontal touch screen. In this way it was ensured that the animal only used the appropriate arm without having to forcefully restrain the unused limb.

The visual targets were identical across conditions, but the spatial plane of presentation was altered. At the start of each trial, a red circular target (70 mm in diameter) appeared at the center of the screen with an additional smaller white circular target (40 mm in diameter; 5.7° of visual angle) on top of it. The red target instructed where the monkey should touch and the white target instructed where the animal should maintain eye fixation. After a baseline period of 500 ms, one of eight green-colored peripheral targets appeared (70 mm in diameter). All eight targets were equally spaced (45°) and appeared randomly, based on a randomized-block design. The peripheral target appeared 5 times at each location for a total of 40 trials per condition. After a variable instructed delay period (IDP, 2000 ms +/- 500 ms) the red central target extinguished and the white target jumped to the peripheral target. This served as the go signal (GO) instructing the animal to move the eyes and hand from the central target to the peripheral target (Fig. 2.1). The movements were made from the center of the central target to the center of the peripheral target (roughly 80 mm, see Fig. 2.2). Once the eyes and hand arrived at the

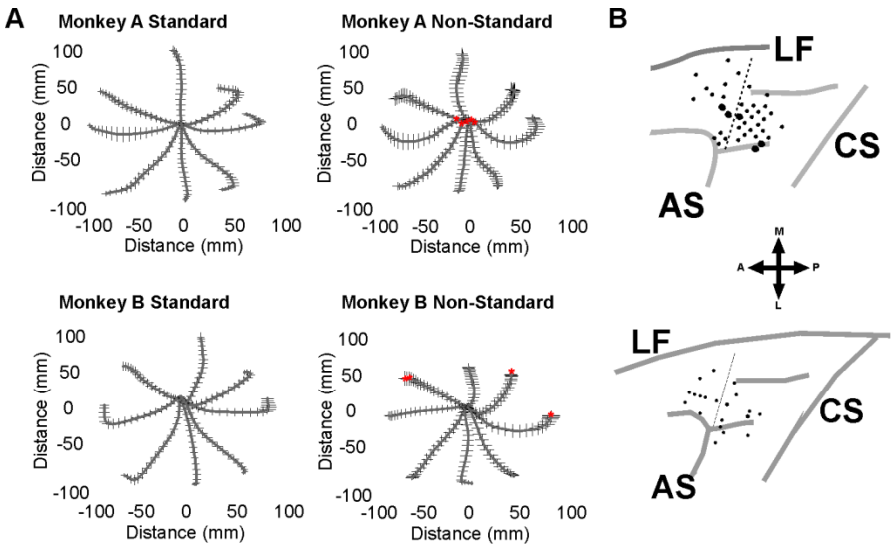

Figure 2.2. **A.** Mean reach trajectories. Black lines: mean movement trajectories, black tick marks: standard deviations. Red asterisks denote trajectory segments that were significantly ($P < 0.05$) more variable in comparison to the standard condition. **B.** Penetration sites for monkey A (top panel) and monkey B (bottom panel). Larger dots indicate where recordings were obtained on two occasions. AS: arcuate sulcus. CS: central sulcus. LF: Longitudinal fissure. Arrows show anterior, posterior, medial, and lateral directions, dotted line denotes division between penetration sites classified as rostral (left of line) or caudal (right of line).

peripheral target, the monkey was required to hold them there for 500 ms, after which a liquid reward was delivered to the animal. Additionally, to reinforce similar hand paths between conditions, movement alleys were included to ensure that reaches were directed along a fairly straight trajectory. These alleys were set at ± 40 mm from a straight line spanning from the central to the peripheral targets. If the monkey's hand deviated beyond the set alley, the trial would stop. To provide feedback on the current position of the hand, a cross-hair representing the position of the finger on the touch screen was displayed.

In the *standard condition,* the actions of the eyes and hand remained congruent. The visual presentation of the task and the reaching movements were both made on the horizontal touch-sensitive screen placed in front of the animal (Fig. 2.1A). In the *non-standard* condition, the actions of the eyes and hand were decoupled: the visual presentation of the task was on the vertical screen while the animal's limb movement remained on the horizontal touch screen (Fig. 2.1B). Thus, the animal was required to direct its gaze along the vertical monitor but move its finger along the horizontal monitor in order to displace the cursor from the central to the peripheral target. To ensure that the animal did not track its hand position extrafoveally, an opaque screen was placed 10 cm above the animal's arm to block vision of the limb. For each condition, two epochs during the trial were considered, the instructed delay epoch (IDP) and the movement epoch (MOVE). IDP was comprised of the 500 ms baseline period and the first 1000 ms of the instructed delay. MOVE was comprised of the last 500 ms of the instruction delay up until 500 ms after movement onset.

We also had a *gaze-only* condition, in order to determine if the oscillatory activity within the sub-regions of PMd was affected solely by the overall shift in gaze angle between conditions. Gaze-only data were collected for every recording. The visual display consisted of 9 white

circles (40 mm in diameter; 5.7° of visual angle) that appeared in the same locations as the white targets that appeared during the experimental conditions. The monkey was instructed to fixate on each of these white circles while maintaining both hands beside the horizontal touch screen. The white circles appeared one at a time in each location 3 times for a total of 27 saccades for each plane.

Muscle activity was recorded from 13 proximal-arm muscles in separate recording sessions. Pairs of Teflon-insulated 50 μm single-stranded stainless steel wires were implanted percutaneously. Implantations were verified by passing current through the wires to evoke focal muscular contractions (< 1.0 mA, 30 Hz, 300 ms train; (Sergio and Kalaska 2003). Multi-unit electromyography (EMG) activity was amplified, band-pass filtered (100-3000 Hz), half-wave rectified, integrated (5 ms time bins) and digitized on-line at 200 Hz. The muscles studied included the anterior deltoid, medial deltoid, posterior deltoid, dorsoepitrochlearis, infraspinatus, latissimus dorsi, pectoralis, supraspinatus, teres major, rostral trapezius, caudal trapezius, triceps lateralis, and triceps medialis. These recordings were performed to assess the general effects of the standard and non-standard tasks on EMG activity and were not designed as a definitive biomechanical study of the muscle properties.

Behavioural and muscle data analysis.

Hand paths recorded from the touch sensitive monitor were analyzed to confirm that the movements were biomechanically similar between conditions. The individual movement paths were first low-pass filtered at 10 Hz and the movement onsets and endpoints were automatically scored as 8% peak velocity at the beginning and end of the velocity profile respectively. The movements were then cut at the onsets and endpoints and divided into 21 equal segments. The five trials for each direction were then pooled and the means and standard deviations were

calculated at each segment along the path. An equality of variance test was performed between the two conditions on the mean x and y components of the trajectory for each target (Snedecor and Cochrane 1989). Since a given trial was only kept if the animal went from the central to the peripheral target within a somewhat narrow alleyway, this test determined if, despite this behavioural training, there were any systematic differences in movement variability between tasks. Mean reaction times (from the GO-signal to 8% peak velocity) were also calculated for each condition and paired-samples t-tests were performed to compare reaction times between the standard and non-standard conditions. Repeated measures ANOVAs were performed on the EMG data during the IDP and MOVE epochs for each muscle recorded in order to determine the effect of target (motion direction) and condition (standard and non-standard) on maximum EMG amplitude. It was expected that reach direction would have an effect on EMG amplitude, but condition would not.

Neural Recordings

Monkeys were implanted with a recording cylinder under standard aseptic surgical techniques (Kalaska et al. 1989). Briefly, a plexiglass cylinder (used to hold the electrode manipulandum) was positioned on the 19 mm craniotomy and fixed into place using cranioplastic acrylic and titanium neurosurgical screws. A small metal fixation pole used to stabilize the head during recording was also implanted into the acrylic. The stereotaxic coordinates for chamber placement over PMd (both monkeys; Interaural AP: +16 mm; ML: +11 mm) were determined using *The Rhesus Monkey Brain in Stereotaxic Coordinates* (Paxinos et al. 2000). The border between rostral and caudal PMd, and primary motor cortex (M1) was drawn according to previously proposed physiological and cytoarchitectonic criteria (Fujii et al. 2000). The experiments began a week after surgery following a complete recovery.

Local field potentials and single units were collected from the extracellular recordings within PMd. A hydraulic multi-channel driver (MCM-4, FHC inc., Bowdoin ME) mounted to the implanted chamber was used in conjunction with a multi-channel processing system (MCP, Alpha-Omega Engineering, Israel). Standard tungsten microelectrodes (impedance 1-3 megaohms, FHC Inc., Bowdoin ME) were used for recording the neural activity within PMd. The multidriver provided simultaneous recordings from up to two penetration sites at a time. Neural activity from each electrode was preamplified (5000x), band-pass filtered (1 Hz-10 kHz) and split into lower (LFP) and higher (single units) frequencies. Higher frequency signals were sampled at 12.5 kHz and passed through the multi-spike detector (Hawkins et al. 2012). The lower frequency signals (below 100 Hz) were sampled at 390.6 Hz.

Data analyses

Directional tuning was determined based on previous methods (Hawkins et al. 2012;Georgopoulos et al. 1982). Briefly, a sinusoidal regression on the mean discharge rates for each target direction was performed and the goodness of the regression fit was calculated. The regression equation was then re-expressed in terms of the peak of the sine wave, which is the direction for which the cell was most active (i.e. the "preferred direction") (Georgopoulos et al. 1982). A bootstrap test was then performed using 1000 shuffled activities to determine the significance of the tuning based on a 95% confidence interval. The mean firing rates of each cell were then normalized to each cell's individual mean baseline firing rate. The baseline firing rate was calculated as the mean firing rate during the first 300 ms of each trial when the animal was instructed to hold its hand at the central target. This generated a normalized firing rate for comparison with the LFP data, which were also normalized to the same baseline time period (see below). Significance was determined by performing a three-way mixed ANOVA with condition, (standard versus non-standard) and time (early versus late) as within-subject factors and location

(PMdr versus PMdc) as between subject factor. All ANOVA results were reported with Greenhouse-Geisser-corrected *p*-values, and post hoc comparisons were corrected for multiple comparisons (Bonferroni). All successfully recorded LFP sites were included in all analyses. The converted data was analyzed in MATLAB (Mathworks, USA) using both custom written and open source (Chronux.org) programmes. Chronux script files were used to analyze the spectral profiles and generate time-frequency spectrograms for all penetrations for both conditions (Pesaran et al. 2002; Jarvis and Mitra 2001). We used spectral analysis to categorize the power at different frequency bands. To estimate the frequency structure of the LFP activity, we used the multitaper spectrum analysis (previously described by Jarvis & Mitra, 2001; Pesaran et al., 2002). The multitaper technique provides an optimal estimate of the spectrum by reducing spectral leakage and variance of the estimate by averaging the spectral estimates from several orthogonal tapers (Jarvis and Mitra 2001). The orthogonal tapers are Slepian np prolate functions (Jarvis and Mitra 2001). A Fourier transform was then applied to the tapered signal. The multitaper estimates of the spectrum Sx (f), for each recording were then calculated (Scherberger et al. 2005; Pesaran et al. 2002). The spectrum was z-transformed to the baseline period, which consisted of 300 ms at the start of each trial during which time the animal was maintaining eyes and hand at the central target. Normalizing to a baseline period was necessary to compare between conditions and locations. No significant differences were observed between baseline activity when comparing between conditions within each region, $P > 0.05$. By normalizing to a baseline period, spectrograms were calculated using a 200 ms window shifted in 50 ms increments with a 3 Hz frequency resolution. Mean spectra reflect the spectra z-transformed from individual trials, then collapsed across target directions and electrode sites within the respective PMd region.

To determine the statistical significance of task-related differences ($P < 0.05$), the

normalized spectra from each electrode site was divided into 4 frequency bands (0-10 Hz, 10-30 Hz, 30-45 Hz, and 45-70 Hz). Data from above 70 Hz were not presented because the pattern of activity within this range has been shown to be closely related to spiking activity (Ray and Maunsell 2011) (Zanos et al. 2012; Zanos et al. 2011). The average spectral value across time for each frequency band was determined for each condition (standard and non-standard). A bootstrapping procedure was used to assess whether the difference in power between the two conditions could have occurred by chance, based on the assumption that if power was the same between the two conditions, then the distribution of differences of the bootstrapped estimates of LFP power between conditions would be normally distributed and centered around 0 difference. This test was implemented as follows. The empirical estimate of power was obtained by calculating the power difference between standard and non-standard conditions. A bootstrapped distribution was created by random reassignment of the condition label (standard/nonstandard) for each observation within these distributions and the mean power difference re-calculated. This was repeated 1,000 times to generate a distribution of 1,000 bootstrapped power difference values that could be expected if the observed power differences were due to chance (i.e. random condition assignment). The bootstrapped differences were then rank ordered. The high and low limits of the 95% confidence interval (CI) were defined as the 25th and 975th largest power values (2-tailed test). Activity from an electrode site was considered to have undergone a significant shift in power between conditions if the calculated power difference between conditions fell outside of the 95% CI of the distribution of its bootstrapped LFP powers (i.e., the null hypothesis that the mean value for power of 0 can be rejected at alpha = 0.05, 2-tailed test). The time points and frequency ranges that were significantly different between standard and non-standard conditions were recorded. To generate spectrograms that displayed the task related

differences, we subtracted the standard from the non-standard spectrum for each site and averaged across the population for each region. All values that were not significant were set to zero, any value above zero represents stronger power for that time-frequency bin within the standard condition and any value below zero represents stronger power within the non-standard condition, using an alpha value of 0.05.

To determine topographical differences between PMdr and PMdc we compared the activity between each region during each condition. The same methods were used as the ones described for the task related analysis, however bootstrapping was done between PMdr and PMdc for each condition.

Lastly, we analysed the oscillatory activity in the gaze-only condition to determine if the overall shift in gaze angle that occurred between the two planes associated with each conditions had an effect on the oscillatory activity within PMd. All recorded sites from PMdr and PMdc were tested in gaze-only conditions. Only a sub-portion of these sites was used for this analysis. The mean power (0-70 Hz) at each gaze location was calculated from a 500 ms window while the animal was fixating at each target. Within each condition, the mean power across the nine target locations was computed. A bootstrapping procedure was used to assess whether the difference in power between the two gaze planes could have occurred by chance (for details see above).

RESULTS

The current results demonstrate changes in the neural activity within PMd when performing a coupled versus decoupled reaching movement. The change in neural activity differed between PMdr and PMdc suggesting functional differences between these regions. These results did not arise from differences in limb biomechanics or gaze angle and support our

hypothesis that these regions are involved in visuomotor transformations for non-standard mapping.

Behavioral Results

To ensure that any oscillatory differences seen between conditions were not a result of differences in the movement of the hand, we compared hand trajectories between conditions. We wanted to ensure that the biomechanical features of the limb movements were identical throughout the experiment. This guarantees that the interpretations of the LFP data are not affected by a difference in limb movements. The use of alleys helped support the animal in maintaining similar hand trajectories during both conditions (see methods). Figure 2.2A shows the mean reach trajectories during both conditions for each animal. Except for a few segments, there were no significant differences in the reach trajectories between standard and non-standard conditions. An analysis of the EMG data revealed that for 11 of 13 muscles there was no main effect of condition during the IDP and MOVE epochs ($p>0.01$). For two muscles, medial deltoid and teres major, there was a marginal effect of condition on EMG activity during the IDP epoch ($0.05>p>0.01$). This may have been due to a slight alteration in the animals' starting posture in reaction to the board placed over their arm in the non-standard condition. There was, as expected, a main effect of target for all proximal arm muscles studied during the movement epoch ($p<0.01$). Lastly, reaction times between the standard (M = 537.9 ms, SEM +/- 12.82) and non-standard (M = 522 ms, SEM +/- 9.89) conditions were also not significantly different (t (45) = .927, p = 0.359). Taken collectively, these results strengthen the conclusion that any neural differences observed between conditions are not a direct result of changes in the biomechanics of the reaching movement, but rather the control of the movement.

Neural Activity

We obtained 66 (59 from monkey A, 7 from monkey B) LFP recordings and classified 36 of these recordings as coming from PMdr and 30 recordings as coming from PMdc based on the stereotaxic coordinates of the recording chamber and the penetration location in the chamber (Fig. 2.2B). All successfully recorded LFP sites were included in the analysis . In addition, 52 single cells were recorded within PMd (28 PMdr and 24 PMdc) during both conditions, of which only 29 were found to be task-related (directionally tuned during either the IDP or MOVE epochs). In support of our hypothesis, we observed that oscillatory and single unit activity in PMd were modulated by the type of eye-hand coordination: standard (direct object interaction) or non-standard (decoupled effectors). In addition, we observed that the temporal and spectral profile of change depended on the region (rostral or caudal) of PMd sampled.

Task related differences within PMd

Oscillatory activity

Our first main finding was that we observed salient differences in the oscillatory activity during performance on the standard condition when compared to the non-standard condition in both sub-regions of PMd. We analyzed the neural activity within two epochs (see methods). During the IDP epoch, the animal received information about the location of the peripheral target but was required to maintain hand and eye position at the central location. Thus during this epoch the early stages of movement planning would be occurring. Figure 2.3 shows an example of the increase in power that occurs across each frequency band for a single PMdc recording site during both epochs. The population spectrum from each animal for each epoch is also shown in Figure 2.3C and D to demonstrate the similarity in spectral profile between animals. Because of these similarities, all analyses were pooled between animals. The MOVE epoch represents both the very late stages of planning and the early stages of the movement (see methods). During this

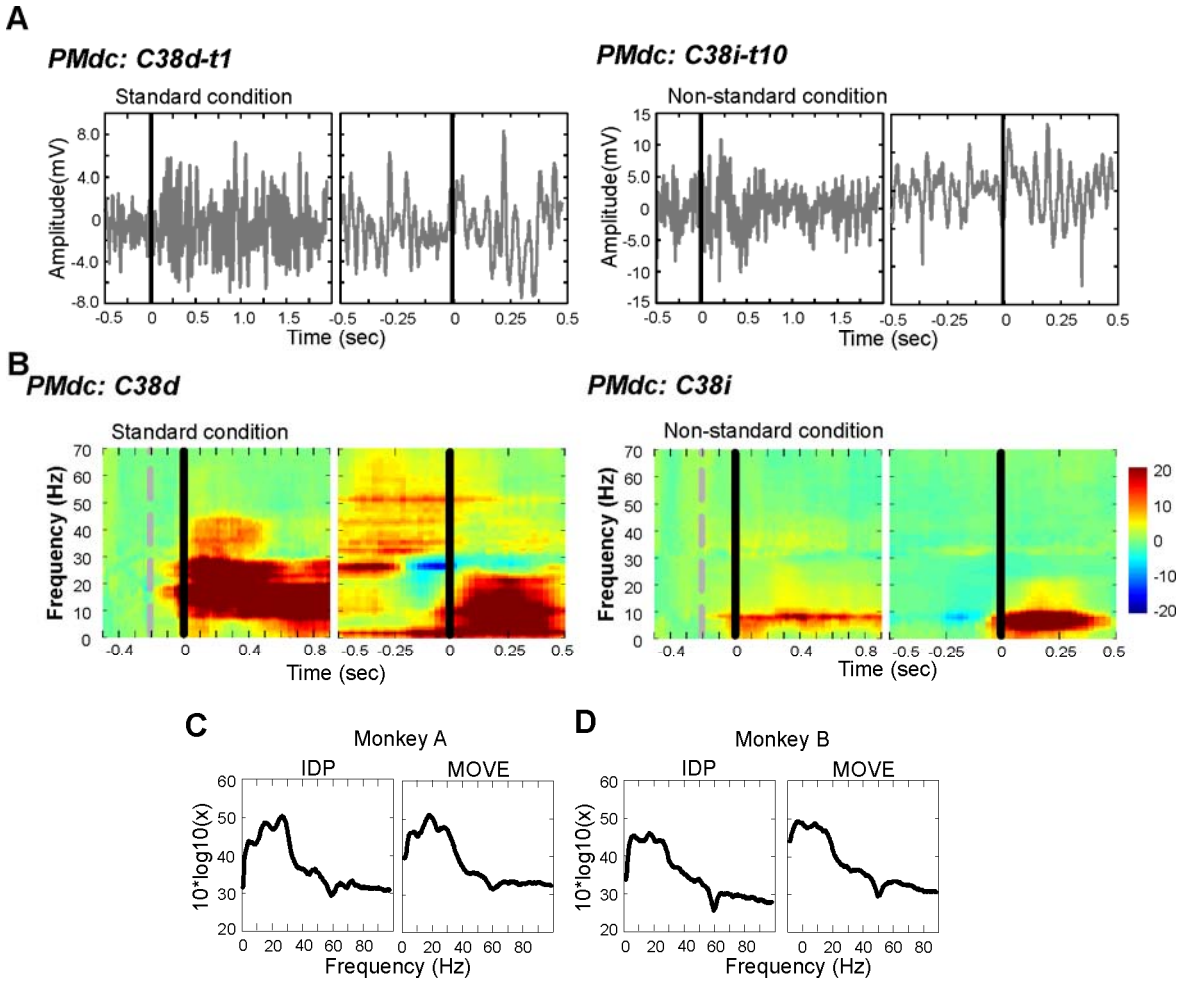

Figure 2.3. Example recordings for a PMdc site. **A,** Example broadband LFP during IDP and MOVE epochs for both conditions. Black line indicates peripheral target (IDP epoch) or movement onset (MOVE epoch). **B,** Example time-frequency spectrograms of oscillatory activity during each epoch and condition. **C, D,** Example spectral power during the IDP and MOVE epochs demonstrating similarity between animals.

epoch the movement has already been planned and there is an anticipation of the GO signal. Additionally, the second 500 ms of this epoch represents the first 500 ms of the reaching movement, which was the same between conditions (i.e., only the eye movement coupling varied between conditions; Fig. 2.1).

During the IDP epoch, changes to the overall oscillatory activity occurred when the eyes and hand were decoupled versus when they were congruent (Fig. 2.4, left panels). Shortly following peripheral cue onset (Black vertical line) there was an increase in oscillatory activity that occurred in both regions of PMd during both conditions (Fig. 2.4 A, B, C and D, left panels). To see task related differences more clearly, Figures 2.4E and F display the main differences in power across conditions, masked for significance (see methods). We observed a significant increase in PMdr oscillatory power within the 10-70 Hz range during the non-standard condition relative to the standard condition (Fig. 2.4E, left panel $P<0.05$). Contrary to this finding, PMdc showed a reduction in oscillatory activity between conditions within the 0-45 Hz range (Fig. 2.4F, left panel $P<0.05$). Figure 2.5 displays the z-score for each frequency bin across time and allows for a more in depth look at the pattern of change between conditions. As shown in Figure 2.4B, the oscillatory activity within PMdr shows a greater increase in power during the non-standard when compared to the standard condition (Fig. 2.5B, C and D, top left panels $P<0.05$). On the other hand, stronger oscillatory activity occurred for the standard when compared to non-standard condition within PMdc (Fig. 2.5A, B and C, bottom left panels $P<0.05$).

Our findings during the MOVE period showed more subtle differences in oscillatory activity when the eyes and hand were decoupled (Fig. 2.4 A, B, C and D, right panels). Task-related differences were only observed within the 0-10 Hz range prior to movement onset for both PMdr and PMdc (Fig. 2.4E and F, right panels). Both regions showed a significant reduction in

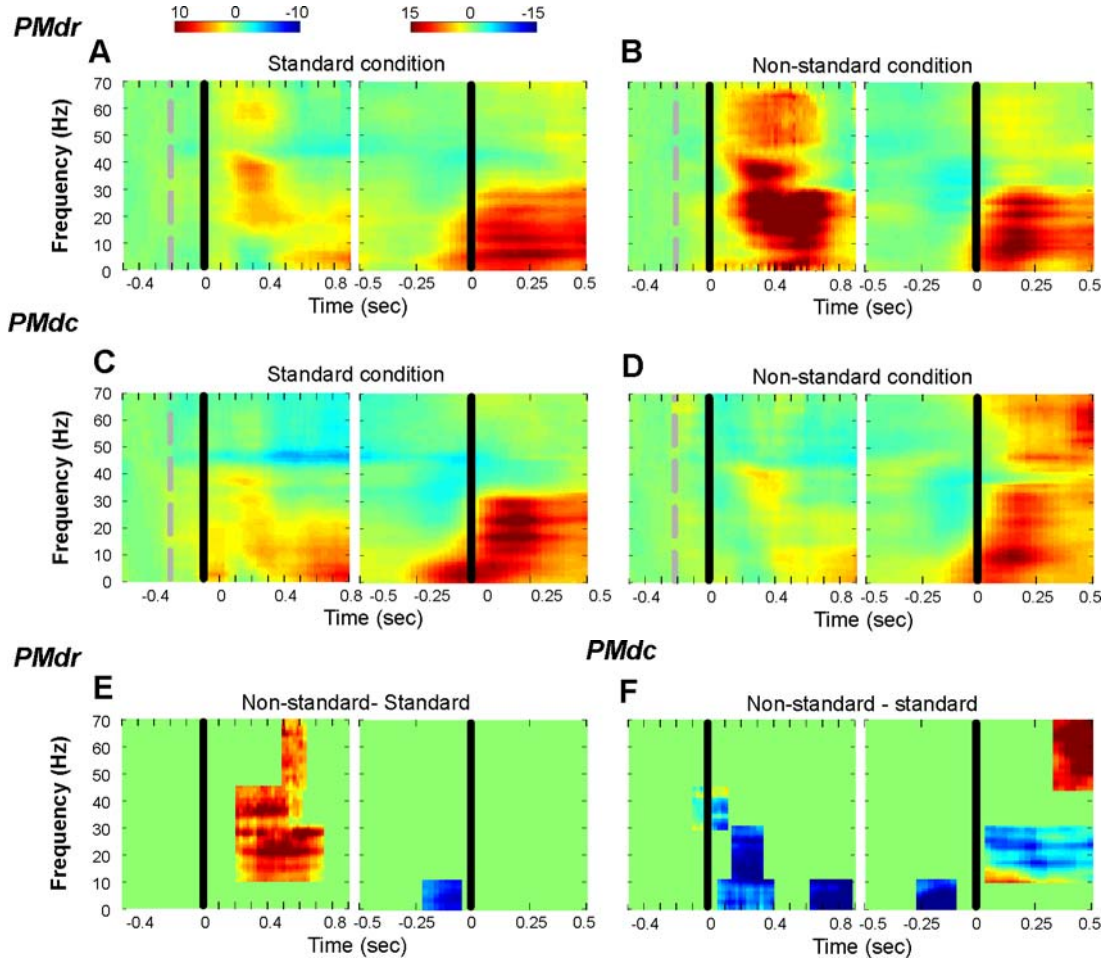

Figure 2.4. Population time-frequency spectrograms of oscillatory activity during the IDP and MOVE epochs. **A, B**, Population spectrograms of PMdr power during standard (left panels) and non-standard (right panel) conditions. **C, D,** Population spectrograms of PMdc power for standard (left panel) and non-standard (right panels) conditions. **E, F,** Population spectrogram showing only significant differences between standard and non-standard conditions within PMdr (E) and PMdc (F). Each time-frequency bin was masked at 95% CI based on bootstrapped data (see methods). Colors above zero indicate greater power within the non-standard condition and colors below zero indicate greater power within the standard condition. Black line indicates peripheral target onset during IDP epochs and movement onset during MOVE epochs, gray dashed line indicates end of the baseline period. Power is color-coded on a log scale.

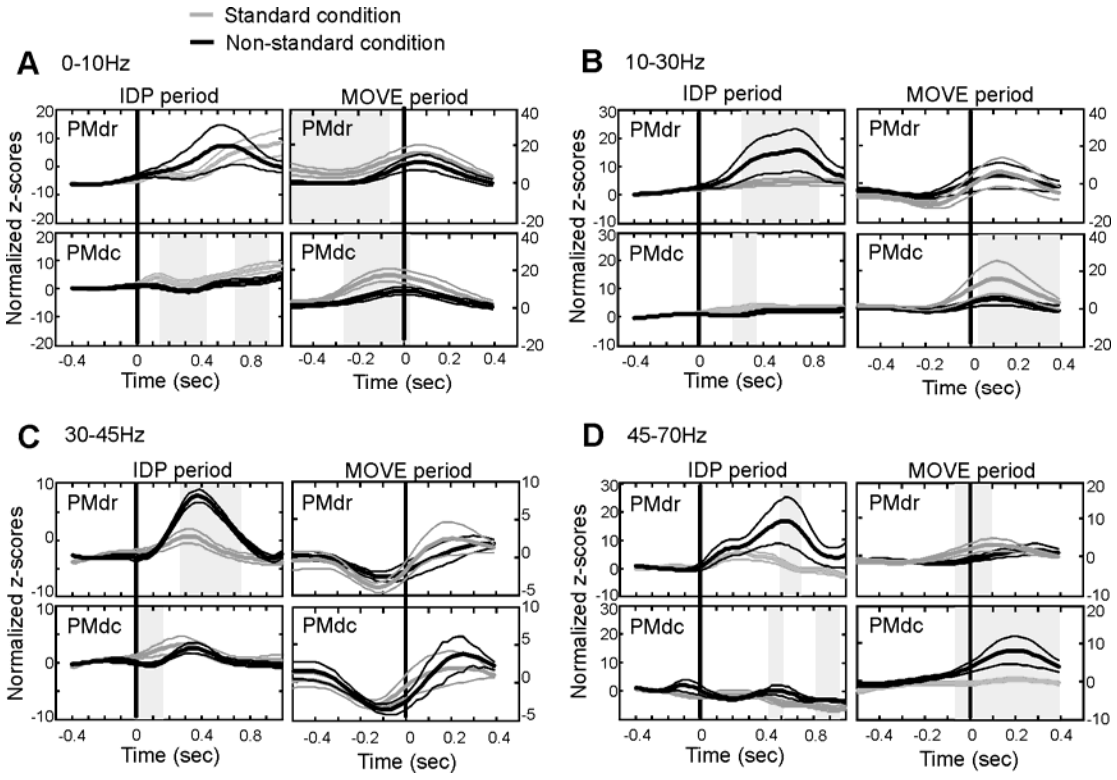

Figure 2.5. Time course of task related differences in power during the IDP (left panels) and MOVE (right panels) epochs, segregated by frequency band. Z-score values are broken up into 0-10Hz (A), 10-30Hz (B), 30-45Hz (C), 45-70Hz (D) frequency ranges. Black line represents peripheral cue onset (left panels) and movement onset (right panels)**.** Gray bars represent when the power was significantly different between condition, $P < 0.05$.

oscillatory activity during the non-standard when compared to the standard condition within this frequency range (Fig. 2.5A, right panels $P<0.05$). Following movement onset PMdc shows both a reduction of power within the 10-30 Hz range (Fig. 2.5B, right bottom panel $P<0.05$) and an enhancement of power within the 45-70 Hz range (Fig. 2.5D, right bottom panel $P<0.05$). These results demonstrate that just prior to movement, both PMdr and PMdc activity was modulated by decoupling the action of the eyes from the hand. By movement onset these conditional differences were less evident, with PMdc showing slight differences between reaching movements (Fig. 2.4E and F).

Spiking activity

The task-related differences observed within the LFP data are also supported by single cell findings (Fig. 2.6). In line with the observed increase in oscillatory activity, a significant increase in firing rate can also be observed within PMdr during the planning phase of a non-standard when compared to a standard reach (Fig. 2.6B, and 2.7A, $P<0.01$). Contrary to the observations in the oscillatory activity within PMdc, a significant increase in firing rate also occurs during decoupled reaching movements within this region (Fig. 2.7A, $P<0.01$). During the MOVE period, we decided to separate the analysis into an early (before movement) and late (after movement began) period to address whether the spike activity follows the same pattern observed for the LFPs during this MOVE period. In this analysis, we observed that task-related differences in spiking activity occurred only after movement onset in both regions (Fig. 2.7B, $P<0.01$). PMdc was most active during standard reaching movements and firing rates decreased during eye-hand decoupling (Fig. 2.7B, late epoch $P<0.01$). PMdr, however, showed enhanced spiking activity only following movement onset (late epoch) during non-standard reaches, while

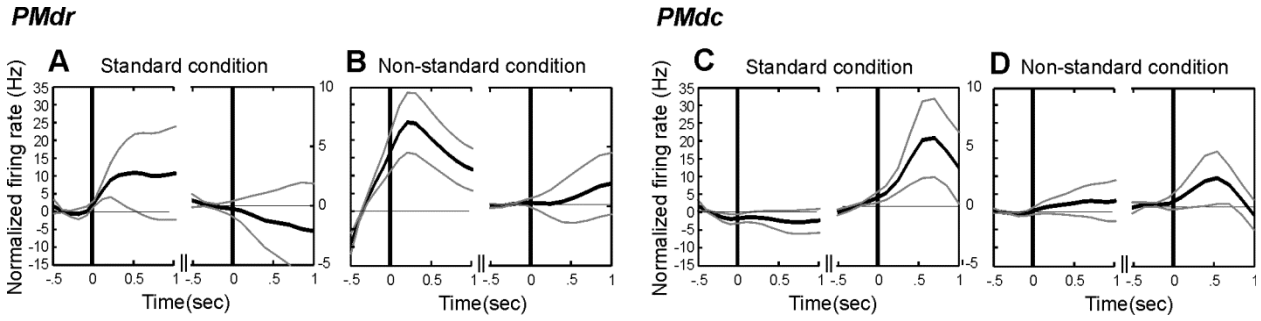

Figure 2.6. Mean discharge rates of single cells within PMd across the tasks. **A, B,** Mean normalized firing rates for PMdr during standard (A) and non-standard (B) condition. **C, D,** Mean normalized firing rates for PMdc during standard (C) and non-standard (D) conditions. Black lines represent peripheral cue onset during the IDP epoch (left panels) and movement onset during the MOVE epoch (left panels).

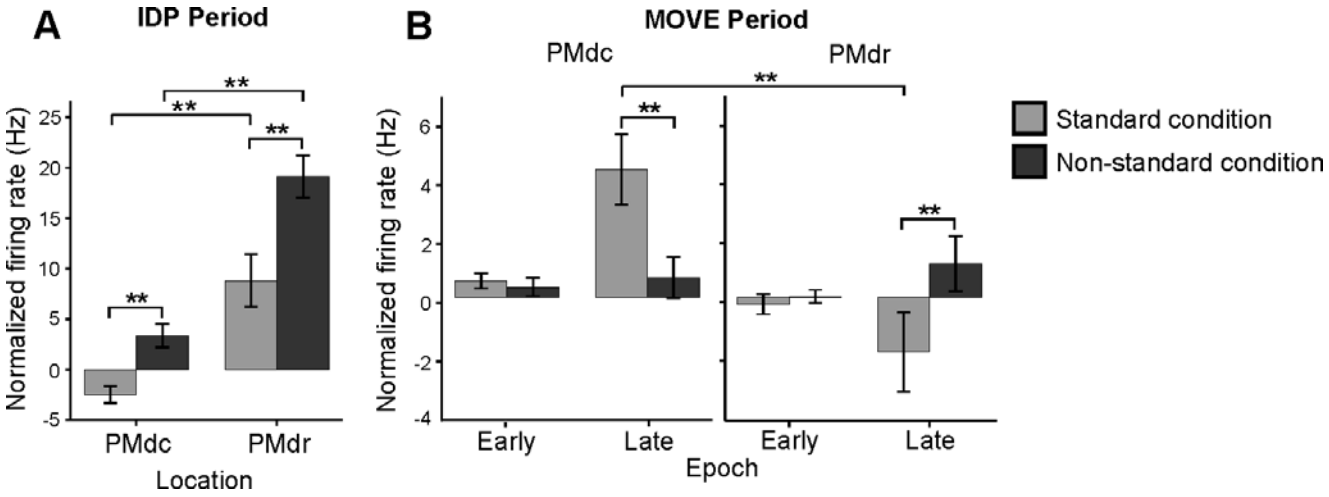

Figure 2.7. Histogram demonstrating significant difference in the normalized mean firing rates between conditions and locations. **A**, Normalized firing rates as a function of condition and location during the IDP epoch. **B,** Normalized firing rates during MOVE epoch broken up into early (before movement onset) and late (after movement onset) periods. Significant difference between either conditions or locations are represented by asterisks (* P <0.05, ** P <0.01).

standard reaches showed a significant reduction in mean firing rate (Fig. 2.7B, $P<0.01$). This suggests that by the late planning stage (early MOVE epoch), task-related differences that occurred during the early planning period become absent and movement-related differences are only observed following movement onset.

Topographical differences in eye-hand decoupling

Oscillatory activity

In support of our hypothesis, we also observed topographical differences between PMdr and PMdc in the modulation of oscillatory activity between conditions. The most striking finding was the significantly greater power in oscillatory activity during eye-hand decoupling within PMdr following peripheral cue onset (Fig. 2.4E, right panel). PMdc, on the other hand, demonstrated a reduction in power when decoupling the eyes from the hand (Fig. 2.4F, right panel). To more explicitly evaluate these topographical differences during the IDP and MOVE epochs of a given condition, we plotted the relative power differences between regions for each of 4 frequency bands (Fig. 2.8). Within the IDP epoch, a similar pattern of oscillatory activity can be seen between regions in the standard condition (Fig. 2.8A). Topographical differences were only observed in the 45-70 Hz range (Fig. 2.8A, left panel $P<0.05$). During the non-standard condition, however, clear differences in power can be observed across many frequencies ranges (10-70 Hz, Fig. 2.8A, right panel $P<0.05$).

By the late planning and movement stage, PMdr and PMdc once again demonstrate similarity in the pattern of oscillatory activity during both conditions (Fig. 2.5, right panel and Fig. 2.8B). In summary, during the early planning of a non-standard reach, PMdr shows enhanced oscillatory activity compared to PMdc. By the late planning and early movement phase, while the oscillatory activity within PMdr and PMdc are both modulated between

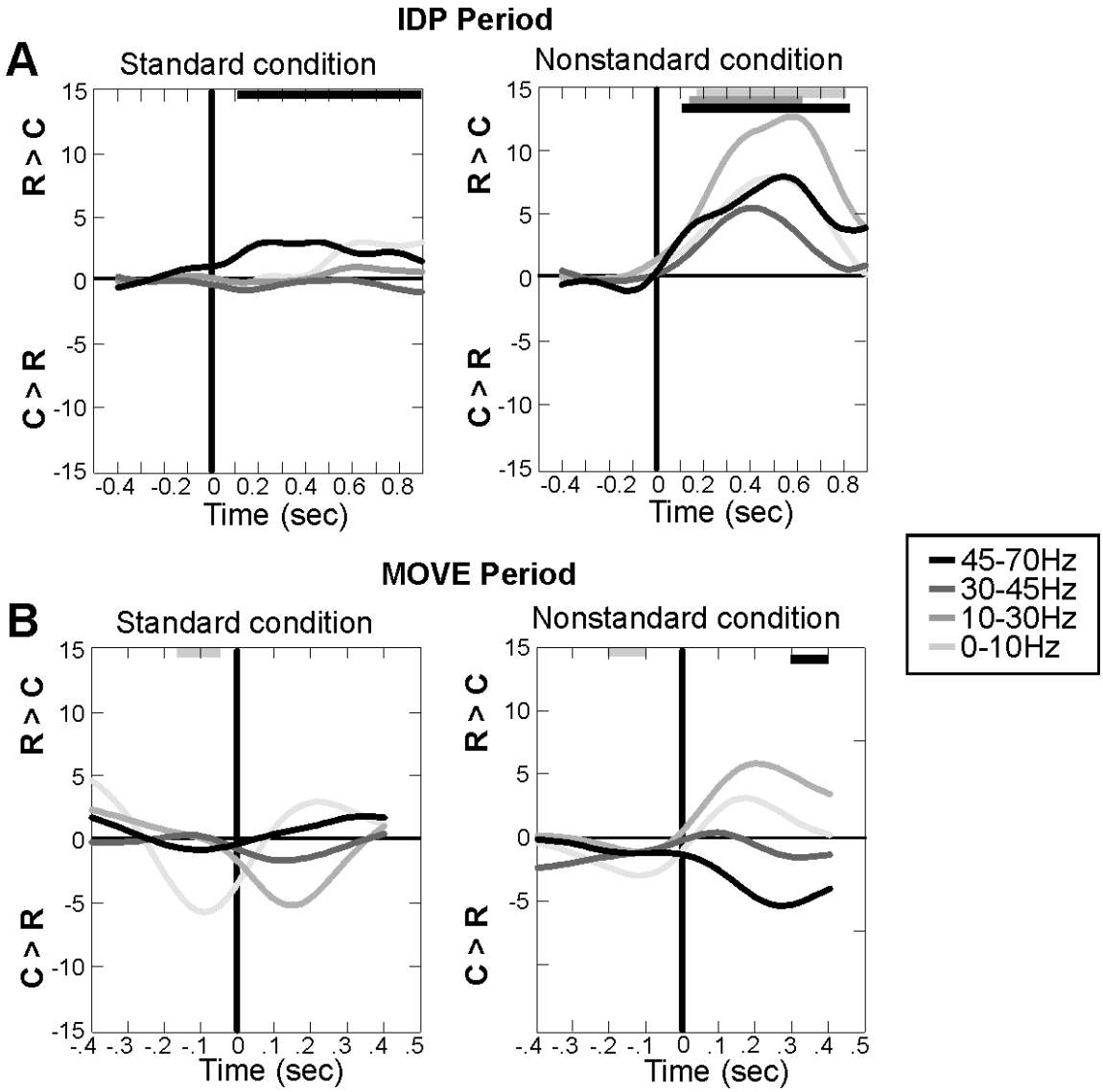

Figure 2.8. Topographical difference in oscillatory activity during the IDP (A) and MOVE (B) epochs. Positive z-score values reflect stronger oscillatory activity within PMdr whereas negative z-score values represent stronger activity within PMdc. Vertical black bars represent onset of peripheral cue **A**, and movement onset **B.** R > C; activity in rostral is stronger than in caudal PMd. C > R; activity in caudal is stronger than rostral PMd.

conditions, there were less obvious topographical differences in the way that this activity was modulated.

Spiking activity

In support of our LFP finding, we also observed distinct topographical differences during the IDP epoch, and subtle differences between PMdr and PMdc during the MOVE period (Fig. 2.7B). Specifically, during the IDP epoch PMdr showed a significantly greater mean discharge rate when compared to PMdc for both conditions (Fig. 2.7A, $P<0.01$). In line with the oscillatory activity results, the greatest mean discharge rate for PMdr was observed during the non-standard condition, when the eyes and hand were decoupled (Fig. 2.6B and 2.8A, $P<0.01$). Figure 2.8B illustrates that by late planning (early MOVE epoch), no significant topographical differences can be seen during either conditions ($P>0.05$). During this epoch we only observed topographical differences in the single unit activity after movement onset (late MOVE epoch) and restricted to the standard condition (Fig. 2.7B, $P<0.01$). Despite some minor differences from the LFP findings, the single unit activity supports the hypothesis that functional differences exist between PMdr and PMdc and how they contribute to the performance of visuomotor transformations.

Gaze effects

In an effort to determine whether the changes in oscillatory and single unit activity between conditions arose solely from the shift in gaze angle attributable to the different viewing planes, a gaze-only condition was analyzed (see methods). Since the visual display in the non-standard condition was presented on a vertical monitor and in the standard condition was presented on a horizontal monitor, the animal's overall gaze angle (but not head position) changed between conditions. During the gaze-only condition, the animal fixated nine points on the horizontal and vertical screens. These fixation points corresponded to the location of the

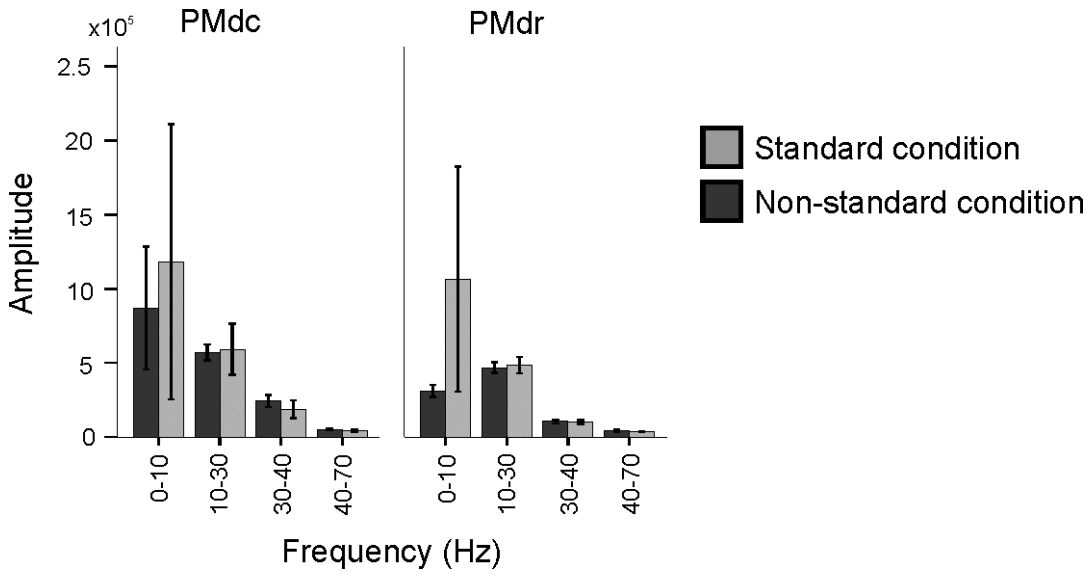

Figure 2.9: Gaze control bar graph. Mean amplitude and standard deviation during standard and non-standard conditions for PMdr (A) and PMdc (B). Bootstrapping methods revealed no significant difference in overall activity between conditions for each region ($P > 0.05$).

targets in the experimental conditions. The animal was instructed to fixate the points while maintaining it's hands on levers to the side of the monitor. Any significant difference observed between conditions was considered to be related to gaze effects.

Within both PMdr and PMdc, no effects of gaze were observed for the frequency bands we tested (0-70Hz, Fig. 2.9, $P > 0.05$). These data suggest that the changes we observed in oscillatory activity between standard and non-standard conditions were not attributable solely to changes in overall gaze angle between the experimental conditions.

DISCUSSION

We report two principal findings following an examination of oscillatory activity in dorsal premotor cortex during coupled versus decoupled visually-guided reaches. First, we observed task-related differences in PMd. Second, topographical differences were seen in the spectral profiles from PMdr and PMdc, during both planning and execution of standard and non-standard reach. Based on our results, we suggest that the rostral portion of dorsal premotor cortex plays a crucial role in breaking the tight linkage that exists for eye-hand coordination. While the caudal portion of the dorsal premotor cortex plays a role in monitoring and updating the ongoing decoupled movement. We provide physiological data supporting previous anatomical work, which suggest distinct roles for PMdr and PMdc in the control of visually-guided reaching movements.

Task related differences in PMd: oscillatory activity

In the present study, our non-standard task required a decoupling of the eyes and the hand to different spatial locations, while the hand movements between conditions were biomechanically equivalent. Thus, our non-standard condition required a learned association. Dorsal premotor cortex is integral to the planning of conditional sensorimotor tasks, and lesions

lead to impaired performance on these tasks (Wise et al. 1996; Halsband and Passingham 1985; Petrides 1985; Halsband and Passingham 1982; Petrides 1997; Petrides 1982; Chen and Wise 1995). Consistent with our hypothesis, we observed that non-standard reaches evoked region- and epoch-specific increases in oscillatory activity.

Similar to previous findings (Prado et al. 2005; Clavagnier et al. 2007; Gail et al. 2009), PMdr was more active during the early planning phase of decoupled versus coupled reaching movements both at the single cell level and within the 30-70 Hz gamma range. Oscillations within premotor regions are poorly understood. However, based on general principles of cortical microcircuits, power increases in the gamma range may be attributed to increased or surplus local synchrony (Pesaran et al. 2002; von Stein and Sarnthein 2000; Denker et al. 2011). When combined with known anatomical connectivity, we suggest that this increase in gamma power within PMdr could be related to the additional cognitive processes, such as spatial working memory and divided attention, putatively required for non-standard movements. These data also support behavioural evidence suggesting that an increase in neural processing is necessary during non-standard visuomotor transformations (Gorbet and Sergio 2009).

The ability to perform decoupled reaching movements likely requires communication between prefrontal and premotor regions (Hoshi and Tanji 2000; Abe and Hanakawa 2009; Hoshi 2006). The dorso-lateral prefrontal cortex (DLPFC) and PMdr are highly interconnected (Lu et al. 1994; Tachibana et al. 2004) and become functionally coupled when a motor plan either requires the integration of a diverse set of instructions (Hoshi and Tanji 2000; Abe and Hanakawa 2009; Hoshi 2006) or during cognitive manipulations (Abe and Hanakawa 2009). The increase in information received by PMdr to plan decoupled reaches would require enhanced local processing and integration and may thus be reflected in the increased gamma oscillatory

activity that occurs within PMdr during the non-standard condition. Similarly, if PMdc cells are important particularly when planning a 'decoupled' movements, one might expect the observed enhancement in gamma synchrony during the early planning phase of decoupled movements in PMdc, which is absent in our results during the early planning period. Gamma band oscillations are however observed within PMdc during the movement epoch of non-standard compared to standard reaches (Fig. 2.5D). Consistent with the commonly suggested function of gamma oscillations (Pesaran et al. 2002; von Stein and Sarnthein 2000; Denker et al. 2011), the enhanced local synchrony that is occurring during a decoupled reach may reflect the online monitoring of the ballistic motor plan. Executing a non-standard reach requires the actions of the eyes and the hand to remain decoupled and thus requires additional online reach monitoring and movement guidance using proprioceptive or somesthetic feedback. Area PEc located with the anterior portion of the superior parietal lobule houses somatosensory cells (Weinrich et al. 1984; Kalaska 1996; Breveglieri et al. 2006) and has a strong anatomical connection with area PMdc (Johnson et al. 1996). This is consistent with our oscillatory results demonstrating stronger oscillatory power within the 45-70 Hz gamma range in PMdc when compared to PMdr during decoupled reaches (Fig. 2.8B). Additionally, only modest increases in gamma oscillations were observed during standard reaching movements, where the reliance on proprioceptive inputs is not as crucial relative to decoupled eye-hand situations. Decoupled reaches also require a signal that inhibits the natural tendency to link the movements of the eyes and the hand. Recently, Gail and colleagues (2009) suggested that the enhanced spiking activity observed in PMd during a non-standard reaching movement reflects such an inhibiting signal to overrule the "default" visuomotor network for standard reaches (Gail et al. 2009; Everling et al. 1999; Schlag-Rey et al. 1997). This is in line with our spiking data, which also demonstrates an increase in the discharge

rate of single cells during the planning phase of non-standard reaching movements. In order for PMdr to provide an inhibitory output signal, it must first be able to receive information about the spatial disparity between gaze and limb position. The enhanced oscillatory activity observed within PMdr during non-standard reach planning may serve this purpose, which may then drive the increase in output signals (single units) that would be needed to inhibit the 'default' visuomotor network, as suggested by others (Gorbet et al. 2004; Gail et al. 2009). Such an arrangement would make PMdr a crucial node in the sensorimotor transformation of non-standard limb movements, though this interpretation raises further questions. In contrast, PMdc demonstrates a decrease in oscillatory activity during non-standard relative to standard reach planning. This reduction in power may represent inhibitory inputs to PMdc, which would be important for allowing the eyes and hand to decouple. Recently, we have found that the mean discharge in single cells recorded from superior parietal areas during the same experiment presented here, is significantly reduced during non-standard task planning (Hawkins et al. 2012). The decoupling of goal/gaze spatial location and sensed limb location may underlie the reduction in activity in these bimodal cells. The subsequent transmission of these signals to premotor planning areas, observable in the input-driven LFP signal, may thus represent the crucial transformation of information that would be needed to decouple the actions of the limb and gaze to successfully perform the task used in these studies.

If the role of PMd is to instruct or inhibit other regions during non-standard conditions, and across-region or more 'global' synchronization is associated with lower frequency oscillations, then one might expect an increase in beta and lower frequencies for the non-standard task. Sub-gamma frequencies including beta are observed when a region is integrating independent distant signals or for 'top down' processing as opposed to engaging in local

processing (Donner and Siegel 2011; Siegel et al. 2012). Consistent with this, our results demonstrate that within PMdr there is an increase in low frequency power during the early planning period of a non-standard compared to standard movement (Fig. 2.5B). Based on the aforementioned idea, the increase in low frequency power seen in the early planning period of a non-standard reach may reflect the integration of the cognitive rule into the motor action allowing for a new relative position code of the eyes and hand.

Contrary to these observations, PMdc showed a reduction in low frequency power during the planning and movement periods in the non-standard condition (notice both epochs, Fig. 2.5A and B). Under natural reaching situations, the brain must integrate hand and eye signals to arrive at the proper behaviour, as in the standard version of the task. Perhaps within PMdc, performance during the non-standard condition requires that these signals continue to be segregated, not integrated, just as the planes of movement of the hand and eyes are separated in space. Thus, while PMdr normally functions to integrate the signals from various regions of the brain for successful eye-hand decoupling, the suppression of beta or lower frequencies would be expected during non-standard reaching within PMdc if this is an area of importance for eye-hand coupling. Cautious interpretation is warranted, however, since the oscillatory functions within PMd are largely unknown, and the present results suggest a complex repertoire of oscillations that reveal temporal and spectral differences even within PMd.

Functional and anatomical separation within PMd

Most PMd single-unit studies have not separated PMd into its rostral-caudal sub-divisions. A re-examination of the literature has revealed that the majority of cells that respond to conditional visuomotor associations appear to be located within PMdr, while cells within PMdc demonstrate mostly movement related activity (Picard and Strick 2001; Grafton et al. 1998). The

authors of these reviews suggest the term "Pre-PMd" for PMdr, reflecting the cognitive conditional visuomotor associations that have been commonly observed there. The functional separation in the activity of PMd cell assemblies in the current study support this proposed distinction: PMdr was more active during decoupled reaching movements, when the movement relied on a transformational rule to be incorporated into the reaching movement. By the late planning/early movement phase of both standard and non-standard movements, PMdc had stronger oscillatory and single unit activity. During this period concerned with movement execution rather than planning, the salient features would be the biomechanical details of the movement, which did not vary with task in the present study (Picard and Strick 2001; Boussaoud 2001; Scott and Kalaska 1997; Toni et al. 2001; Scott et al. 1997). Left open is the question of how information within PMdr affects the final movement programming in PMdc, SMA, M1 or spinal cord structures, given the evidence that there are few if any direct connections between PMdr and these other areas (Barbas and Pandya 1987; Kurata 1991; Luppino and Rizzolatti 2000). It has been suggested that PMdr, a rostral motor region, plays a large role in relaying prefrontal signals to pre-SMA and CMAr to eventually reach the more caudal motor regions like SMA, PMdc and finally M1 (Lu et al. 1994; Takada et al. 2004; Morecraft et al. 2004). These connections are important because they may provide a pathway for information flow from DLPFC and PMdr, and thus allow signals important for decoupled reaching to reach the final motor plan. Another avenue for PMdr activity to influence the motor plan may be via the cortico-striatal connections between PMdr and the basal ganglia (BG) (Tachibana et al. 2004). Considering that PMdr is thought to play a role in inhibiting the natural tendency to couple the eyes and hand during decoupled reaching movements (Gorbet et al. 2004; Gail et al. 2009), its connection with BG structures may help mediate the inhibitory signal that would be necessary to

accomplish this type of reaching movement. Recently, SMA has been shown to play a key role in proactive control, the ability to stop a movement based on endogenous signals (Chen et al. 2010; Jaffard et al. 2008). Proactive control is key to our ability to inhibit our natural tendency to couple the eyes and the hand. Thus this region may also play a key role in our ability to decouple the eyes and hand. Finally, based on the strong reciprocal connections that the premotor and parietal cortices share (Picard and Strick 2001; Matelli et al. 1998; Lu et al. 1994; Luppino and Rizzolatti 2000; Geyer et al. 2000; Pandya and Yeterian 1984), information from PMdr may provide the parietal lobe with signals necessary to incorporate a rule into the ongoing movement.

In conclusion, the task-related oscillatory activity in dorsal premotor cortex observed in the present study supports necessary but separate roles for rostral and caudal sub-regions in the control of non-standard reaching, a behavior performed in everyday life. PMdr activity appears to be more involved in integrating the rule-based aspects of a visually-guided reach, while PMdc is more involved in the online updating of the decoupled eye and hand movements. We propose that dorsal premotor cortex, particularly the rostral portion, plays a crucial role in breaking the tight linkage that exists for eye-hand coupling. We also provide physiological data that suggest distinct roles for PMdr and PMdc in the control of visually-guided reaching movements. On a practical level, these results indicate that caution should be taken when comparing data obtained from studies using direct object manipulation to studies using non-standard, decoupled target/object interaction.

Acknowledgements

We would like to thank Taiwo McGregor, Tyrone Lew, Dr. Bogdan Neagu and and Dr. Hongying Wang for their exceptional technical and surgical assistance, as well as Natasha

Down, Veronica Scavo, and Julie Panakos for their invaluable animal care expertise. This work was supported by Canadian Institutes of Health Research grant MOP-74634 (LS), the Canadian Foundation for Innovation and the Ontario Innovation Trust (LS), and the Ontario Ministry of Training, Colleges, and Universities (OGSST to PS).

Chapter Three

Decoupling the actions of the eyes from the hand alters beta and gamma synchrony within SPL

Patricia F. Sayegh, Kara M. Hawkins, Bogdan Neagu, J. Douglas Crawford, Kari L. Hoffman, and Lauren E. Sergio

Reprinted with permission from Journal of Neurophysiology: Patricia F. Sayegh, Kara M. Hawkins, Bogdan Neagu, J. Douglas Crawford, Kari L. Hoffman, Lauren E. Sergio (2014) Decoupling the actions of the eyes from the hand alters beta and gamma synchrony within SPL. Journal of Neurophysiology , JN-00793-2013R2.

ABSTRACT

Eye-hand coordination is crucial for our ability to interact with the world around us. However, much of the visually guided reaches that we perform require a spatial decoupling between gaze direction and hand orientation. These complex decoupled reaching movements are in contrast to more standard coupled eye and hand reaching movements in which the eyes and the hand are coupled. The superior parietal lobule receives converging eye and hand signals, however what is yet to be understood is how the activity within this region is modulated during decoupled eye and hand reaches. To address this, we recorded local field potentials (LFPs) within SPL from two rhesus macaques during coupled versus decoupled eye and hand movements. Overall we observed a distinct separation in synchrony within the lower 10-20 Hz beta range from that in the higher 30-40 Hz gamma range. Specifically, within the early planning phase beta synchrony dominated, however the onset of this sustained beta oscillation occurred later during eye-hand decoupled versus coupled reaches. As the task progressed there was a switch to low frequency and gamma-dominated responses, specifically for decoupled reaches. More importantly, we observed LFP activity to be a stronger task (coupled vs. decoupled) and state (planning vs. execution) predictor than that of single units alone. Our results provide further insight into the computations of SPL for visuomotor transformations, and highlight the necessity of accounting for the decoupled eye-hand nature of a motor task when interpreting movement control research data.

INTRODUCTION

Eye-hand coordination is an important aspect of our ability to perform different types of visually guided reaches, allowing us to interact with objects in a variety of ways. We can reach for objects we are not looking at, manipulate a tool like a joy-stick, and even perform

laparoscopic surgery. These types of complex eye-hand coordination tasks usually require the location of the eyes and the hand to remain decoupled throughout the movement, a type of action referred to as a decoupled, or eye-hand decoupled, reach (Wise et al. 1996). Decoupled reaches require an implicit spatial algorithm and/or an explicit cognitive rule to be incorporated into the motor plan in order to relate the visual stimulus to the direction of the end effector movement (Wise et al. 1996; Murray et al. 2000; Sergio et al. 2009). This differs from the more basic forms of visually guided reaches in which the visual object guiding the movement is the spatial target of the action itself, referred to as a standard, or eye-hand coupled, reach (Wise et al. 1996). Decoupled reaching requires inhibition of the natural tendency to link the actions of the eyes and the hand (Gielen et al. 1984; Prablanc et al. 1979; Henriques et al. 1998; Neggers and Bekkering 2000; Gauthier and Mussa Ivaldi 1988; Morasso 1981; Sergio and Scott 1998; Vercher et al. 1994; Gorbet and Sergio 2009; Terao et al. 2002), as well as additional processing to calculate the new spatial mapping between the eyes and the hand (Sergio et al. 2009; Gorbet et al. 2004; Granek and Sergio 2012)**.**

Although previous human and animal studies have found that performing decoupled reaches alters the activity of regions located within the parietofrontal reach network (Battaglia-Mayer et al. 2001; Prado et al. 2005; Granek et al. 2010; Gorbet et al. 2004; Sayegh et al. 2013; Gail et al. 2009; Gail et al. 2009; Hawkins et al. 2013; Andersen et al. 1987; Andersen et al. 1997; Grafton et al. 1996; Connolly et al. 2000; Hawkins et al. 2012), many of these studies focused only on foveated versus extra-foveated reaching (Battaglia-Mayer et al. 2001; Prado et al. 2005; Clavagnier et al. 2007; Gail et al. 2009; Andersen et al. 1997). Thus, the specific contribution of parietofrontal regions, known to integrate eye and hand information, to the control of decoupled but foveated movements is largely unknown.

Situated between sensory and motor cortices, SPL integrates eye and hand signals in order to successfully calculate the reach vector under sensory guidance (Graziano et al. 2000; Vesia and Crawford 2012; Rushworth et al. 1997a; Battaglia-Mayer and Caminiti 2002; Vesia et al. 2010; Grefkes et al. 2004; Andersen et al. 1987). Recently, we have found that during an identical decoupled reach task, single units within SPL demonstrate a reduction in the mean discharge rate during decoupled reach planning and execution (Hawkins et al. 2013). In order to fully characterise the contribution of a region to a particular behaviour, analyzing both the single units and oscillatory activity will provide a richer repertoire of information than one technique alone. While spiking activity is known to reflect supra-threshold inputs or outputs from pyramidal cells, LFPs reflects sub-threshold inputs within local cell assemblies (Scherberger et al. 2005). In addition, LFP activity is thought to be a better predictor of certain behavioural states compared to the activity of single units alone (Mitzdorf 1985; Scherberger et al. 2005; Pesaran et al. 2002; Engel and Fries 2010). Thus it is reasonable to suggest that spike and LFP activity each carry a different set of information and can therefore be complementary tools for brain analysis (Pesaran et al. 2002; Sanes and Donoghue 1993). Finally, because LFP activity has been shown to have a stronger relationship with blood-oxygen-level dependent (BOLD) function magnetic resonance imaging (fMRI) (Goense and Logothetis 2008; Nir et al. 2007) than single unit activity (Fries et al. 2001), the results obtained from LFP studies can help bridge the gap between neurophysiological data in animals and human fMRI recordings. The results of the current study will thus enrich the findings from our previous report on the single unit activity within SPL, and improve our understanding about the computations of SPL in eye-hand decoupled reaches.

Given the crucial role of the SPL in the integration of vision and proprioception for limb guidance, we hypothesize that a spatial decoupling between the actions of the eyes and the hand

will affect the neural activity within SPL during reach planning and execution. Decoupling the eyes from the hand will provide incongruent eye and hand signals. Thus a greater reliance on proprioceptive input will be required during decoupled reaches when the visual information about the reach target is inaccurate (Buneo and Andersen 2006; Rushworth et al. 1997a; Engel et al. 2002; Flanders et al. 1992; Rushworth et al. 1997b; Nixon et al. 1992). We predict that these incongruent eye and hand signals will modulate the LFPs within SPL in a way that differs from that which occurs during direct object interaction. An exploratory aspect of the current study was to examine *how* LFP activity in the different frequency bands varies in both the planning and execution phases of a decoupled relative to coupled reach. A second aim of this study was to test the hypothesis that LFP activity within SPL will vary *between* the planning and execution phases of the movement, when movement control switches from a planning, feedforward, and movement inhibition phase, to an execution, proprioceptive feedback and efference copy phase. We discuss our findings in the context of other research characterising the alteration of activity in the parietofrontal movement control network during the control of complex, rule-based behaviours.

METHODS

Animals and Apparatus

Two rhesus monkeys (Female *Macaca mulatta*, both 5.2 kg) were trained to perform a visually instructed delayed reaching task under coupled and decoupled eye-hand conditions as described previously (Sayegh et al. 2013; Hawkins et al. 2013). All surgical and animal handling procedures were in accordance with *Canadian Council on Animal Care* guidelines on the use of laboratory animals, and pre-approved by the *York University Animal Care Committee*.

During the experiment, the monkey was seated in a custom-built primate chair 40 cm in

front of a 38.1 cm vertical screen, which was set at monkey eye level and centered with her midline. An additional 38.1 cm horizontal touch sensitive screen (Touch Controls Inc, San Diego CA) was set in front of the animal, between the animal's waist and xyphoid process, so that she could reach over the entire surface of the screen comfortably (Fig. 3.1). The horizontal touch screen was designed to detect spatial displacements as small as 3 mm using infrared beams, at a sampling rate of 100 Hz. Continuous tracking of the eye was monitored using the ISCAN-ETL 200 Eye Tracking System (ISCAN Inc, Burlington MA) at a sampling rate of 60 Hz. To minimize any interference from the non-reaching limb, the animal was trained to maintain its non-reaching hand on a metal lever just beyond the lower corner of the horizontal touch screen throughout the experiment. Only when the metal lever was depressed would the tasks begin and continue. In this way it was ensured that the animal only used the appropriate arm without having to forcefully restrain the unused limb.

Behavioural Task

The schematic describing the sequence of each trial is shown in Figure 3.1 and is as follows: a red circular target (70 mm in diameter) appeared at the center of the screen with an additional smaller white circular target (40 mm in diameter; 5.7° of visual angle) on top of it. The monkey was instructed to touch the red target and maintain eye fixation on the white target. After a baseline period of 500 ms, one of eight green-coloured peripheral targets appeared (70 mm in diameter). All eight targets were equally spaced (45°) and appeared randomly, based on a randomized-block design. The peripheral target appeared 5 times at each location for a total of 40 trials per condition. After a variable instructed delay period (IDP, 2000 ms +/- 500 ms, Gaussian distribution) the red central target extinguished and the white target jumped to the peripheral target. This served as the go signal (GO) instructing the animal to move the eyes and

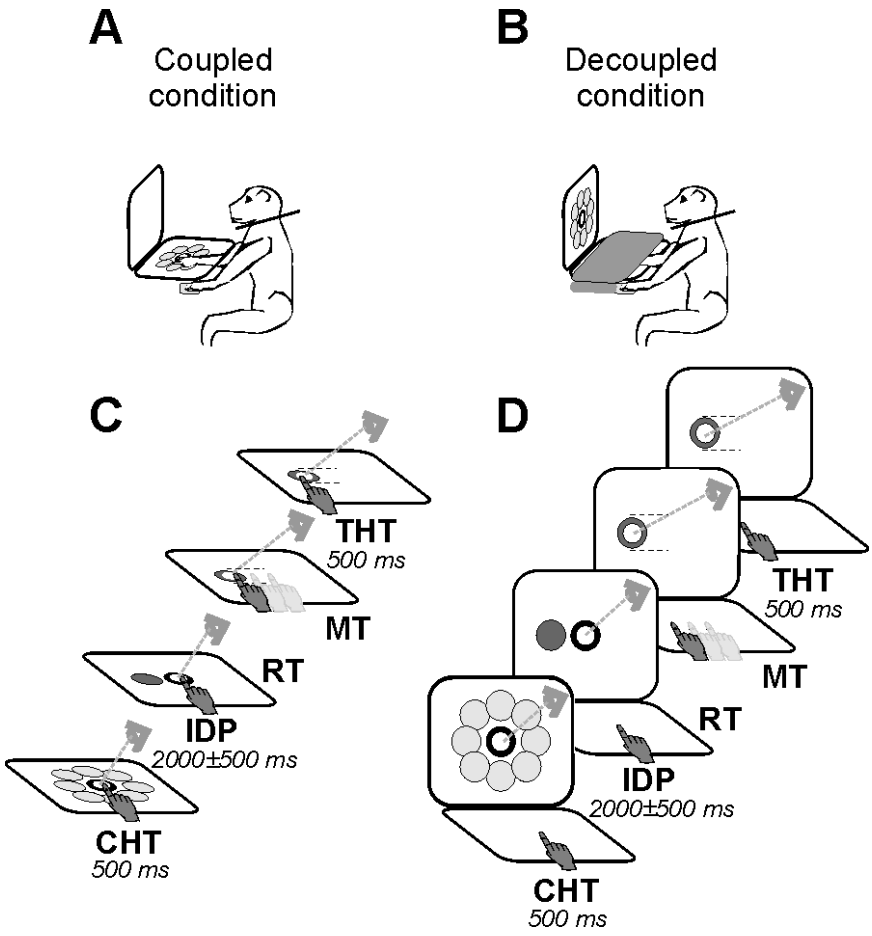

Figure 3.1. Experimental setup and trial timing. **A, C,** Schematic of the standard condition. **B, D,** Schematic of the decoupled conditions. Arm movements were always made over the horizontal touch screen. During each trial, one of eight equally spaced (45°, light grey circles) peripheral targets were presented on either a touch-sensitive screen placed over the animal's lap (**A**) or on a monitor positioned vertically 40 cm away from the animal's frontal plane (**B**). Epochs - CHT: centre hold time, IDP: instructed delay period, RT: reaction time, MT: movement time, THT: target hold time. The baseline epoch came from within the centre hold time epoch.The animal's head was fixed throughout the experiment.

hand from the central target to the peripheral target (Fig. 3.1). Once the eyes and hand arrived at the peripheral target, the monkey was required to hold both the eyes and the hand there for 500 ms. The movements were made from the middle of the center target to the middle of the peripheral target (roughly 80mm, Fig. 3.2Cand D). Visual presentation of the task was identical across conditions. In the *coupled* condition, the actions of the eyes and hand remained congruent. The visual presentation of the targets and the reaching movements were both made on the horizontal touch-sensitive screen placed in front of the animal (Fig. 3.1A). In the *decoupled* condition, the actions of the eyes and hand were incongruent. The visual presentation of the targets was on the vertical screen while the animal's limb movements remained on the horizontal touch screen (Fig. 3.1B). Thus, the animal was required to direct its gaze along the vertical monitor but move its hand along the horizontal touch screen in order to displace the cursor from the central to the peripheral target. To ensure that the animal did not track its hand position extra-foveally, an opaque screen was placed 100 mm over the animal's arm to block vision of the limb. For each condition, two epochs during the trial were considered. The delay epoch (IDP) comprised of the 500 ms baseline period and the first 2000 ms of the instructed delay period. While this epoch length means that a small percentage of trials will include early reaction time, we found in preliminary analyses that the results were stable using a longer epoch. The movement epoch (MOVE) is aligned to the onset of the reach and is comprised of the last 500 ms of the instruction delay period and 500 ms after movement onset. The animals were trained to perform similar movements during both conditions and the biomechanical features of the reach movements were monitored to insure that the movement profiles were similar between conditions. To reinforce similar hand paths between conditions, movement alleys were included to ensure that reaches were directed along a fairly straight trajectory (Fig.3.1). These alleys were

set at ± 40 mm from a straight line spanning from the central to the peripheral targets. If the cursor moved outside of these alleys the trial would stop. To provide feedback on the current position of the hand, a cross-hair representing the position of the hand on the touch screen was displayed. Muscle activity was also recorded from 13 proximal-arm muscles in separate recording sessions. Pairs of Teflon-insulated 50 μm single-stranded stainless steel wires were implanted percutaneously. Implantations were verified by passing current through the wires to evoke focal muscular contractions (< 1.0 mA, 30 Hz, 300 ms train; (Sergio and Kalaska 2003). Multi-unit electromyography (EMG) activity was amplified, band-pass filtered (100-3000 Hz), half-wave rectified, integrated (5 ms time bins) and digitized on-line at 200 Hz. The muscles studied included the anterior deltoid, medial deltoid, posterior deltoid, dorsoepitrochlearis, infraspinatus, latissimus dorsi, pectoralis, supraspinatus, teres major, rostral trapezius, caudal trapezius, triceps lateralis, and triceps medialis. These recordings were performed to assess the general effects of the coupled and decoupled tasks on EMG activity and were not designed as a definitive biomechanical study of the muscle properties.

A *gaze-only* control task, which has been described previously in detail (Sayegh et al. 2013; Hawkins et al. 2013), was also included in order to determine if the neural activity was affected solely by the overall shift in gaze angle. This condition was performed for every recording. The visual display consisted of 9 white circles (40 mm in diameter; 5.7° of visual angle) that appeared one at a time in the same locations (i.e. one central and 8 peripheral) as the white targets that appeared during the experimental conditions. The monkey was instructed to fixate on each of these white circles while maintaining both hands beside the horizontal touch screen. The white circles appeared in each location 3 times for a total of 27 fixation points for each plane.

Behavioural analyses

To confirm that the movements were biomechanically similar between conditions, hand paths were recorded and analyzed. The individual movement paths were first low-pass filtered at 10 Hz and the movement onsets and endpoints were scored as 8% peak velocity. The movements were then divided into 21 equal segments. The five trials for each direction were pooled and the mean standard deviations were calculated at each segment along the path for both the coupled and decoupled tasks. An equality of variance test was performed between the two conditions on the mean X and Y components of the trajectory for each target (Snedecor and Cochrane 1989). Mean reaction times (from the GO-signal movement onset) and mean reach velocity (from movement onset to the end of the movement) were also calculated for each condition and paired-samples t-tests were performed to compare reaction times and velocity between the coupled and decoupled conditions. Repeated measures ANOVAs were performed on the EMG data during the IDP and MOVE epochs for each muscle recorded in order to determine the effect of target (reach direction) and condition (coupled vs. decoupled) on maximum EMG amplitude. It was expected that reach direction would have an effect on EMG amplitude, but task condition would not.

Neural Recordings

Monkeys were implanted with a recording cylinder under standard aseptic surgical techniques (Kalaska et al. 1989). The stereotaxic coordinates for chamber placement over SPL (Monkey A, Interaural; A: -12.30 mm, L: 18.40 mm and Monkey B, Interaural; A: -7.80 mm, L: 00.00 mm, Fig. 3.2A and B) were determined using *The Rhesus Monkey Brain in Stereotaxic Coordinates* (Paxinos et al. 2000). Space limitations for Monkey A, due to a previously implanted premotor chamber and a posterior head-post, required the chamber to be positioned on

a 25° angle in order to allow access to the desired brain regions through deep electrode penetrations in the medial-anterior quadrant of the chamber (Fig. 3.2A and C). Thus, while the surface entry points are more rostral, the angle and depth of the electrodes provided access to neurons from within the medial intraparietal sulcus. A hydraulic multi-channel driver (MCM-4, FHC inc., Bowdoin ME) mounted to the implanted chamber was used in conjunction with a multi-channel processing system (MCP, Alpha-Omega Engineering, Israel). The multidriver provided simultaneous recording from up to two electrodes at a time and allowed us to examine the local field potential (LFP) collected at each electrode site. Neural activity from each electrode was pre-amplified (5000x) band-pass filtered (1 Hz-10 kHz) and split into lower (LFP) and higher (single units) frequencies. Higher frequency signals were sampled at 12.5 kHz and spikes of single units were sorted using template matching (Hawkins et al. 2013). The LFP (below 100 Hz) was sampled at 390.6 Hz. Following the completion of all experiments, anatomical brain images of both animals were obtained using a 3T Siemens Tim Trio MRI scanner to verify chamber location (T1-anatomical, FOV: 131 x 122.8 mm, TR: 2300 ms, TE: 3.54 ms, Flip Angle: 9 degrees).

Data analyses

Local field potentials

All successfully recorded LFP sites were used for all of the analyses reported in this k paper. Open source Chronux script files were used in MATLAB (The Mathworks, Inc., Natic MA) to analyze the spectral data and to generate time-frequency spectrograms for all penetrations in both conditions (Pesaran et al. 2002; Jarvis and Mitra 2001). To estimate the frequency structure of the LFP activity, we used the multitaper spectrum analysis (previously described in (Pesaran et al. 2002; Jarvis and Mitra 2001)). The multitaper estimates of the

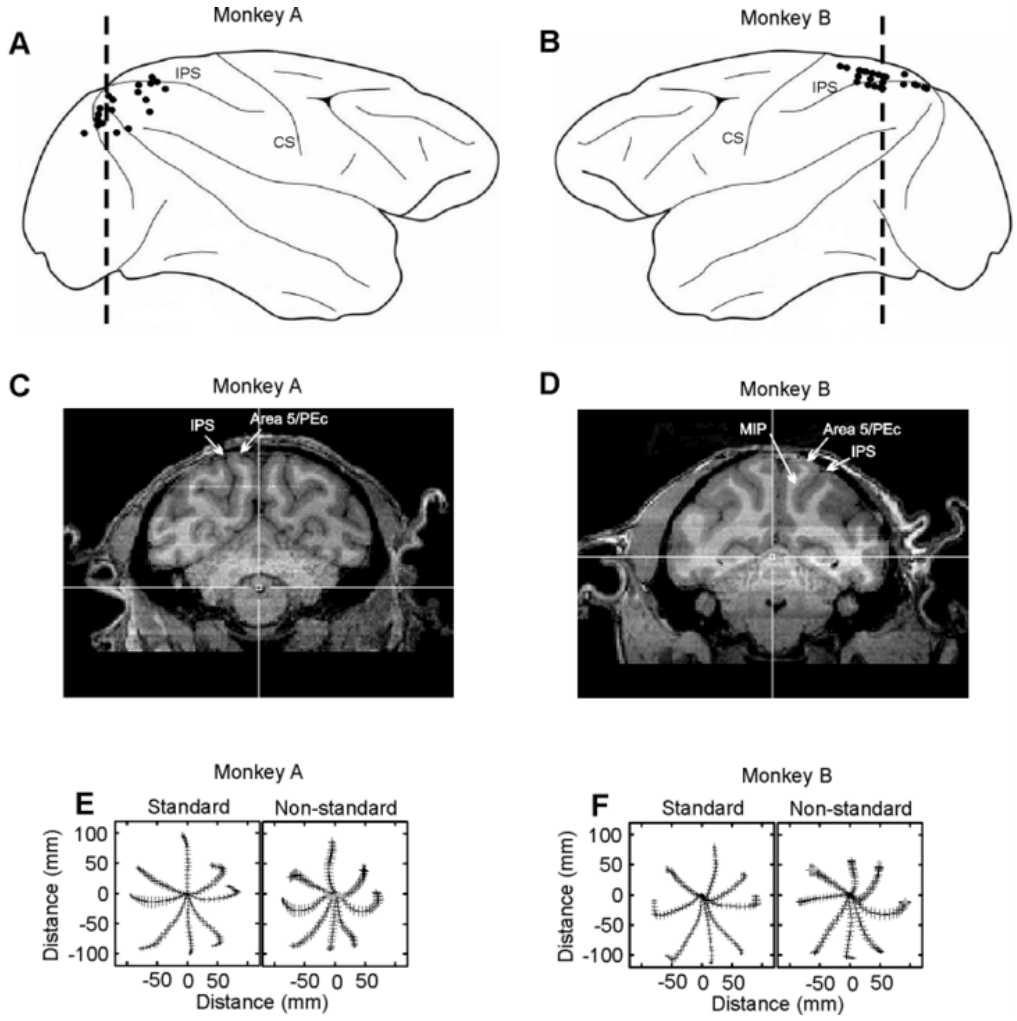

Figure 3.2. Penetration sites for *monkey A* (*A*) and *monkey B* (*B*). Larger dots indicate where recordings were obtained on two occasions. CS, central sulcus; IPS, intraparietal sulcus. Arrows show anterior, posterior, medial, and lateral directions; dotted line denotes division between penetration sites classified as rostral (left of line) or caudal (right of line). *C* and *D*: MRI images representing chamber location for *monkey A* (*C*) and *monkey B* (*D*). The level of the slice is represented by the dashed line in *A* and *B*. PEc, superior parietal lobule area (caudal portion); MIP, medial intraparietal area (posterior parietal cortex). *E* and *F*: represent the mean reach trajectories for *monkey A* (*E*) and *monkey B* (*F*). Black lines represent the mean movement trajectories; black tick marks represent the standard deviations. Gray asterisks denote trajectory segments that were significantly ($P < 0.05$) more variable compared with the standard condition.

spectrum Sx(f) were calculated for each recording (Scherberger et al. 2005; Pesaran et al. 2002). Normalizing to a baseline period was necessary to directly compare between conditions, therefore the spectrum for each site was z-transformed to its own baseline period centered on the final 350-500 ms of the baseline window, which reflected the most stable time window prior to directional cue onset (averaged across trials) (See fig. 3.3D). Spectrograms were then calculated using a 500 ms window shifted in 20 ms increments with a 6 Hz frequency resolution. Currently there is some discrepancy regarding the relationship of high frequency gamma activity with spiking activity. While some research suggest that a strong relationship exists (Ray and Maunsell 2011; Zanos et al. 2012; Zanos et al. 2011), others suggest a difference between spiking and high gamma activity (Pesaran et al. 2002; Flint et al. 2012). To remain consistent with our previous work we decided to only include data from below 60 Hz (Sayegh et al. 2013).

To determine significant task related differences (at a $P < 0.05$ alpha level), the normalized spectra from each trial for each electrode site was calculated. The average spectral value across each time-frequency bin was determined for each condition. A bootstrapping permutation test (Sayegh et al. 2013; Hawkins et al. 2013; Sergio and Kalaska 2003) was used to assess whether the difference in power between the two conditions was significant. According to the null hypothesis, power would be the same irrespective of condition (coupled/decoupled), as such the observed difference in mean power would not exceed the 95% confidence limits of a distribution of differences in LFP power. The difference distribution is obtained by shuffling (permuting) the condition assignment of each trial, taking the power difference, then repeating this 1000 times. To depict the regularity of significant differences for each time and frequency bin across the population of SPL sites, we generated a color plot mapping the proportion of sites showing significant differences at a given point in time and a given frequency. A Receiver-

operating characteristic (ROC) analysis was performed on the spectrum to measure the discriminability of two alternatives by an ideal observer. Here, we calculated the probability of an ideal observer correctly predicting the behavioural epoch (IDP versus MOVE) and of correctly predicting the task (coupled versus decoupled). ROC values were determined across the population of sites (N=44) using the normalized power values at each time and frequency band used to generate the average spectra. To determine the ROC values for predicting the state of the animal (planning versus execution) we pooled the ROC values from each condition for each epoch separately.

Lastly, we analysed the oscillatory activity in the gaze-only condition to determine if the overall shift in gaze angle that occurred from viewing the stimuli in two different planes had an effect on the oscillatory activity within SPL. The mean power (0-70 Hz) at each gaze location was calculated from a 500 ms window while the animal was fixating at each target. Within each condition, the mean power across the nine target locations was computed. The permutation procedure described above was used to assess whether the difference in power between the two gaze planes could have occurred by chance.

Single Units

A single unit analysis was previously described elsewhere (Hawkins et al. 2013), however a subset of the data was selected for a distinct analysis in this study. See (Hawkins et al. 2013) for details on single unit isolation and task-selective analysis. Cells that were directionally tuned to the epoch of interest were selected and mean firing rates were normalized to individual baseline firing rates. Baseline firing rates were calculated as the mean firing rate during the first 300 ms of each trial when the animal was instructed to hold their hand at the central target. This generated a normalized firing rate for comparison with the LFP data, which were also

normalized to the same baseline time period. Significant task related differences were determined by performing paired-samples t-test between the spike rates during each condition. As was done for the LFP data, single units were tested in the gaze-only condition to assess the effect of the viewing plane on spike activity. Lastly, an ROC analysis was performed on the firing rates of all task-related single units. Area under the curve (AUC) values were determined across the population of cells (N=26, IDP epoch; N=17, MOVE epoch) using a sliding window analysis with the same timing as that used for the LFPs. We compared the firing rates of each cell during the coupled versus decoupled conditions to generate ROC values for task probability. To determine the ROC values for predicting the behavioral state (planning versus execution) we pooled the firing rate for each condition and compared across epochs.

RESULTS

Behavioral Results

To ensure that task related differences in the neural data were not a result of differences in the movement of the hand we compared the hand trajectories between the two conditions. Our comparisons confirm that the kinematic and electromyographic features of the limb movement between task conditions were not significantly different. Therefore we can interpret the task-related differences in the neural data as being due to rule-processing rather than motor behaviour. The use of alleys helped support the animal in maintaining similar hand trajectories during both conditions (see methods). Figure 3.2C and D shows the mean reach trajectories during both conditions for each animal. Except for a few segments, there were no significant differences in the extent or variability of the reach trajectories between coupled and decoupled conditions ($P>0.05$). To analyze reach kinematics the mean reach velocity was calculated for each animal and no significantly different between conditions was observed ($P > 0.05$). An

analysis of the EMG data revealed that for 11 of 13 muscles there was no main effect of condition during the IDP and MOVE epochs (p>0.01). For two muscles, medial deltoid and teres major, there was a marginal effect of condition on EMG activity during the IDP period (0.05>p>0.01). This may have been due to a slight alteration in the animals' starting posture in reaction to the board placed over their arm in the plane dissociation condition. There was, as expected, a main effect of target for all proximal arm muscles studied during the movement epoch (p<0.01). Lastly, reaction times between the coupled (M = 537.9 ms, SEM +/- 12.82) and decoupled (M = 522 ms, SEM +/- 9.89) conditions were also not significantly different (t (45) = .927, p = 0.359). Taken collectively, these results strengthen the conclusion that any neural differences observed between conditions are not a direct result of changes in the kinematics or biomechanics of the reaching movement, but rather the neural control of the movement.

Neural results

We obtained 44 LFP recordings from SPL (28 from monkey A, 16 from monkey B; Fig. 3.2). All successfully recorded LFP sites were used for the analysis of this project. In addition, 91 single cells were recorded during each condition, of which only 41 (45%) were found to be task-related (see (Hawkins et al. 2013). In line with our first hypothesis, the neural activity within SPL, both at the single cell and LFP level, changed between conditions. In support of our second hypothesis we observed that the magnitude of these changes varied with behavioural epoch.

Task related differences during IDP epoch

We observed salient differences in the oscillatory activity within SPL during coupled versus decoupled reaches (example site, Fig. 3.3). Specifically we observed strong synchrony within the 10-20 Hz beta frequency band shortly after peripheral cue onset for each site (Fig.

3A). The signal is more easily seen in Figure 3.3C for both conditions. This was consistent across the population (Fig. 3.4A-C). Importantly, there was a delay in the oscillatory activity within this range during the IDP of decoupled relative to coupled reaches (10-20Hz, compare Fig. 3.4A to B). Figure 3.4C shows the number of sites within the population that showed significant task-related differences ($P < 0.05$). The heightened beta synchrony in the coupled condition emerged more quickly after directional cue onset than that observed during the decoupled condition (Fig. 3.4D). As the task progressed, these differences diminished so that by approximately 500 ms into movement planning, power within the beta band was indistinguishable between conditions. In concert with the 10-20 Hz IDP oscillation, we also observed a reduction in the mean firing rate of single cells during this epoch in the decoupled condition relative to the coupled one (Fig. 3.5A, $P < 0.05$). Furthermore, similar to the oscillatory activity results (Fig. 3.4D), as the task progressed this difference in mean firing rate was no longer significant (Fig. 3.5A, $P > 0.05$). We also observed a reduction of gamma-band activity for both conditions following the peripheral cue onset (Fig. 3.4A and B). This gamma band reduction was stronger during the coupled relative to the decoupled condition (Fig. 3.4D). As the task progressed, gamma synchrony continued to increase during the IDP, and continued to be stronger in the decoupled condition, right up until the GO cue that signaled the beginning of the MOVE epoch.

Task related differences during MOVE epoch

Whereas 10-20 Hz beta synchrony in SPL dominated the IDP, by movement onset this pattern shifted to reveal even stronger synchrony that was focused in the gamma (>25 Hz) and low frequency (< 10 Hz) bands (Fig. 3.3B, Fig. 3.4E-G). Across the population, a clear enhancement in oscillatory power within the low-frequency band occurred roughly 200 ms

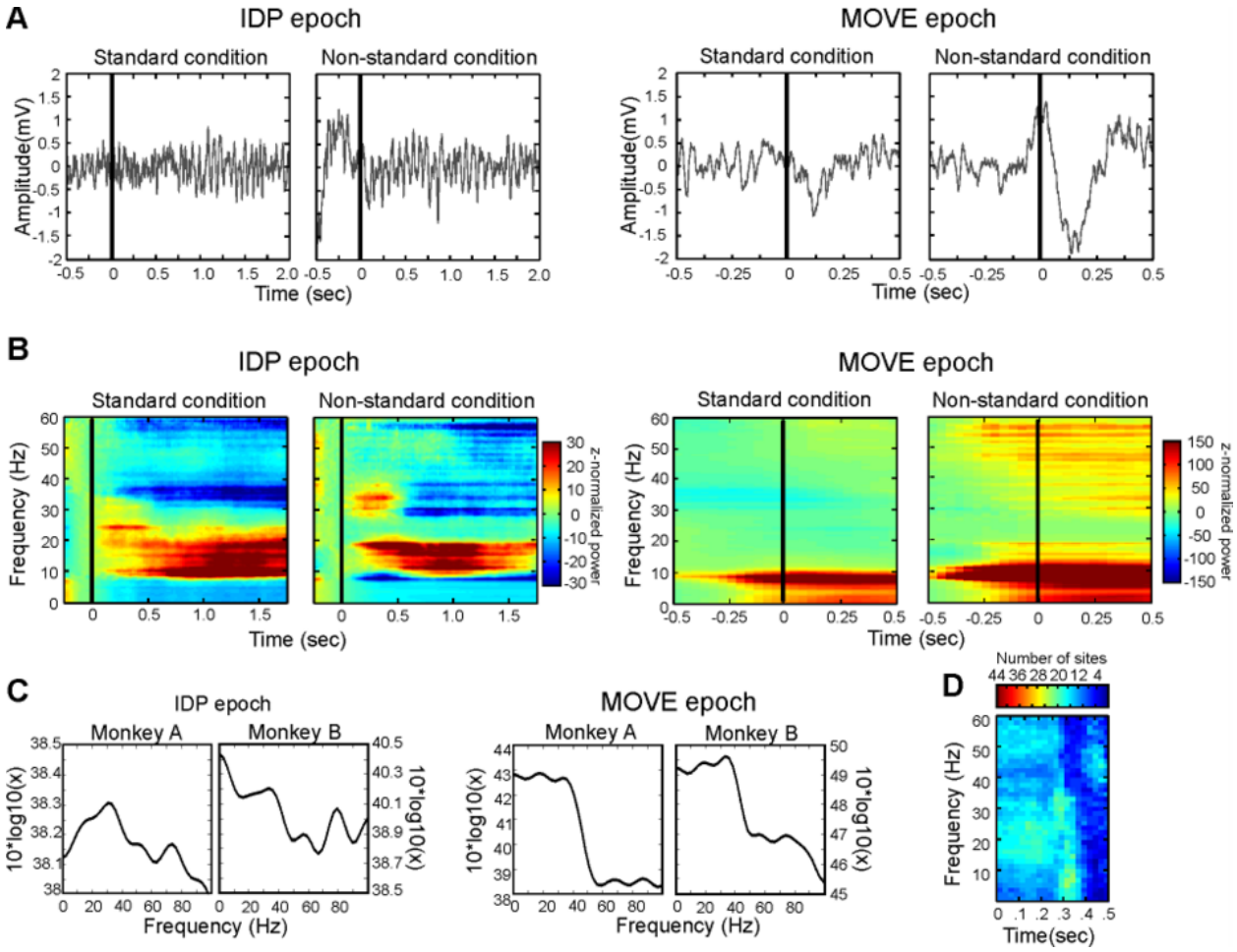

Figure 3.3. Example recordings for SPL. **A,** Example broadband LFP during IDP epoch (left panels) and MOVE epoch (right panels) for both conditions. Black line indicates peripheral target (IDP epoch) or movement onset (MOVE epoch). **B,** Example time-frequency spectrograms of oscillatory activity during each epoch and condition. Black vertical lines represent the onset of the peripheral cue (IDP epoch) and movement onset (MOVE epoch). **C,** Example spectral power during the IDP and MOVE epochs demonstrating similarity between animals. **D,** Number of sites that show a significant difference for each frequency range across the baseline period ($P < 0.05$). The baseline used for z normalization was taken in the later part of the epoch, when the condition-specific effects had dissipated. Color bar represents number of sites.

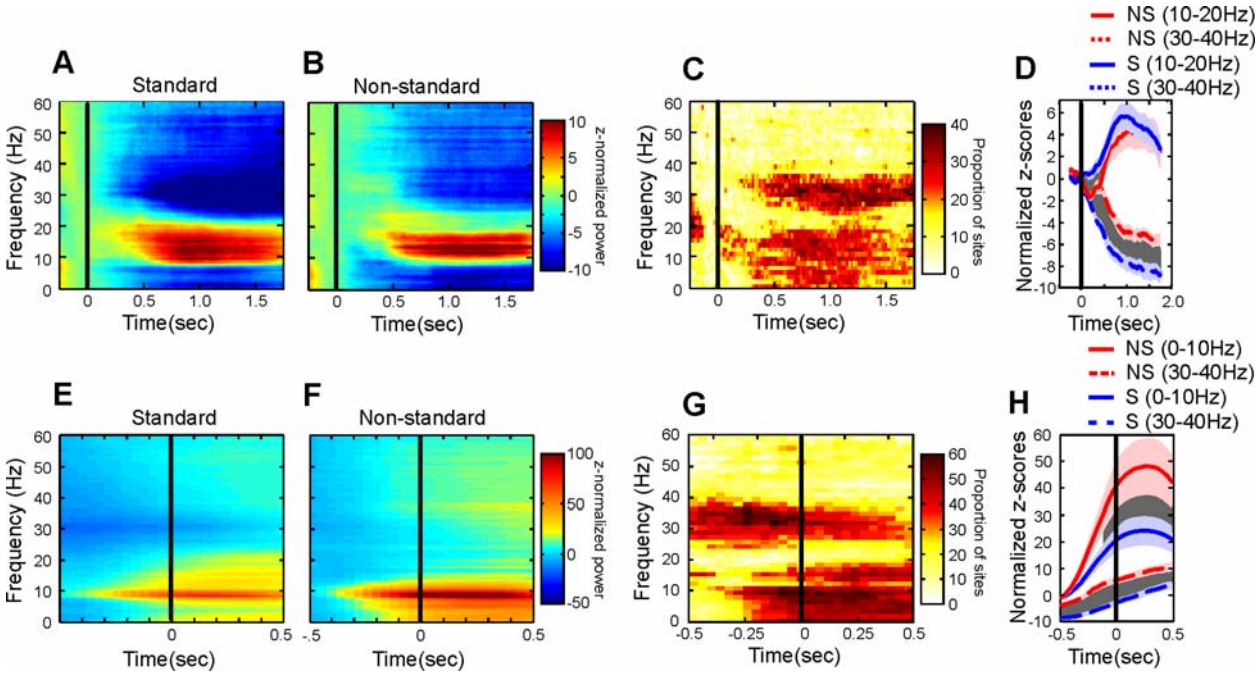

Figure 3.4. Population time-frequency spectrograms of oscillatory activity during the IDP and MOVE epochs. **A, B,** Population spectrograms of activity during the IDP epoch for standard (**A**) and decoupled (**B**) conditions. Power is color-coded on a log scale. **C,** Proportion of sites that show a significant difference for each frequency range across the IDP period ($P < 0.05$). Color bar represents number of sites. **D,** Population mean normalized z-scores for beta band activity (10-20Hz). Dark shaded region represent significant difference between conditions, $P < 0.05$. Blue and red shading represent jackknife error bars for standard and decoupled conditions. **E,F** Same as A and B for MOVE epoch during standard (**E**) and decoupled (**F**) conditions. **G,** Same as C for MOVE epoch. **H,** Same as D for low (10Hz) and high (30-40Hz) frequency activity. Black vertical lines indicates peripheral target onset during IDP epochs and movement onset during MOVE epochs.

before the onset of the reach movement (Fig. 3.4E and F). Furthermore, this activity was stronger during decoupled compared to coupled reaches (Figure 3.4H, $P > 0.05$). Prior to movement onset, during the late planning phase of the reach, many sites also showed significant alterations in the gamma frequency band (30-60 Hz, Figure 3.4E-G). As the task progressed, gamma band activity became stronger and similar to the IDP epoch, the 30-40 Hz low gamma band was significantly enhanced during the decoupled compared to the coupled condition (Fig. 3.4G and H, $P > 0.05$). Figure 3.4G shows not only the timecourse of the gamma recovery at the end of the IDP/beginning of the MOVE epoch, but also that the low-gamma power is stronger and occurs earlier in the decoupled condition (Fig. 3.4G,H). In summary, as the end of the delay approaches and reaching behaviour progresses from planning a decoupled reaching movement to executing one, a significant enhancement in the oscillatory power under 10 Hz and in the low-gamma band occurs relative to that observed during coupled reaches. In support of the LFP findings, we also observed an enhancement in the mean discharge rate of single units within SPL during decoupled reaching relative to direct target interaction, albeit at a slower timecourse that begins after the start of the MOVE epoch (Fig. 3.5B, $P<0.05$).

Task probability estimates

We calculated the average ROC probability for each site in predicting the correct condition (coupled versus decoupled) and behavioural state (planning versus execution) of the animal. Whereas the lower beta band range (10-20 Hz) was a dominant oscillatory frequency across conditions, our results showed that the greatest task predictability (coupled/decoupled) was within the low-gamma frequency range (30-40Hz) during both the planning (Fig. 3.6A and B) and movement epochs (Fig. 3.6C and D). Furthermore, oscillations within the gamma band showed stronger task predictability than the single units, specifically during the late planning

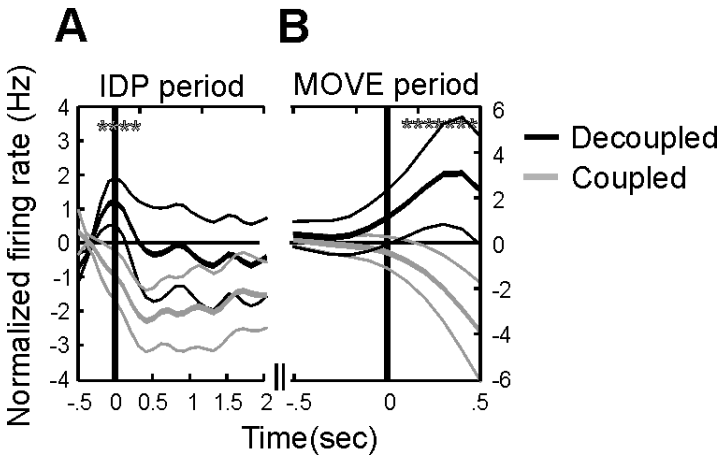

Figure 3.5. Mean normalized firing rates of single cells during the IDP epoch (**A**) and MOVE epoch (**B**). Black lines represent peripheral cue onset during the IDP epoch (left panels) and movement onset during the MOVE epoch (left panels). Asterisks denote significance, $P < 0.05$.

phase (Fig. 3.6 B and D). Thus gamma band activity was a better predictor of the type of reach the animal was performing. In contrast to the task discrimination, the behavioural state of the animal was most strongly discriminated by the 10-20 Hz frequency band (AUC = 0.8861, planning versus execution), compared to that of spiking (AUC = 0.5277) or low-gamma band activity (AUC = 0.6715). In summary, although gamma-band activity was good at predicting the type of reach the animal was performing, beta-band activity was better at predicting the behavioural epoch, providing a reliable signature of the delay epoch. These results support the idea that oscillatory activity carries a richer set of information than single unit firing rate alone.

Gaze-related differences

Performance during each condition required arm movements that were biomechanically similar (Fig. 2C and D), however, the overall eye-in-head angle shifted between conditions equivalent to the gaze angle since the head was fixed in place. To ensure that the task-related differences we observed were not a direct result of this change in gaze angle, we recorded and analysed the neural activity during a gaze-only condition (see methods). No change in single unit mean discharge rate occurred within SPL, as previously reported (Hawkins et al. 2013). Similarly, we found no effect of gaze plane on any frequency range of the oscillatory activity within SPL (Fig. 3.7, $P > 0.05$).

DISCUSSION

Patient data and limited imaging studies suggest that parietal and premotor areas are crucial to the control of goal-directed voluntary movement, and may contribute to eye-limb coordination under conditions requiring cognitive rule integration. How key nodes within this network help to accomplish goal-directed voluntary movement in the face of decoupled gaze-hand mapping is not yet understood. The vast amount of research available on SPL activity has

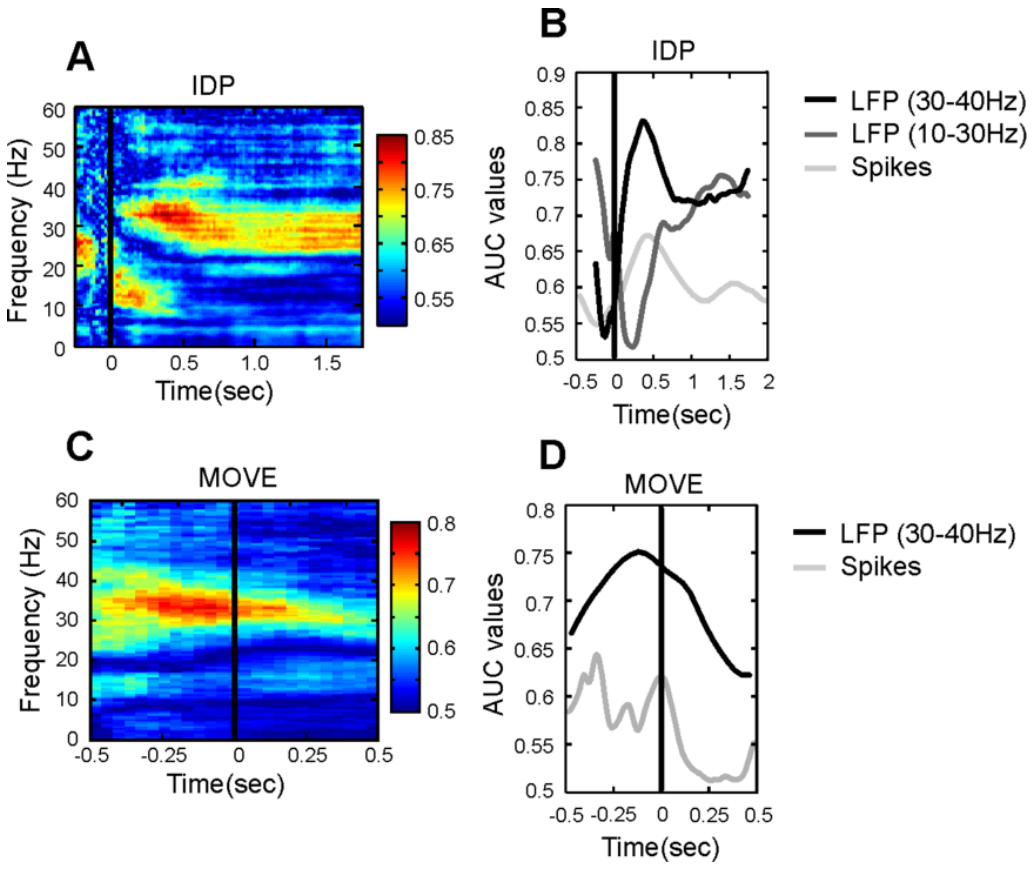

Figure 3.6: ROC task probability estimates during the IDP (**A**) and MOVE (**C**) epochs. Color plots denote task probability values. **B, D,** Mean population ROC task probability estimates for spikes (gray line) and LFPs (black lines). Black vertical lines represent onset of the peripheral cue during the IDP epochs or movement onset during the MOVE epochs.

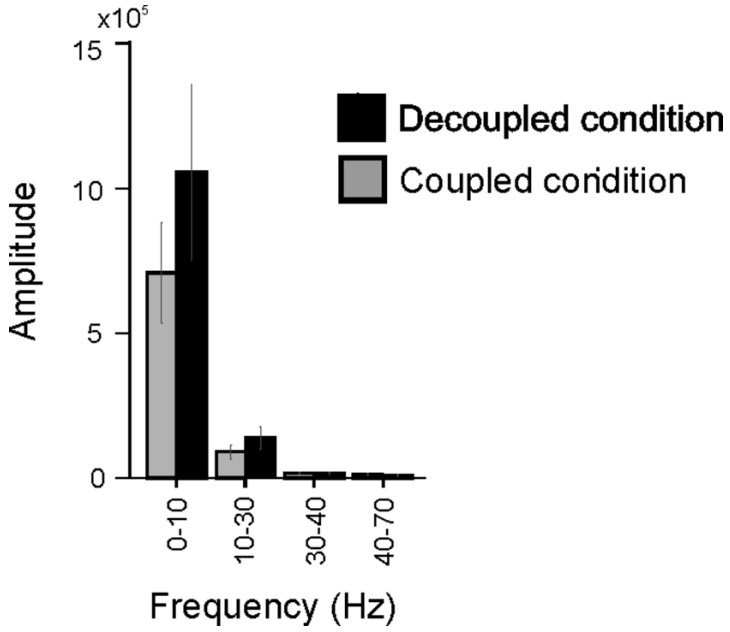

Figure 3.7: Gaze control condition. Mean amplitude and standard deviation during standard and decoupled conditions. Bootstrapping methods revealed no significant difference in overall activity between conditions for each region (P = 0.50 for 0-10 Hz, P = 0.81 for 10-30 Hz, P = 0.15 for 30-45 Hz, P = 0.06 for 45-70 Hz).

demonstrated its importance in the general representation of posture and movement of the body and eyes for visuomotor transformations (Kalaska et al. 1997; Kalaska 1996; Caminiti et al. 1998; Andersen et al. 1997; Breveglieri et al. 2006)**.** Specifically, the SPL is thought to be involved in transforming sensory information into the appropriate reference frames to guide hand movements (Batista et al. 1999; Buneo et al. 2002; Vesia and Crawford 2012; Galletti et al. 2003; Kalaska et al. 1983)**.** Regions within SPL are important in the planning and execution of goal-directed reaches (Prado et al. 2005; Galletti et al. 2003; Culham et al. 2006; Colby and Goldberg 1999; Colby 1998; Galletti et al. 1999)maintaining an internal representation of ones body in the surrounding space (Mountcastle et al. 1975; Breveglieri et al. 2006), and calculating the reach vector from the initial hand position (Vesia et al. 2010; Eskandar and Assad 1999). Taken collectively, while it is known that SPL shows reach-related activity, our investigation into the oscillatory and single unit activity within SPL demonstrates that this activity varies depending on the type of visuomotor transformation being performed, specifically between the different stages of the movement. The oscillatory activity during the IDP, a period concerned with planning and holding the motor plan in working memory, was dominated by synchrony within the 10-20 Hz frequency range. This activity was specifically evident during the coupled transformation, while, in contrast, the contribution of 10-20 Hz oscillations to the decoupled IDP seemed to be disrupted, at least in the early part of the epoch. As the task progressed we observed a clear distinction in the role of SPL to the planning versus the execution of a decoupled motor act. By late planning and movement onset there was a switch in low frequency and gamma-dominated response, specifically for decoupled reaches. This switch may represent the increased reliance on proprioceptive inputs and online control mechanisms required during decoupled eye-hand coordination (Battaglia-Mayer and Caminiti 2002; Battaglia-Mayer and

Caminiti 2002).

Planning a decoupled reach: Decreased neural activity within SPL

The planning of a decoupled reaching movement produced a significant delay in the dominant beta oscillation (10-20 Hz) and single cell activity within SPL when compared to coupled reach planning. Previous work into the contribution of SPL to the planning of visually-guided reaches has shown that cells within this region receive converging information from the eyes, as visual feedback, and the arm, as proprioceptive feedback (Kalaska 1996; Kalaska and Crammond 1995b). As a result, it has been suggested that the regions within SPL preferentially represent automatic or sensory driven reaching movements (Gail et al. 2009; Pisella et al. 2000; Desmurget et al. 1999). Coupled reaching movements that involve direct interaction with objects of interest are innate and natural to produce, while decoupled reaching movements are not innate and must be learned over time (Sergio et al. 2009; Bo et al. 2006; Piaget 1965). Successfully decoupling the action of the eyes from that of the hand will demand inhibition of our natural tendency to couple them, thus increasing the processing that must occur to incorporate the transformational rule into the motor plan (Sergio et al. 2009; Gorbet and Sergio 2009).

Sub-gamma frequencies (<30Hz), including beta oscillations, are primarily observed within the infragranular layers of a region and thus are suggested to reflect feedback projections to from distant signals or involved in 'top down' neural processing (Maier et al. 2010; Bosman et al. 2012; Bastos et al. 2012) . This is in contrast to neuronal synchrony and spike-field coherence in the gamma range which are observed in the superficial and granular cortical layers of a region and thus suggested to reflect 'bottom up' processing (Engel and Fries 2010; Bastos et al. 2012; Donner and Siegel 2011; Siegel et al. 2012; Brovelli et al. 2004; Buschman et al. 2012). This idea is further supported by recent work into the functional role of beta oscillations by Engel and

Fries (2010). They suggest that beta oscillations signal the current behavioural state, or the 'status quo', by promoting preferential or top-down processing of that state (such as the motor plan) (Scherberger et al. 2005; Pesaran et al. 2002; Engel and Fries 2010). In the present study it is important to clarify the different uses of the word feedback/feedforward. In the movement control sense, feedback refers to updating the current state of the system using incoming sensory information once the movement has begun. In the neural anatomical sense, top-down types of anatomical feedback are thought to modulate typical integration or processing of incoming signals into a given region, as may occur following memory, attention, context, or voluntary inhibition of a typical response.

Our results demonstrate 1) enhanced beta synchrony during the delay epoch, and 2) a delay of this oscillation during decoupled reaches. Based on the observations that SPL integrates eye and hand signals from various regions of the brain (Graziano et al. 2000; Battaglia-Mayer and Caminiti 2002), the appearance of beta may be a signal to indicate that the behaviour has been planned successfully, possibly as a 'hold' signal to maintaining the current motor plan. Indeed others have observed increases in beta band activity during working memory paradigms (Pesaran et al. 2002) when the motor plan would need to be held. Beta coherence has also been observed between area 5 and M1 during movement hold (Witham et al. 2007) and enhanced beta synchrony is associated with motor slowing in healthy (Pogosyan et al. 2009) and Parkinsonian patients (Schnitzler and Gross 2005). In addition beta band activity shows strong state (planning versus execution) predictability (see section below, Pesaran et al. 2002).

Our observation of a delay in beta synchrony during decoupled reaching movements may indicate that eye-hand segregation leads to a neural interference or a delay of this top-down control over movement planning. Indeed the incongruent eye and hand signals will demand

additional processing to incorporate the new spatial transformation into the motor plan (Gorbet and Sergio 2009), as discussed below. The additional processing would require more time to calculate the transformed reach vector and incorporate the new spatial transformation between the eyes and the hand, a requirement that may be reflected in the delayed beta band and single unit activity observed here. These results also support a functional role for beta in the planning of visually guided movements, possibly as a signal for indicating the maintenance of an already established movement plan prior to execution.

In contrast to the task-related beta band differences, we observed gamma band synchrony that was *reduced* during the delay of coupled compared to decoupled reaches. Previous reports have observed enhanced gamma synchrony within early sensory areas during active sensory processing, whereas alpha/beta band synchrony is generally reduced. Proprioceptive information arising from the somatosensory cortex and visual information arising from the primary visual cortex terminate in the superficial layers of SPL (Pandya and Seltzer 1982; Rockland and Pandya 1979), where gamma oscillations often dominate (Maier et al. 2010; Bosman et al. 2012; Bastos et al. 2012). The incongruent signal between eye and hand locations will require additional processing between parietal and frontal regions (Matelli and Luppino 2001; Geyer et al. 2000; Gorbet and Sergio 2009) so that the correct relative position code can be calculated to guide the eyes and the hand to their new appropriate spatial locations. The extra reliance on proprioceptive and visual signals is important in calculating the spatial transformation required for decoupled reach, and we propose that the increase in gamma synchrony is a reflection of this extra-reliance, relative to a coupled reach.

Executing decoupled reaches: enhanced SPL activity

As the trial progresses, the pattern of neural activity shifts to one of enhanced activity

during the execution of decoupled reaches. This shift occurs prior to movement onset in the low-frequency (5-10 Hz) and low-gamma oscillations (30-40 Hz) within SPL. Note here that the clearly delineated bands of activity do not fall strictly within typical EEG bands; namely, our 'beta' covers the high alpha range (10 Hz), and our time resolution during the MOVE epoch prohibits a clear delineation within low-frequency bands (e.g. delta from theta and even lower alpha).

During visually-guided reaching movements, SPL receives information to maintain an updated representation about the relative position between the hand and the reach goal in eye-centered coordinates (Buneo and Andersen 2006; Rushworth et al. 1997a; Jackson et al. 2009; Wolpert et al. 1998). The rapid online updating about limb position relies on forward model predictions that combine efference copy motor commands, sensory feedback (visual and proprioceptive), and an internal model regarding the dynamics of the arm (Buneo and Andersen 2006; Vesia and Crawford 2012; Battaglia-Mayer et al. 2012; Wolpert et al. 1998; Desmurget and Grafton 2000; Desmurget et al. 1999). During coupled eye and hand reaches, the visual and proprioceptive information regarding the location of the limb and its relative position to the reach target are in alignment and thus provide equally accurate information. During decoupled reaching movements, SPL is receiving mismatched visual and sensory information. Thus in order for SPL to maintain an updated representation of the position of the hand relative to the target the hand position must be derived predominantly from proprioceptive feedback and efference copy information (Buneo and Andersen 2006; Rushworth et al. 1997a; Engel et al. 2002; Flanders et al. 1992; Rushworth et al. 1997b; Nixon et al. 1992). Numerous research studies suggest that a reach performed under visually reliable situations is controlled in eye-centered coordinates (Buneo and Andersen 2006; Vesia and Crawford 2012). However, when visual information is

unreliable, a limb-centered posture defined coordinate system must be used to control the reach (Batista et al. 1999; Buneo and Andersen 2006; Rushworth et al. 1997a; Jackson et al. 2000; Pellijeff et al. 2006; Jackson et al. 2009). Within SPL the frames of references used to plan and control reaching movements are highly flexible and task specific (Buneo et al. 2002; Battaglia-Mayer and Caminiti 2002; Battaglia-Mayer and Caminiti 2002; Newport et al. 2006). In addition, damage to the SPL results in misreaching due to proprioceptive deficits that impair the integration of visual and proprioceptive information (Blangero et al. 2007). Together these results suggest that during a decoupled, context dependent visuomotor transformations the reliability of the visual information provided could influence how the updated limb state is determined (Buneo and Andersen 2006). However future investigations specifically designed to test this hypothesis will need to be conducted in order to address this suggestion.

As previously stated, proprioceptive inputs from sensorimotor cortex terminate in the superficial layers of SPL (Pandya and Seltzer 1982; Rockland and Pandya 1979) where gamma oscillations dominate (Maier et al. 2010; Bosman et al. 2012; Bastos et al. 2012). If executing a decoupled reach relies more heavily on proprioceptive and efference copy processing versus a coupled reach, than enhanced gamma-band activity during these types of movements are not surprising. This also helps to explain the progressive increase in gamma band synchrony observed in the current study as the trial progresses. In order to maintain an updated representation regarding the current state of the limb, SPL must be able to incorporate proprioceptive feedback into the ongoing motor command (Buneo and Andersen 2006; Rushworth et al. 1997a; Jackson et al. 2009; Wolpert et al. 1998). The reciprocal communication between parietal and frontal structures (such as PMd) are likely critical to the incorporation of an updated estimate regarding limb position to the current motor plan throughout movement

execution (Wise et al. 1997; Matelli et al. 1998; Luppino and Rizzolatti 2000; Geyer et al. 2000). Since alpha/beta synchrony has been suggested to reflect top-down, feedback processing (Maier et al. 2010; Bosman et al. 2012; Bastos et al. 2012), one possibility is that the enhanced low frequency synchrony (10 Hz), observed in the present study, could signal the maintenance of the updated limb estimates to the motor plan. This is also supported in the ROC analysis, which demonstrates beta band activity to be the strongest predictor of behavioral state (see Probability estimates section,). Future studies examining the synchrony between parietal and premotor structures during decoupled reaches would need to be conducted in order to address this possibility.

Probability estimates

In addition to characterizing the oscillatory activity within SPL during different types of reaching movements, we also looked at the receiver-operating characteristic for task epoch and condition probability estimates. We found that oscillations within the beta and gamma bands showed either strong task epoch or strong condition predictability. Gamma-band activity, and to a lesser extent single units, were a stronger predictor of which condition the animal was performing (coupled versus decoupled) than beta-band activity. In contrast, beta-band activity was observed to be a better predictor of the behavioural state of the animal (i.e. task epoch - planning versus execution) than spikes and gamma band activity. Previously, Pesaran (2002) and others have found that they could decode the behavioural state of the animal (planning versus execution) more reliably with beta band activity, while gamma band and single unit activity could reliably be used to decode the movement direction (Scherberger et al. 2005; Pesaran et al. 2002; Engel and Fries 2010). Previous work by Battaglia-Mayer and colleagues has demonstrated that SPL neurons combine different eye and hand information into a global-tuning

field, representing different frames of reference for eye-hand coordination (Battaglia-Mayer et al. 2001; Battaglia-Mayer and Caminiti 2002). This idea fits with Pesaran's (2002) conclusion that gamma band and single unit activity carry information about movement direction, which alters the relative position of the eyes and the hand. Similarly, our finding that gamma band and single unit activity carry information about which condition is being performed is in agreement with these findings. Performance of the decoupled task required an overall shift in the relative position of the eyes and the hand. These results support the idea that SPL activity is modulated by different types of reaching movements. In addition it supports previous work that has found LFP activity to carry a richer set of information than single units alone.

Conclusion

The current report supports and expands upon recent work demonstrating that different types of visually-guided reaching movements alter the activity of regions within the parietofrontal reach network. Although the role of SPL in reach planning and execution is well understood, its role in decoupled visuomotor transformations has not been thoroughly studied. The current work presented here supports the role of SPL in decoupled reach planning and execution. Specifically, we suggest that because of the nature of decoupled reaching movements, decoupling the action of the eyes from that of the hand will alter the weight of proprioceptive feedback and online monitoring required during a decoupled relative to a coupled movement. This increased reliance on prioprioceptive and efference copy information will manifest itself as enhanced neural processing (increased firing rate and activity) during the movement and suggests that SPL may have a prominent role in providing ongoing proprioceptive and efference copy information about the hand.

Chapter Four

The contribution of different cortical regions to the control of coupled versus decoupled reach movements

Patricia F. Sayegh, Kara M. Hawkins, Kari L. Hoffman, and Lauren E. Sergio

Submitted to the Journal of Neuroscience

ABSTRACT

Humans are able to exhibit a wide range of motor behaviours, most of which involve an interaction with a visual object. Eye-hand coordination, crucial for our ability to interact with the world around us, has become more complex throughout our evolution. In many circumstances, successful interaction with an object requires a spatial decoupling between gaze direction and hand motion. This differs from more natural types of reaches that couple the eyes and the hand towards the same spatial target. Reaching movements rely on brain regions located within the parietofrontal reach network. Importantly, decoupled -but not coupled- reaches are affected during certain neurological conditions, and are known to only develop later in childhood. Recently, we have shown that different sub-regions within SPL and PMd are altered during different types of visually guided reaching movements. To fully characterize these results, we measured the spike-field coherency within region of SPL and PMd while monkeys performed coupled versus decoupled visually guided reaches. We were specifically interested in quantifying how these regions select and transmit information required to integrate sensory and rule-based information for motor performance. We observed stronger spike-field coherence within PMdr and superficial regions of SPL during decoupled reaches while PMdc and deeper regions of SPL hand stronger coherence during coupled reaches. These results were supported by an imaging literature review on human fMRI data. Our results support the proposal of altered cortical control during complex eye-hand coordination and highlight the necessity to account for the different eye-hand compatibilities in motor control research.

INTRODUCTION

The brain's ability to perform various types of visually-guided reaches enables our various interactions with objects around us. . The core network of brain regions that support

these diverse set of behaviours includes the dorsal premotor (PMd) and superior parietal lobule (SPL), highly interconnected regions that are part of the parietofrontal reach network (Sergio et al. 2009; Kalaska et al. 1998; Battaglia-Mayer et al. 2001; Caminiti et al. 1999; Prado et al. 2005; Granek et al. 2010; Gorbet et al. 2004; Picard and Strick 2001; Wise et al. 1997; Johnson et al. 1996; Gail et al. 2009; Grafton et al. 1996; Connolly et al. 2000). The most basic, natural reach we can perform couples eye and hand movements to the same spatial location, commonly referred to as a *standard,* coupled reach. However, many of our interactions require a spatial decoupling of eyes and hand targets (Wise et al. 1996). These *non-standard* decoupled reaches require some form of training to learn the necessary visuomotor transformation (Sergio et al. 2009; Bo et al. 2006; Piaget 1965). Recently, we and other groups have demonstrated that dissociating the eye from the hand *alters* the cortical activity of regions such as PMd and SPL, through psychophysical (Granek and Sergio 2014; Gorbet and Sergio 2009), imaging (Prado et al. 2005; Clavagnier et al. 2007; Granek et al. 2010; Gorbet et al. 2004; Connolly et al. 2000), neurophysiological (Sayegh et al. 2013; Gail et al. 2009; Hawkins et al. 2013; Sayegh et al. 2014) and patient (Granek et al. 2012; Granek et al. 2013) work. Further, rostral PMd and regions located within the caudal-superficial portion of SPL have been suggested to have a strong role in the visuomotor transformations necessary during decoupled reaches (Prado et al. 2005; Granek et al. 2012; Battaglia-Mayer et al. 2012; Sayegh et al. 2013; Perenin and Vighetto 1988; Blangero et al. 2007; Rossetti et al. 2005; Pisella et al. 2009; Pisella et al. 2000; Grea et al. 2002; Granek and Sergio 2014; Hawkins et al. 2013). Caudal PMd and deeper regions of SPL, however, seem to preferentially process coupled reaches (Prado et al. 2005; Sayegh et al. 2013; Hawkins et al. 2013).

While advancing our understanding of how parietal and frontal regions contribute to

visuomotor transformation, most research has focused on characterizing the activity of single units or local field potentials (LFP) alone. What is lacking is a comprehensive view of the local computations within these regions and, importantly, how they change to accommodate the different types of reach behaviours. The present study examined the relationship between the spikes to the field. We measured the spike-fieldcoherency (SFC) within sub-regions of PMd and SPL to determine how the coordination of neural activity changed during coupled versus decoupled reaches. SFC measures the communication between neuronal groups that are processing task-related information, enabling inputs to have a greater impact on the local population (Womelsdorf and Fries 2006; Fries 2005; Roberts et al. 2013). Regions exhibiting strong neuronal coherency during movement are thought to promote the selection and transmission of information required to integrate sensory information for motor performance (Womelsdorf and Fries 2006; Fries 2005). Here we demonstrate that coherency in all regions examined is affected by the type of visuomotor mapping performed.

METHODS

Animals and Apparatus

The methods for this study have been extensively described elsewhere (Sayegh et al. 2013; Hawkins et al. 2013). Briefly, two rhesus monkeys (Female *Macaca mulatta*, both 5.2 kg) were trained to perform a visually instructed, delayed reaching task in coupled and decoupled conditions. All surgical and animal handling procedures were in accordance with *Canadian Council on Animal Care* guidelines on the use of laboratory animals, and pre-approved by the *York University Animal Care Committee*. Each monkey was seated in front of a 38.1 cm vertical screen with an additional 38.1 cm horizontal touch sensitive screen (Touch Controls Inc, San Diego CA) set in front of the animal (Figure 4.1). The horizontal touch screen was designed to

detect spatial displacements as small as 3 mm using infrared beams, at a sampling rate of 100 Hz. Continuous tracking of the eye was monitored using the ISCAN-ETL 200 Eye Tracking System (ISCAN Inc, Burlington MA) at a sampling rate of 60 Hz.

Behavioural Task

The sequence of events is illustrated in Figure 4.1. Each trial began with the appearance of a red circular target (70 mm in diameter) at the center of the screen, which the monkey was instructed to touch. An additional smaller white circular target (40 mm in diameter; 5.7° of visual angle) appeared on top of the red circle, which instructed the monkey to maintain eye fixation. After a 500msec baseline period, one of eight equally spaced green-colored peripheral targets appeared randomly (70 mm in diameter, visual angle relative to fixation). The peripheral target appeared 5 times at each location for a total of 40 trials per condition. After a variable instructed delay period (IDP, 2000 ms +/- 500 ms) the red central target disappeared and the white target jumped to the peripheral target. Following this target jump the animal moved their eyes and hand towards the peripheral target. These reaching movements were made from the middle of the center target to the middle of the peripheral target (roughly 80mm). Once the eye and hand arrived at the peripheral target, the monkey was required to hold both the eye and the hand there for 500 ms. The visual presentation of the task was identical across conditions however during the eye-hand *coupled condition,* visual presentation and the reaching movements were both made on the horizontal touch-sensitive screen (Figure 4.1A). In the eye-hand *decoupled condition*, visual presentation of the task was on the vertical screen while the animal's limb movement remained on the horizontal touch screen (Figure 4.1B). This allowed us to decouple the spatial target of the eyes from that of the hand. To prevent extra-foveal tracking of the hand, an opaque screen was placed 100 mm over the animal's arm to block vision of the limb. To provide

feedback on the current position of the hand, a cross-hair representing the position of the finger on the touch screen was displayed. The animals were trained to perform similar movements during both conditions and the biomechanical features of the movements were recorded to confirm this similarity (Sayegh et al. 2013; Hawkins et al. 2013). For each condition, two epochs during the trial were considered. The delay epoch (IDP) comprised the 500 ms baseline period and the first 2000 ms of the instructed delay period. The movement epoch (MOVE) comprised the last 500 ms of the instruction delay period and 500 ms after movement onset.

The monkeys also performed a *gaze-only* control task to determine if the neural activity was affected solely by the overall shift in gaze angle. This condition has been described elsewhere (Sayegh et al. 2013; Hawkins et al. 2013). Briefly, before the start of each condition nine white circles (40 mm in diameter; 5.7° of visual angle) appeared one at a time in the same locations as the targets that appeared during the experimental conditions (i.e. one central and 8 peripheral). The monkey was instructed to fixate on each of these white circles while maintaining both hands beside the horizontal touch screen. The white circles appeared in each location 3 times for a total of 27 fixation points for each plane.

Neural Recordings

Monkeys were implanted with a recording cylinder under standard aseptic surgical techniques (Sayegh et al. 2013; Hawkins et al. 2013; Kalaska et al. 1989). The stereotaxic coordinates for chamber placement can be seen in Figure 4.2. Placement over PMd (Monkey A; Interaural A: 16 mm; L: 11 mm; Monkey B; Interaural A: 16 mm; L: 11 mm) and over SPL (Monkey A, Interaural; A: -12.30 mm, L: 18.40 mm and Monkey B, Interaural; A: -7.80 mm, L: 00.00 mm) were determined using *The Rhesus Monkey Brain in Stereotaxic Coordinates* (Paxinos et al. 2000). The border between rostral and caudal PMd, and primary motor cortex

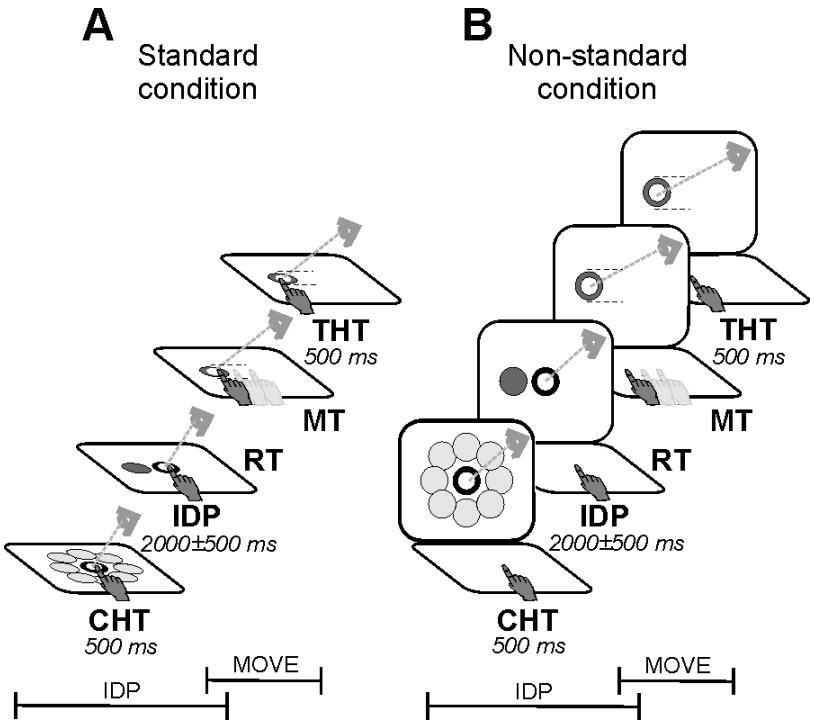

Figure 4.1. Experimental setup and trial timing for the coupled(**A**), and decoupled (**B**) conditions. At the start of each trial a red center target would apear with a smaller white target on top. The animal had to touch and look at these targets. After a variable delay one of eight equally spaced (45°, light grey circles) peripheral targets were presented on either a touch-sensitive screen placed over the animal's lap (**A**) or on a monitor positioned vertically 40 cm away from the animal's frontal plane (**B**). Epochs - CHT: centre hold time, IDP: instructed delay period, RT: reaction time, MT: movement time, THT: target hold time. The baseline epoch came from within the centre hold time epoch. The animal's head was fixed throughout the experiment.

(M1) was drawn according to previously proposed physiological and cytoarchitectonic criteria (Fujii et al. 2000). Because of the location of Monkey`s A premotor chamber and a posterior head-post, space limitations required the SPL chamber to be positioned on a 25° angle in order to allow access to the desired brain regions through deep electrode penetrations in the medial-anterior quadrant of the chamber. Thus, while the surface entry points are more rostral, the angle and depth of the electrodes provided access to neurons from within the medial intraparietal sulcus. A hydraulic multi-channel driver (MCM-4, FHC inc., Bowdoin ME) in conjunction with a multi-channel processing system (MCP, Alpha-Omega Engineering, Israel) provided simultaneous recording from up to two penetration sites at a time. This allowed us to examine the local field potential (LFP) and single units collected at each electrode site. Neural activity from each electrode was preamplified (5000x) band-pass filtered (1 Hz-10 kHz) and split into lower (LFP) and higher (single units) frequencies. Higher frequency signals were sampled at 12.5 kHz and spikes of single units were sorted using template matching (Hawkins et al. 2013). The LFP (below 100 Hz) was sampled at 390.6 Hz (Sayegh et al. 2013). Following the completion of all experiments, anatomical brain images of both animals were obtained using a 3T Siemans Tim Trio MRI scanner to verify chamber location (T1-weighted anatomical images, FOV: 131 x 122.8 mm, TR: 2300 ms, TE: 3.54 ms, Flip Angle: 9 degrees).

Data analyses

Behavioural analyses.

To confirm that the reaching movements were biomechanically similar between conditions, hand paths were recorded and analyzed. The results of these analyses have been extensively reported in previous papers using the same dataset (Sayegh et al. 2013; Hawkins et al. 2013; Sayegh et al. 2014). In additions, to reinforce similar hand paths between conditions,

movement alleys were included to ensure that reaches were directed along a fairly straight trajectory (Figure 4.1). These alleys were set at ± 40 mm from a straight line spanning from the central to the peripheral targets. If the cursor moved outside of these alleys the trial would stop. Our comparisons confirm that the kinematic and electromyographic features of the limb movement between task conditions were not significantly different. In addition, as previously reported (Sayegh et al. 2013; Hawkins et al. 2013; Sayegh et al. 2014), there was no significant difference in the neural activity recording during the gaze-only control task. Therefore we can interpret the task-related differences in the neural data as being due to rule-processing rather than motor behaviour.

Spike-Field Coherency

Only task-related single units were used for this analysis. A cell was determined to be task-related if it displayed directional tuning during either the IDP or MOVE epoch. Directional tuning was determined based on previously described methods (Sayegh et al. 2013; Hawkins et al. 2013; Georgopoulos et al. 1982). All LFPs that were collected simultaneously with a task-related single unit were used for analysis. Task-related cells and LFPs were grouping based on depth in order to separate superficial (gyrus, depths <2.2 mm past dura, defined based on average grey matter thickness) from deep (sulcus, depths >2.2 mm past dura, generally 4-8 mm, i.e. deep enough to enter the anterior wall of the IPS) recordings (Figure 4.2 E and F). Because of the location of our recordings, the superficial group is suggested to be recorded from area PEc while the deeper recordings are suggested to be from MIP regions. Open source Chronux script files (www.chronux.org) were used in MATLAB (The Mathworks, Inc., Natick MA) to analyze the spectral data and to generate time-frequency coherency plots for all spike-field pairs for both conditions (Pesaran et al. 2002; Jarvis and Mitra 2001). Spike-field coherence was determined

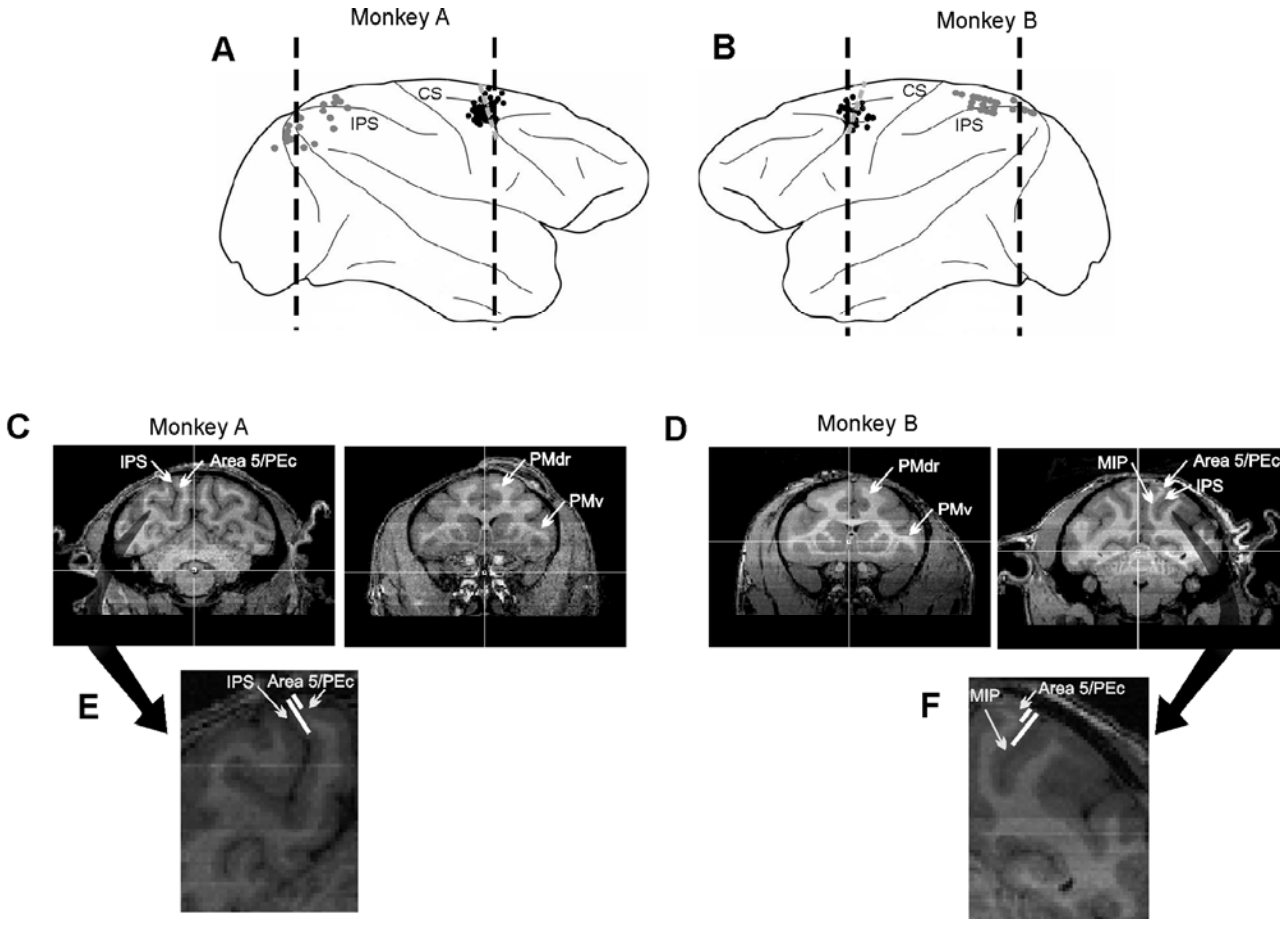

Figure 4.2. Penetration and chamber location sites for monkey A (**A** and **C**) and monkey B (**B** and **D**). Larger dots indicate where recordings were obtained on two occasions and gray dotted line denotes division between penetration sites classified as rostral (left of line) or caudal (right of line). **E** and **F)** Enlarged section taken from parietal chamber shown in C and D. White lines shows depth information, smaller line is 2.2mm and larger line is 5 mm to show the regions within SPL that were being recorded from based on depth. AS: arcuate sulcus. CS: central sulcus. IPS: intraparietal sulcus. PMdr: rostral region of the dorsal premotor cortex. PMdc: caudal region of dorsal premotor cortex. MIP: medial intraparietal sulcus.

using multitaper spectrum analysis (previously described in (Pesaran et al. 2002; Pesaran et al. 2008; Jarvis and Mitra 2001) , using a time-bandwidth product of TW = 3 with K = 5 tapers. Z-scores were then calculated for each site by determining the expected standard deviation of the coherency based on the degrees of freedom (V = number of trials * number of tapers). The coherence was then transformed using the assumption that when the coherence is zero, the transformed coherence is distributed as a normal variate with the variance equal to 1 (Pesaran et al. 2002; Jarvis and Mitra 2001). This transformation uses the equation $z = \beta (q - \beta)$ where $q = -\nu - 2 * \log 1 - C$, $\beta = 1.5$, and C is the coherency. The population z-transformed coherence was then calculated and task-related differences were determined using bootstrapping procedures (Sayegh et al. 2013; Hawkins et al. 2013). Because some spike-field pairs were recorded on the same electrode we compared the results obtained from these pairs to spike-field pairs from different electrodes. The same pattern of coherency results were observed between groups and thus the population results represent both groups

Review of imaging studies on eye-hand coordination

In addition to the neural analysis described above, we also performed a review on published data from fMRI studies performed on visually-guided reaching movements. The goal of the imaging literature review was to determine whether the topographical distribution of task-related activity we have observed in monkeys is also apparent in data collected from human participants. An exhaustive pubmed search was done to find fMRI studies that examined coupled or decoupled reaching movements. Results from studies using coupled reaching tasks were included if the final location of the eyes and the hand at the target of a visually-guided reach were congruent. Decoupled reaching tasks were included if a spatial dissociation of eye and hand targets or a context-related visuomotor mapping rule was required to successfully complete the

reach. The reported peak Talairach coordinates of task-related activity within the dorsal premotor and/or superior parietal cortices from each study were plotted onto the surface of the standardized Talairach glass brain template available in BrainVoyger software (BrainVoyager QX version 2.8, Brain Innovation, Maastricht, The Netherlands). Each data point was plotted as a cluster of 2 shaded polygons on the surface of the template brain (see Figure 4.7).

RESULTS

Behavioural results:

As a first step, we analysed the biomechanical features of the reaches performed in each condition. This was to ensure that differences that occurred in the neural activity between tasks were not a direct result from differences in the reach profile. The results of these analysis has been extensively reported previously (Sayegh et al. 2013; Hawkins et al. 2013; Sayegh et al. 2014). Briefly, when comparing between conditions we observed no significant differences in the variability of the reach trajectories ($P>0.05$), in the reach velocity ($P>0.05$), in the reaction times (Coupled: M = 537.9 ms, SEM +/- 12.82, Decoupled: M = 522 ms, SEM +/- 9.89), or in the EMG data ($p>0.01$). Taken collectively, our comparisons confirm that the kinematics and electromyographic features of the limb movement between conditions were not significantly different. Therefore any task-related difference observed within this study can be interpreted as due to differences in the processing of the motor behaviour.

Neural results:

To investigate the coordination between spiking activity and LFP activity during visually guided reaching movements we recorded the activity of 60 task-related single units (29 within SPL, 21 within PMdr, and 11 within PMdc) and 63 LFP recordings (30 within SPL, 17 within PMdr, and 16 within PMdc). SFC measures the relationship of the spiking neurons to the local

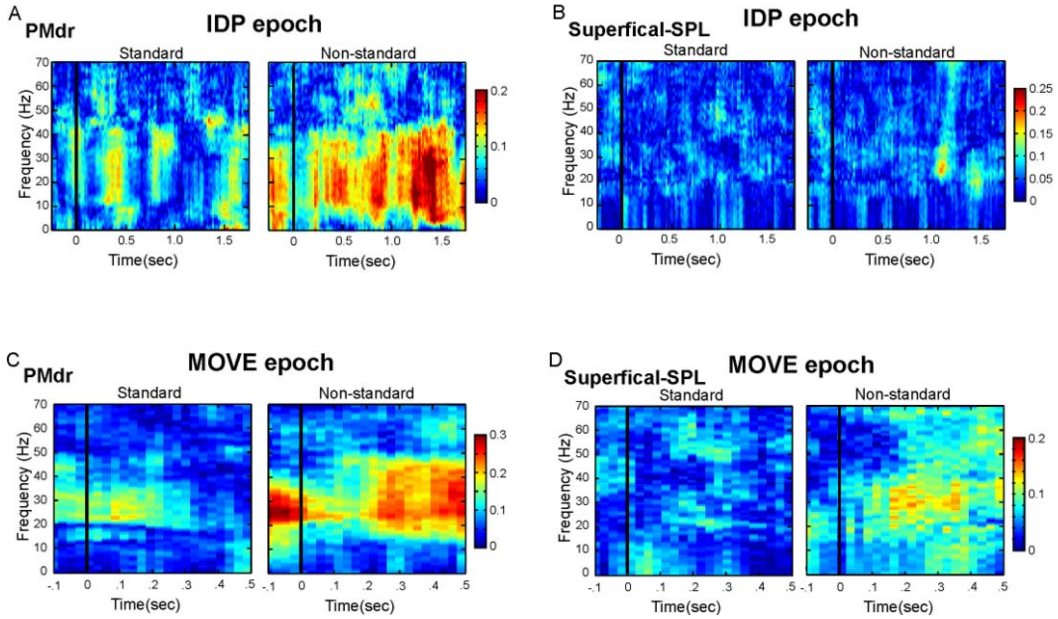

Figure 4.3: Example spike-field coherency. **A** and **C**) PMdr during IDP epoch and MOVE epochs. **B** and **D**) PEc during IDP epoch and MOVE epochs. Results show a different pattern of coherency for each region examined. Results were aligned to peripheral cue onset (A and B) and to movement onset (C and D), represented by the black vertical line. Amplitude is color coded.

field potential (Pesaran et al. 2008; Womelsdorf and Fries 2006) and thus it is an appropriate measure to gain insight into the computations of each of these region to different types of visually guiding reaching movements.

Stronger SFC during decoupled reaches:

Overall significant spike-field coherency occurred within the planning of visually-guided reaching movements (Figure 4.3A and B). However, consistent with our previous reports (Sayegh et al. 2013; Hawkins et al. 2013), we saw an enhancement in the SFC across the population of PMdr and PEc during decoupled reaches when compared to coupled reaches (Figure 4.4). Within PMdr, task-related SFC differences can be observed within the lower 1-10 Hz frequency range during the planning of a decoupled reach (Figure 4.4A, $P < 0.05$). When examining the time course between the SFC of each condition, enhanced SFC during decoupled reaches emerge roughly 700msec after the peripheral cue onset (Figure 4.4a, $P < 0.05$). In addition to these low frequency differences, PMdr also demonstrated enhanced SFC within the 17-38 Hz range during the planning of decoupled relative to coupled reaches (Figure 4.4B, $P < 0.05$). These differences did not occur until late within the planning epoch, occurring roughly 1500 msec after the peripheral cue onset. We observed a similar pattern of results across the population of PEcsites. Strong SFC was observed within the 17-38 Hz range during decoupled versus coupled reach planning (Figure 4.4C, $P < 0.05$). These task-related coherency differences emerged roughly 1200 msec after the peripheral cue onset (Figure 4.4C, $P < 0.05$). Importantly, the beta band SFC observed within the PEcwas within the same range and time frame as the beta-band SFC observed within PMdr.

As the trial progressed to the execution phase of the movement, PMdr and superficial-SPL remained as the two regions that displayed stronger SFC during decoupled versus coupled

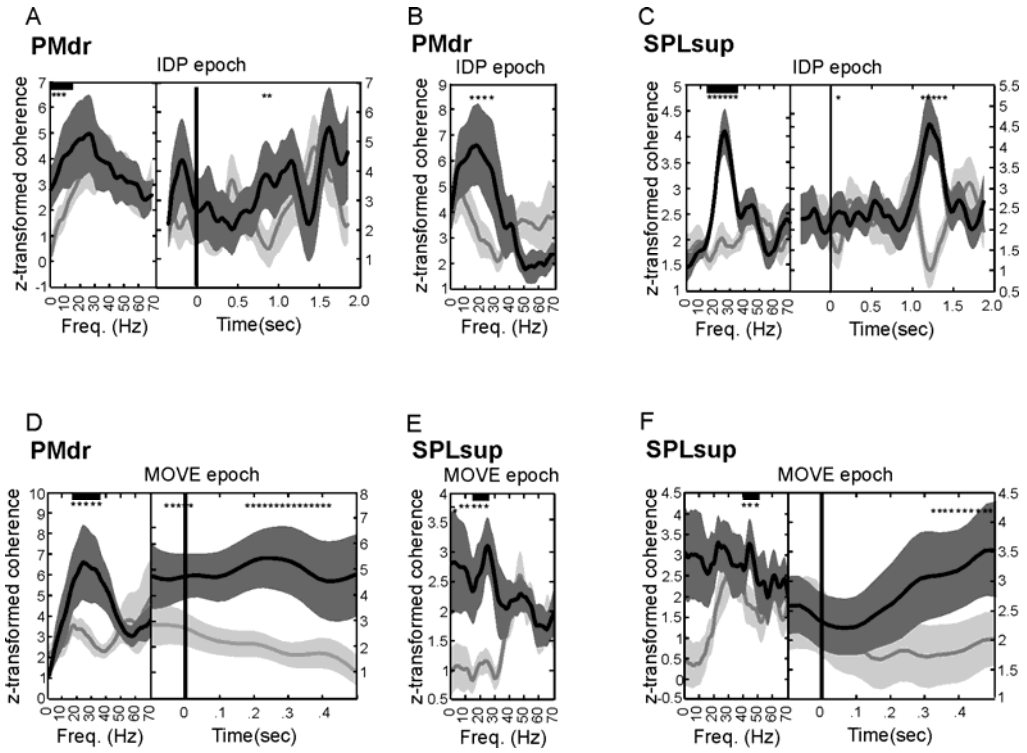

Figure 4.4: Population spike-field coherency line plots. **A** and **D**) PMdr z-transformed coherency during coupled (gray) and decoupled (black) conditions for the IDP (A) and MOVE (D) epochs. Asterisks denotes significance difference between conditions P <0.05. Black horizontal bar shows analysis window for right panel. Right panel show the time course for the frequency range selected across the population. **B**) PMdr z-transformed coherency showing significant difference in the higher 17-38 Hz range, $P < 0.05$. **C** and **E**) PEc z-transformed coherency during coupled (gray) and decoupled (black) conditions for the IDP (C) and MOVE E) epochs. **F**) PEc z-transformed coherency showing significant difference in the lower 1-30 Hz range, $P < 0.05$.

reaches (Figure 4.3C and D). Similar to the planning phase, across the population, PMdr demonstrated significantly greater SFC within the 17-45 Hz range for decoupled when compared to coupled reach execution (Figure 4.4D, $P < 0.05$). These task-related coherency differences began at movement onset and remained significantly different between conditions for the entire epoch (Figure 4.4D, $P < 0.05$). A similar pattern of coherency was observed within PEcas those observed during reach planning. Specifically, PEc demonstrated enhanced SFC within the 1-35 Hz that occurred just prior to movement onset (Figure 4.4E, $P < 0.05$). By reach execution a shift occurred and stronger SFC was observed within the 45 Hz range for decoupled reaches within PEc (Figure 4.4F, $P < 0.05$).

In summary decoupled reaches were associated with enhanced synchrony within PMdr and PEc. PMdr displayed strong alpha-band SFC beginning shortly after the onset of the peripheral cue. As the trial progressed into reach execution, the SFC within PMdr and PEc shifted into beta- and then gamma band synchrony. Taken collectively, these results suggest that PMdr and PEc preferentially process the visuomotor transformations
necessary during decoupled eye-hand reaches.

Stronger SFC during coupled reach planning:

Contrary to the observations of PMdr and PEc activity described in the above section, SFC within PMdc and MIP were significantly stronger during the performance of a coupled reach when compared to a decoupled reach (Figure 4.5A and B). During coupled reach planning, PMdc displayed stronger SFC within the 48-70 Hz range than during decoupled reach planning (Figure 4.6A, $P < 0.05$). When observing the time-course of these differences, they emerged roughly 400 msec after the peripheral cue was displayed (Figure 4.6A, $P < 0.05$). Within MIP, we also observed enhanced SFC for coupled versus decoupled reaches. Stronger

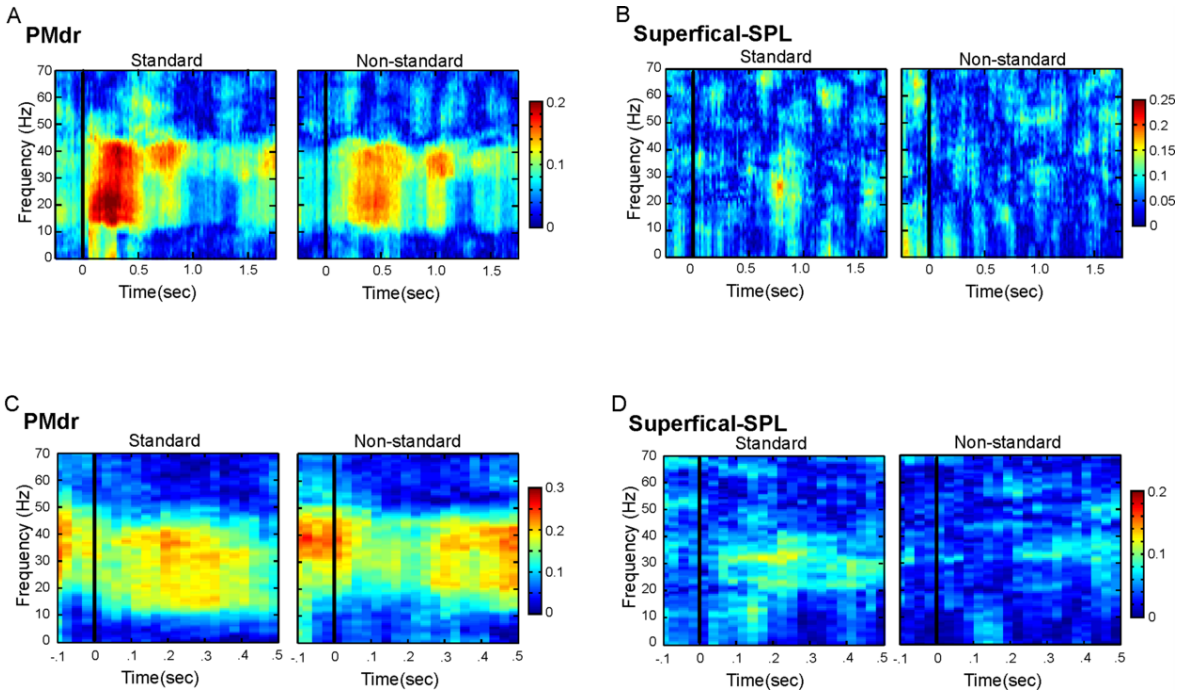

Figure 4.5: Example spike-field coherency. **A** and **C**) PMdc during IDP epoch and MOVE epoch. **B** and **C**) PEc during IDP epoch and MOVE epochs. Results show a different pattern of coherency for each region examined. Results were aligned to peripheral cue onset (A and B) and to movement onset (C and D), represented by the black vertical line. Amplitude is color coded.

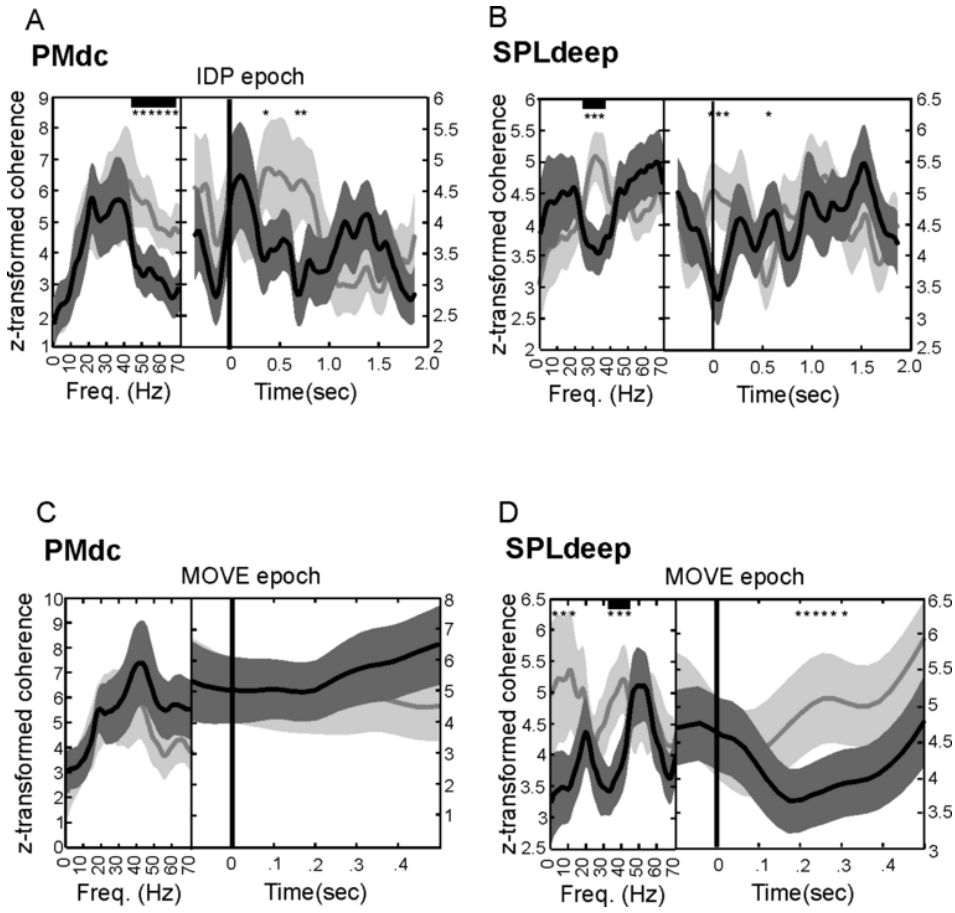

Figure 4.6: Population spike-field coherency line plots. **A** and **C**) PMdc z-transformed coherency during coupled (gray) and decoupled (black) conditions for the IDP (A) and MOVE (D) epochs. Asterisks denotes significance difference between conditions $P < 0.05$. Black vertical line shows peripheral cue or movement onset. Black horizontal bar shows analysis window for right panel. Right panel show the time course for the frequency range selected across the population. **B** and **D**) MIP z-transformed coherency during coupled (gray) and decoupled (black) conditions for the IDP (C) and MOVE E) epochs.

SFC occurred within the 28-38 Hz range at the onset of the peripheral cue (Figure 4.6B, $P < 0.05$). As the trial progressed these task-related differences within MIP disappeared.

During reach execution the pattern of SFC within PMdc and MIP shifted. By the onset of the reach the previously observed task-related differences within PMdc were not observed (Figure 4.6C). However, MIP maintained a stronger SFC for coupled when compared to decoupled reaches (Figure 4.6D). More specifically, stronger SFC was observed within the lower 1-12 Hz and 28-42 Hz range (Figure 4.6D, $P < 0.05$). These task-related differences occurred shortly after the onset of the reaching movement (Figure 4.6D, $P < 0.05$).

Taken collectively, PMdc and the MIP demonstrate enhanced synchrony for coupled when compared to decoupled reaches. PMdc demonstrated enhanced gamma band SFC during the planning of coupled reaches that resolved by movement onset. MIP showed stronger alpha and beta-band synchrony during the planning and execution of coupled reaches. These results suggest that during coupled reach planning, there is enhanced local communication within PMdc and MIP, supporting a stronger role of these regions in coupled visuomotor transformations.

DISCUSSION

Decoupled visually-guided reaches require additional processing in a number of ways compared to coupled reaching movements. First, decoupling the action of the eyes from the hand requires a greater cognitive influence over the sensory to motor transformation. These top-down influences alter the computations that occur in a context-related manner. For instance, a rule regarding the spatial transformation between the eyes and the hand must be incorporated into the upcoming reach plan. Second, because of the natural tendency for the action of the eyes and the hand to move together (Gielen et al. 1984; Prablanc et al. 1979; Henriques et al. 1998; Neggers and Bekkering 2000; Gauthier and Mussa Ivaldi 1988; Morasso 1981; Sergio and Scott

1998; Sergio and Scott 1998; Vercher et al. 1994; Gorbet and Sergio 2009; Terao et al. 2002), the computations involved in decoupled reaching must account for disengaging this linkage (Wise et al. 1996; Murray et al. 2000; Sergio et al. 2009). Finally, incongruent visual and sensory information will result in unreliable visual signals regarding the position of the hand relative to the target. Thus hand position must be derived predominantly from proprioceptive feedback and efference copy information (Buneo and Andersen 2006; Rushworth et al. 1997a; Engel et al. 2002; Flanders et al. 1992; Rushworth et al. 1997b; Nixon et al. 1992). Here, we measured the SFC within premotor and parietal regions because it allows one to determine if a relationship exists between individual neurons and the LFPs (Pesaran et al. 2008) and importantly, to determine how a region is selecting and transmitting information required to integrate sensory information for motor performance (Womelsdorf and Fries 2006; Fries 2005).

PMdr and PEc preferentially process decoupled reaches

To our knowledge we are the first group to show enhanced SFC within PMdr and superior SPL during decoupled reaching. These results support previous observations that these regions play a crucial role in visuomotor transformations when a rule dictates the relationship between the eyes and hand motion (Prado et al. 2005; Picard and Strick 2001; Kurata and Hoffman 1994; Halsband and Passingham 1985; Halsband and Passingham 1982; Sayegh et al. 2013; Gail et al. 2009; Hawkins et al. 2013).

Early within the planning of decoupled reaches PMdr demonstrated enhanced alpha-band SFC. Alpha-band synchrony (6-16Hz) has been observed to dominate during the active inhibition of a not-to-be-applied rule (Buschman et al. 2012). During decoupled reach planning, an inhibitory signal must be present to allow for the dissociation between the eyes and the hand (Gielen et al. 1984; Prablanc et al. 1979; Henriques et al. 1998; Neggers and Bekkering 2000;

Gauthier and Mussa Ivaldi 1988; Morasso 1981; Sergio and Scott 1998; Vercher et al. 1994; Gorbet and Sergio 2009; Terao et al. 2002). We propose that the observed enhanced alpha-band synchrony may signal the decoupling between the eyes and the hand. Additional research, such as muscimol studies targeting PMdr, would be an elegant way of examining the importance of alpha band synchrony to decoupled reach planning.

As the trial progressed from planning into movement we observed stronger beta-band (17-38 Hz) SFC within PMdr. Spike-field coherency within the beta band range has previously been shown to dominate within the infragranular cortical layers where many feedback projections terminate. Such an arrangement is indicative of top-down control (Engel and Fries 2010; Maier et al. 2010; Bosman et al. 2012; Bastos et al. 2012; Spaak et al. 2012) and, importantly, beta band activity is thought to be involved in the high-order executive function of rule selection within the prefrontal cortex (Buschman et al. 2012). PMdr and the dorso-lateral prefrontal cortex (DLPFC) have been shown to become functionally coupled when a motor behaviour is guided by a rule (Murray et al. 2000; Luppino et al. 2003; Abe and Hanakawa 2009; White and Wise 1999) and thus it is possible that the strong synchronization of the spikes and LFPs at the beta band range reflects the integration of the spatial rule into the motor plan. Further, long-range beta-band synchronization mediates top-down processing (Buschman and Miller 2007) between regions. PMdr is likely communicating the rule updated motor plan to other reach related regions. The high degree of communication between PMdr and SPL is essential for motor control (Battaglia-Mayer et al. 2001; Caminiti et al. 1999; Wise et al. 1997; Matelli et al. 1998; Luppino and Rizzolatti 2000). Importantly, both PMdr and PEc demonstrated enhanced beta-band-SFC within the same timeframe. The reciprocal communication between these regions, along with the necessary top-down control during decoupled reaches, is likely

driving the enhanced beta-band-synchrony, allowing PMdr to communicate the updated motor plan to other reach related regions.

During movement, the incongruent eye and hand signals require online processing in regions of SPL, such as PEc, where proprioceptive feedback is integrated into the ongoing motor command in order to monitor limb position and update body position (Buneo and Andersen 2006; Rushworth et al. 1997a; Jackson et al. 2009; Wolpert et al. 1998). Shortly after movement onset, we observed strong gamma-band synchronization between the spikes and LFPs within PMdr and superficial-SPL. Neuronal synchrony and coherency within the gamma-band range is observed within the superficial and granular cortical layers of a region, indicative of 'bottom-up' or feed-forward processing (Maier et al. 2010; Bosman et al. 2012; Bastos et al. 2012). During reach execution, this enhanced gamma SFC is likely reflecting the extra weight placed on proprioceptive and efference copy processing within SPL. Similarly, we propose that the observed gamma-band synchrony within PMdr reflects online error correction during the remapping of the relative position of the arm to the eyes (Caminiti et al. 1991; Lee and van Donkelaar 2006; Pesaran et al. 2006; Crammond and Kalaska 1996).

In summary, we observed no differences in behaviour between coupled and decoupled reaches. Thus the observed enhancements in synchrony within these regions provided insight into the enhanced processing that occurs during decoupled reach planning and execution. We suggest that the early computations within PMdr and PEc reflect rule-integration and inhibition of eye-hand coupling. By reach onset the local computation shifts to reflect the enhanced proprioceptive control needed during decoupled reach execution.

PMdc and deep SPL preferentially process coupled reaches

Compared to PMdr, PMdc is more directly connected to the motor system (M1),

preferentially coding limb movement parameters primarily when arm movements are controlled by visual or somatosensory information, and thus plays a more active role in the computations of coupled reaches (Prado et al. 2005; Picard and Strick 2001; Lee and van Donkelaar 2006; Sayegh et al. 2013; Gail et al. 2009). Similar observations were made for regions like the medial intraparietal sulcus (MIPs) located deep within SPL(Colby 1998). Although the MIPs is involved in the planning and execution of goal-directed reaches (Colby 1998), it is suggested to have a more active role in the online automatic corrections of coupled reaching movements (Prado et al. 2005; Clavagnier et al. 2007).

Here we observed greater SFC in PMdc and MIP within the gamma-band range during the planning of coupled versus decoupled reaches. During coupled reaches the visual target is guiding the action itself. This innate reaching behaviour does not require much cognitive control (Sergio et al. 2009; Bo et al. 2006; Gorbet and Sergio 2009). As gamma-band synchrony is indicative of bottom-up processing (Maier et al. 2010; Bosman et al. 2012; Bastos et al. 2012), the observed enhancements in gamma-band SFC during coupled reaches within PMdc and MIP is suggested to be reflecting the local biomechanical computations required to perform a simple reaching task.

Comparisons with human primate reach control

In summary, our work supports the idea of altered cortical control during different types of visuomotor mappings and highlights the need to account for the decoupled nature of a motor task when interpreting movement control research data. These data support the enhanced role of PMdc and MIP regions in preferentially processing coupled reaches (Prado et al. 2005; Clavagnier et al. 2007; Gail et al. 2009; Hawkins et al. 2013), distinct from the role of PMdr and

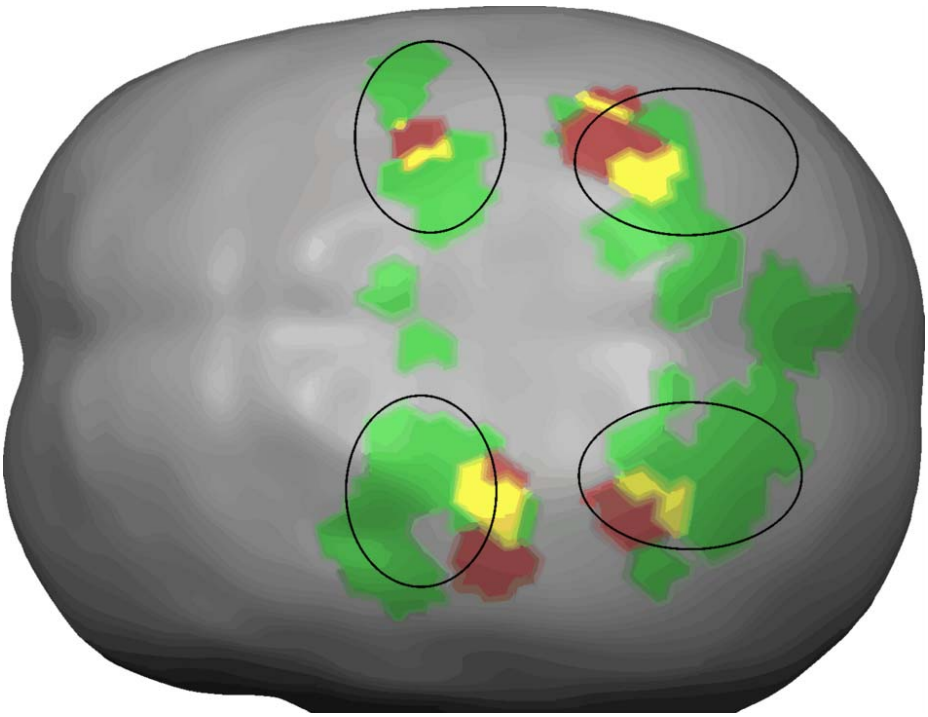

Figure 4.7: Review of previous fMRI studies on visually guided reaching. The reported peak Talairach coordinates of task-related activity within the dorsal premotor and/or superior parietal cortices(represented by the circles) from each study were plotted. Activity that occurred during coupled reaches are in red, decoupled reaches in green, and overlapped activity in yellow (Prado et al. 2005; Granek et al. 2010; Gorbet et al. 2004; Gorbet and Sergio 2007; Grafton et al. 1998; Filimon et al. 2009; Kertzman et al. 1997).

superior-caudal regions of SPL during decoupled reaches (Prado et al. 2005; Clavagnier et al. 2007; Sayegh et al. 2013). To look for evidence of a similar functional topography in the human brain, we undertook a imaging literature review examining fMRI findings reported in the literature for eye-hand coupled versus decoupled tasks. The observed pattern of activity associated with these different visuomotor mappings suggests delineation in the cortical activity of coupled

versus decoupled reaching in the human brain, and is in line with our research on non-human primates (Figure 4.7). Strikingly, human brain activity associated with decoupled reach tended to occur within the rostral portion of PMd and the superior-caudal portion of SPL. Activity associated with coupled reaches was localized to the caudal portion of PMd and deep regions within SPL surrounding mIPS. This pattern of activity, parallel to our observations in non-human primates, not only supports our neurophysiological studies, but also helps to bridge the gap between animal and human studies due to the strong relationship between LFPs and fMRI (Goense and Logothetis 2008; Nir et al. 2007). Lastly while research into the cortical control of different types of reaching behaviour exists, many of these studies focus on characterising how reach-related regions respond during fixation paradigms (Buneo et al. 2002; Pesaran et al. 2006; Gail et al. 2009; Andersen 1995), a type of decoupled reach. However, we have demonstrated changes in cortical activity of many regions within the parietofrontal reach network associated with eye-hand decoupling. Thus, our findings emphasize the importance of accounting for the nature of eye-hand visuomotor mapping when interpreting movement control data.

Chapter Five

Summary and Conclusion

5.1 Summary and Conclusion

The basic skill of coordinating vision and limb motion in order to interact with external objects requires a sophisticated level of control, and is carried out by numerous interconnected areas of the brain. The general innate linkage of the action of the eyes to the hand allows for coupled reaching movements to be more natural to produce (Wise et al. 1996; Sergio et al. 2009; Bo et al. 2006; Neggers and Bekkering 2000; Piaget 1965). However, many of our daily interactions involve actions that require a decoupling of the eyes from the hand, such as during tool use. Our ability to perform these types of reaches are not innate and must be learned over time (Wise et al. 1996; Sergio et al. 2009; Bo et al. 2006; Neggers and Bekkering 2000; Piaget 1965). Although patient (Granek et al. 2012; Battaglia-Mayer et al. 2012; Blangero et al. 2007; Pisella et al. 2009; Karnath and Perenin 2005) and imaging research (Prado et al. 2005; Granek et al. 2010; Gorbet et al. 2004) has supported the involvement of the cortical regions controlling decoupled or rule-based visually-guided reaching, how the particular nodes and the local computations are altered within this interconnected network has yet to be fully characterized. As such, the current dissertation explored specifically how these region are affected during eye hand decoupled reaching using a method that allowed for an in-depth, detailed examination of brain activity not possible with clinical and behavioural research (see Figure 4.7).

The three studies in this dissertation provide novel insight into the contribution of numerous cortical regions to the control of complex eye-hand coordination. Since we used a reaching task that required movement of the eyes and hand towards the cued target, we were one of the first groups to explore the cortical control of 'natural' reaching behaviour during coupled and decoupled situations. As such we can directly compare how decoupled reaching movements differ from coupled reaches in a more natural situation.

In chapter two, my **first goal** was to decipher the role of PMd in different types of reaching movements. To address this, we trained two rhesus macaques to perform coupled and decoupled reaching movements. Once trained, we recorded the neural activity (single unit and LFP) within PMd during their performance on these tasks. To address my **second goal** we divided the recorded activity, based on the topographical organization within PMd, into rostral and caudal groups. Here, we showed for the first time that during the planning stage PMdr was more active for decoupled when compared to coupled reaches. PMdc on the other hand was more active during coupled reach planning. During the execution phase, while no major difference occurred in the neural activity between PMdr and PMdc during coupled reaches, during decoupled reaches PMdc was more active when compared to both coupled reaches and the activity within PMdr. The results not only highlight the different roles PMdr and PMdc play in different types of visuomotor transformations, but also the necessity within the literature to account for the different sub-region of PMd when interpreting motor control data. These novel findings will be useful to not only the fundamental motor control community, but also to those working in the burgeoning field of neuroprosthetics.

In chapter three, my **third goal** was to understand the role of a different brain region, SPL, during the same reaching behaviours. The same rhesus macaques were studied using identical reach conditions in an effort to record changes in the neural activity (LFP) within SPL. Here, we showed that during the planning phase, the beta-dominated response observed within the LFPs was delayed during decoupled reaches. SPL in general was more active during coupled when compared to decoupled reach planning. By the execution phase this pattern shifted so that SPL was more active during decoupled versus coupled reaches. These results support the idea that decoupled reaches require more cognitive processing, shown in the delayed activity within SPL.

Decoupled reaches will rely on additional proprioceptive control because of the decoupled nature between the eyes and the hand. The extra activity within SPL during decoupled reach execution likely reflects this. What was striking about these results was the fact that these animals were highly over-trained on these tasks. Yet to successfully execute the decoupled behaviour required fairly extensive alterations to the parietofrontal network responsible for its control. Such a finding has implications for the control of decoupled movements in humans, and the effects that attention and aging might have on skilled performance when even highly trained brains are loaded during such movements.

In the fourth chapter, my **fourth goal** was to gain a more comprehensive view of the local computations with PMdr, PMdc, and SPL and how they change to accommodate the different types of reaching behaviours. We examined the SFC within these regions based on the previously recorded activity obtained within projects one and two. As a **fifth goal,** based largely on the results from the spike analysis within SPL, we divided SPL based on the superficial region, PEc, and deep region, MIP to determine if functional differences existed. The results presented here support the previous reports that during coupled reaching movements, PMdc and MIP are more active while during decoupled reaching movements PMdr and PEC are more active. As our work focused solely on the neural activity of non-human primates, our **sixth goal** was to carry out a imaging literature review examining fMRI findings reported in the literature for eye-hand coupled versus decoupled tasks in human primates. Here, we observed a striking similarity between our present results and those of the imaging literature review which support a distinction between PMdr and superfical SPL and PMdc and deep SPL in different types of visually-guided reaching movements.

Taken collectively, these projects provide novel insight to the alternative cortical

networks involved in decoupled eye-hand coordination. We propose that PMdr and superficial regions of SPL are crucial for accurate guidance of a limb during decoupled reaching. Coupled reaches may rely more heavily on the activity within PMdc and deep regions of SPL (for details, see Figure 4.7). More broadly, our results highlight the necessity of accounting for the coupled nature between the eyes and the hand during a motor task when interpreting movement control research data, and when seeking to apply neurophysiological signals to clinical functions.

5.2 Future direction and limitations

As in most experiments, the results presented in the current dissertation have raised a few more questions. Although it is clear that regions of SPL and PMd play different roles in visuomotor transformations that require a decoupling between the eyes from the hand, how exactly does the communication *between* these regions changes? A relevant follow-up study here would be to examine the SFC between the different regions of SPL and PMd to determine how the communication is affected by different eye-hand compatibilities. This analysis would give us a much fuller picture of how the weight of each region within the parietofrontal network shifts between time and across conditions.

Another intriguing question raised here is what is the role of the prefrontal cortex during the rule-integration process required during decoupled types of visuomotor transformations? Specifically because of the strong connection and functional coupling between PMdr and DLPFC (Murray et al. 2000; Luppino et al. 2003; Abe and Hanakawa 2009; White and Wise 1999) and the present observations regarding the role of PMdr, it would be of worth to determine the exact role of DLPFC when a motor behaviour is guided by a rule. Thus research focused on recording the neural activity within this region during similar paradigms would allow one to examine the proposed role this region may play in top-down control (Abe and Hanakawa 2009)

over the necessary visuomotor transformation. It may also be of interest to examine the communication between PMdr and DLPFC. If DLPFC indeed exerts top-down influence over the necessary transformations performed by PMd, analyzing for instance the SFC between these regions would be a great way to explore this idea.

As mentioned previously, decoupled reaches can take many forms. The studies presented here examined how parietal and premotor regions responded during decoupled reaches that depended more heavily, but not exclusively, on sensorimotor recalibration. We did not examine how reaches that required more explicit strategic control affected the activity within these parietofrontal regions. Tasks that use different levels of cursor rotation or arbitrary associations compared directly to coupled reaches must be employed to advance research into the basic control of rule-based behaviour. Some research has been done using an anti-pointing paradigm (Gail et al. 2009; Connolly et al. 2000) or arbitrary cues (Gorbet et al. 2004; Granek et al. 2007; Grafton et al. 1998). Neurophysiological studies, such as the one performed by Gail et al (2009), found stronger neural activity within PMdr during anti-pointing when compared to PMdc and some regions of SPL. Recently, Granek and Sergio (2014) suggested that tasks that rely more heavily on strategic control may depend on more prefrontal and inferior parietal region.

The fundamental research conducted in these series of studies can provide a basis for a myriad of clinical applications, such as being used as an assessment tool for cases of mild brain dysfunction. Preliminary research has demonstrated that mild brain dysfunction can impair performance when the goal of the eye and the hand has been decoupled. Specifically, this assessment tool could be used to detect early stages of Alzheimer's disease, as well as function as a part of the return-to-play protocols following a concussion. Preliminary evidence in our lab (Hawkins, Thayaparan, Bida & Sergio, 2011**)** suggests that decoupled eye-hand coordination

can detect deficits in individuals with just a family history of Alzheimer's disease, without the actual diagnosis itself and even detect deficits in athletes with a history of concussion, but without any current symptoms (Brown et al. 2011). By assessing the integrity of these different networks, we can distinguish subtle brain network-related deficits associated with different dementias. My work represents the fundamental characterization of how the brain plans and executes decoupled reaching movements. These data describe how parieto-frontal networks control such movements in the healthy state, thereby providing insight into the form of the underlying pathology in those situations of mild brain dysfunction where there is a deficit in decoupled movement performance.

In summary, these studies have provided novel information about the contribution of brain areas (summarized in Figure 4.7) to one of our most fundamental human behaviours, the flexibility of eye-hand coordination that allows for the interaction with our environment in a meaningful and skilled way.

References

Abe M and Hanakawa T. Functional coupling underlying motor and cognitive functions of the dorsal premotor cortex. *Behav Brain Res* 198: 1: 13-23, 2009.

Adrian ED and Matthews BH. The interpretation of potential waves in the cortex. *J Physiol* 81: 4: 440-471, 1934a.

Adrian ED and Matthews HC. The berger rhythm: potential changes from the occipital lobes in man. *Brain* 4: 57: 24, 1934b.

Aertsen AM, Gerstein GL, Habib MK and Palm G. Dynamics of neuronal firing correlation: modulation of "effective connectivity". *J Neurophysiol* 61: 5: 900-917, 1989.

Alexander GE and Crutcher MD. Preparation for movement: neural representations of intended direction in three motor areas of the monkey. *J Neurophysiol* 64: 1: 133-150, 1990.

Alink A, Schwiedrzik CM, Kohler A, Singer W and Muckli L. Stimulus predictability reduces responses in primary visual cortex. *J Neurosci* 30: 8: 2960-2966, 2010.

Andersen RA, S.L.,Bradley DC, Xing,J. Multimodal representation of space in the posterior parietal cortex and it's use in planning movements. 20: 303-330, 1997.

Andersen RA. Encoding of intention and spatial location in the posterior parietal cortex. *Cereb Cortex* 457-469, 1995.

Andersen RA and Buneo CA. Intentional maps in posterior parietal cortex. *Annu Rev Neurosci* 25: 189-220, 2002.

Andersen RA, Essick GK and Siegel RM. Neurons of area 7 activated by both visual stimuli and oculomotor behavior. *Exp Brain Res* 67: 2: 316-322, 1987.

Andersen RA, Essick GK and Siegel RM. Encoding of spatial location by posterior parietal neurons. *Science* 230: 4724: 456-458, 1985.

Archambault PS, Ferrari-Toniolo S and Battaglia-Mayer A. Online control of hand trajectory and evolution of motor intention in the parietofrontal system. *J Neurosci* 31: 2: 742-752, 2011.

Asher I, Stark E, Abeles M and Prut Y. Comparison of direction and object selectivity of local field potentials and single units in macaque posterior parietal cortex during prehension. *J Neurophysiol* 97: 5: 3684-3695, 2007.

Baker SN, Kilner JM, Pinches EM and Lemon RN. The role of synchrony and oscillations in the motor output. *Exp Brain Res* 128: 1-2: 109-117, 1999.

Bakola S, Gamberini M, Passarelli L, Fattori P and Galletti C. Cortical connections of parietal field PEc in the macaque: linking vision and somatic sensation for the control of limb action. *Cereb Cortex* 20: 11: 2592-2604, 2010.

Barbas H and Pandya DN. Architecture and frontal cortical connections of the premotor cortex (area 6) in the rhesus monkey. *J Comp Neurol* 256: 2: 211-228, 1987.

Bastos AM, Usrey WM, Adams RA, Mangun GR, Fries P and Friston KJ. Canonical microcircuits for predictive coding. *Neuron* 76: 4: 695-711, 2012.

BATES JA and ETTLINGER G. Posterior biparietal ablations in the monkey. Changes to neurological and behavioral testing. *Arch Neurol* 3: 177-192, 1960.

Batista AP, Buneo CA, Snyder LH and Andersen RA. Reach plans in eye-centered coordinates. *Science* 285: 5425: 257-260, 1999.

Battaglia-Mayer A, Archambault PS and Caminiti R. The cortical network for eye-hand coordination and its relevance to understanding motor disorders of parietal patients. *Neuropsychologia* 44: 13: 2607-2620, 2006.

Battaglia-Mayer A and Caminiti R. Optic ataxia as a result of the breakdown of the global tuning fields of parietal neurones. *Brain* 125: Pt 2: 225-237, 2002.

Battaglia-Mayer A, Caminiti R, Lacquaniti F and Zago M. Multiple levels of representation of reaching in the parieto-frontal network. *Cereb Cortex* 13: 10: 1009-1022, 2003.

Battaglia-Mayer A, Ferraina S, Genovesio A, Marconi B, Squatrito S, Molinari M, Lacquaniti F and Caminiti R. Eye-hand coordination during reaching. II. An analysis of the relationships between visuomanual signals in parietal cortex and parieto-frontal association projections. *Cereb Cortex* 11: 6: 528-544, 2001.

Battaglia-Mayer A, Ferraina S, Mitsuda T, Marconi B, Genovesio A, Onorati P, Lacquaniti F and Caminiti R. Early coding of reaching in the parietooccipital cortex. *J Neurophysiol* 83: 4: 2374-2391, 2000.

Battaglia-Mayer A, Ferrari-Toniolo S, Visco-Comandini F, Archambault PS, Saberi-Moghadam S and Caminiti R. Impairment of Online Control of Hand and Eye Movements in a Monkey Model of Optic Ataxia. *Cereb Cortex* 2012.

Battaglini PP, Muzur A, Galletti C, Skrap M, Brovelli A and Fattori P. Effects of lesions to area V6A in monkeys. *Exp Brain Res* 144: 3: 419-422, 2002.

Battaglini PP, Muzur A and Skrap M. Visuomotor deficits and fast recovery after area V6A lesion in monkeys. *Behav Brain Res* 139: 1-2: 115-122, 2003.

Bedford FL. Perceptual and cognitive spatial learning. *J Exp Psychol* 19: 517-530, 1993.

Berger H. Ueber das Elektroenkephalogramm des Menschen. *Arch Psychiatr Nervenkrankh* 87: 527-570, 1929.

Blangero A, Menz MM, McNamara A and Binkofski F. Parietal modules for reaching. *Neuropsychologia* 47: 6: 1500-1507, 2009.

Blangero A, Ota H, Delporte L, Revol P, Vindras P, Rode G, Boisson D, Vighetto A, Rossetti Y and Pisella L. Optic ataxia is not only 'optic': impaired spatial integration of proprioceptive information. *Neuroimage* 36 Suppl 2: T61-8, 2007.

Blatt GJ, Andersen RA and Stoner GR. Visual receptive field organization and cortico-cortical connections of the lateral intraparietal area (area LIP) in the macaque. *J Comp Neurol* 299: 4: 421-445, 1990.

Bo J, Contreras-Vidal JL, Kagerer FA and Clark JE. Effects of increased complexity of visuo-motor transformations on children's arm movements. *Hum Mov Sci* 25: 4-5: 553-567, 2006.

Bock O. Components of sensorimotor adaptation in young and elderly subjects. *Exp Brain Res* 160: 2: 259-263, 2005.

Bosman CA, Schoffelen JM, Brunet N, Oostenveld R, Bastos AM, Womelsdorf T, Rubehn B, Stieglitz T, De Weerd P and Fries P. Attentional stimulus selection through selective synchronization between monkey visual areas. *Neuron* 75: 5: 875-888, 2012.

Boussaoud D. Attention versus intention in the primate premotor cortex. *Neuroimage* 14: 1 Pt 2: S40-5, 2001.

Boussaoud D. Primate premotor cortex: modulation of preparatory neuronal activity by gaze angle. *J Neurophysiol* 73: 2: 886-890, 1995.

Boussaoud D, Jouffrais C and Bremmer F. Eye position effects on the neuronal activity of dorsal premotor cortex in the macaque monkey. *J Neurophysiol* 80: 3: 1132-1150, 1998.

Boussaoud D and Wise SP. Primate frontal cortex: effects of stimulus and movement. *Exp Brain Res* 95: 1: 28-40, 1993a.

Boussaoud D and Wise SP. Primate frontal cortex: neuronal activity following attentional versus intentional cues. *Exp Brain Res* 95: 1: 15-27, 1993b.

Breveglieri R, Galletti C, Gamberini M, Passarelli L and Fattori P. Somatosensory cells in area PEc of macaque posterior parietal cortex. *J Neurosci* 26: 14: 3679-3684, 2006.

Brink F, Bronk DW and Larrabee MG. Chemical excitation of a nerve. *Ann N Y Acad Sci* 47: 457-485, 1946.

Brovelli A, Ding M, Ledberg A, Chen Y, Nakamura R and Bressler SL. Beta oscillations in a large-scale sensorimotor cortical network: directional influences revealed by Granger causality. *Proc Natl Acad Sci U S A* 101: 26: 9849-9854, 2004.

Brovelli A, Lachaux JP, Kahane P and Boussaoud D. High gamma frequency oscillatory activity dissociates attention from intention in the human premotor cortex. *Neuroimage* 28: 1: 154-164, 2005.

Brown JA, Hughes C and Sergio LE. The detrimental effects of concussion on cognitive-motor integration. *Soc Neurosci Abstr* November: 698.19, 2011.

Buffalo EA, Fries P, Landman R, Buschman TJ and Desimone R. Laminar differences in gamma and alpha coherence in the ventral stream. . *Proc Natl Acad Sci U S A* 108: 11262-11267, 2011.

Bullock TH. Problems in the Comparative Study of Brain Waves. *Yale J Biol Med* 17: 5: 657-680.3, 1945.

Buneo CA and Andersen RA. The posterior parietal cortex: sensorimotor interface for the planning and online control of visually guided movements. *Neuropsychologia* 44: 13: 2594-2606, 2006.

Buneo CA, Jarvis MR, Batista AP and Andersen RA. Properties of spike train spectra in two parietal reach areas. *Exp Brain Res* 153: 2: 134-139, 2003.

Buneo CA, Jarvis MR, Batista AP and Andersen RA. Direct visuomotor transformations for reaching. *Nature* 416: 6881: 632-636, 2002.

Burbaud P, Doegle C, Gross C and Bioulac B. A quantitative study of neuronal discharge in areas 5, 2, and 4 of the monkey during fast arm movements. *J Neurophysiol* 66: 2: 429-443, 1991.

Buschman TJ, Denovellis EL, Diogo C, Bullock D and Miller EK. Synchronous oscillatory neural ensembles for rules in the prefrontal cortex. *Neuron* 76: 4: 838-846, 2012.

Buschman TJ and Miller EK. Top-down versus bottom-up control of attention in the prefrontal and posterior parietal cortices. *Science* 315: 5820: 1860-1862, 2007.

Buzsaki G. *Rhythums of the Brain.* New York: Oxford University Press, 2006, p. 448.

Buzsaki G and Draguhn A. Neuronal oscillations in cortical networks. *Science* 304: 5679: 1926-1929, 2004.

Caminiti R, Ferraina S and Johnson PB. The sources of visual information to the primate frontal lobe: a novel role for the superior parietal lobule. *Cereb Cortex* 6: 3: 319-328, 1996.

Caminiti R, Ferraina S and Mayer AB. Visuomotor transformations: early cortical mechanisms of reaching. *Curr Opin Neurobiol* 8: 6: 753-761, 1998.

Caminiti R, Genovesio A, Marconi B, Battaglia-Mayer A, Onorati P, Ferraina S, Mitsuda T, Giannetti S, Squatrito S, Maioli M and Molinari M. Early coding of reaching: frontal and parietal association connections of parieto-occipital cortex. *Eur J Neurosci* 11: 3339-3345, 1999.

Caminiti R, Johnson PB, Burnod Y, Galli C and Ferraina S. Shift of preferred directions of premotor cortical cells with arm movements performed across the workspace. *Exp Brain Res* 83: 1: 228-232, 1990.

Caminiti R, Johnson PB, Galli C, Ferraina S and Burnod Y. Making arm movements within different parts of space: the premotor and motor cortical representation of a coordinate system for reaching to visual targets. *J Neurosci* 11: 5: 1182-1197, 1991.

Cavada C and Goldman-Rakic PS. Posterior parietal cortex in rhesus monkey: I. Parcellation of areas based on distinctive limbic and sensory corticocortical connections. *J Comp Neurol* 287: 4: 393-421, 1989.

Chen LL and Wise SP. Neuronal activity in the supplementary eye field during acquisition of conditional oculomotor associations. *J Neurophysiol* 73: 3: 1101-1121, 1995.

Chen X, Scangos KW and Stuphorn V. Supplementary motor area exerts proactive and reactive control of arm movements. *J Neurosci* 30: 44: 14657-14675, 2010.

Chrobak JJ and Buzsaki G. Gamma oscillations in the entorhinal cortex of the freely behaving rat. *J Neurosci* 18: 1: 388-398, 1998.

Cisek P, Crammond DJ and Kalaska JF. Neural activity in primary motor and dorsal premotor cortex in reaching tasks with the contralateral versus ipsilateral arm. *J Neurophysiol* 89: 2: 922-942, 2003.

Cisek P and Kalaska JF. Neural correlates of reaching decisions in dorsal premotor cortex: specification of multiple direction choices and final selection of action. *Neuron* 45: 5: 801-814, 2005.

Cisek P and Kalaska JF. Modest gaze-related discharge modulation in monkey dorsal premotor cortex during a reaching task performed with free fixation. *J Neurophysiol* 88: 2: 1064-1072, 2002a.

Cisek P and Kalaska JF. Simultaneous encoding of multiple potential reach directions in dorsal premotor cortex. *J Neurophysiol* 87: 2: 1149-1154, 2002b.

Clavagnier S, Prado J, Kennedy H and Perenin MT. How humans reach: distinct cortical systems for central and peripheral vision. *Neuroscientist* 13: 1: 22-27, 2007.

Clower DM and Boussaoud D. Selective use of perceptual recalibration versus visuomotor skill acquisition. *J Neurophysiol* 84: 2703-2708, 2000.

Clower DM, Hoffman JM, Votaw JR, Faber TL, Woods RP and Alexander GE. Role of posterior parietal cortex in the recalibration of visually guided reaching. *Nature* 383: 6601: 618-621, 1996.

Cohen YE and Andersen RA. A common reference frame for movement plans in the posterior parietal cortex. *Nat Rev Neurosci* 3: 7: 553-562, 2002.

Colby CL. Action-oriented spatial reference frames in cortex. *Neuron* 20: 1: 15-24, 1998.

Colby CL and Duhamel JR. Heterogeneity of extrastriate visual areas and multiple parietal areas in the macaque monkey. *Neuropsychologia* 29: 6: 517-537, 1991.

Colby CL, Gattass R, Olson CR and Gross CG. Topographical organization of cortical afferents to extrastriate visual area PO in the macaque: a dual tracer study. *J Comp Neurol* 269: 3: 392-413, 1988.

Colby CL and Goldberg ME. Space and attention in parietal cortex. *Annu Rev Neurosci* 22: 319-349, 1999.

Connolly JD, Goodale MA, Desouza JF, Menon RS and Vilis T. A comparison of frontoparietal fMRI activation during anti-saccades and anti-pointing. *J Neurophysiol* 84: 3: 1645-1655, 2000.

Cooper NR, Croft RJ, Dominey SJ, Burgess AP and Gruzelier JH. Paradox lost? Exploring the role of alpha oscillations during externally vs. internally directed attention and the implications for idling and inhibition hypotheses. *Int J Psychophysiol* 47: 1: 65-74, 2003.

Crammond DJ and Kalaska JF. Differential relation of discharge in primary motor cortex and premotor cortex to movements versus actively maintained postures during a reaching task. *Exp Brain Res* 108: 1: 45-61, 1996.

Crammond DJ and Kalaska JF. Modulation of preparatory neuronal activity in dorsal premotor cortex due to stimulus-response compatibility. *J Neurophysiol* 71: 3: 1281-1284, 1994.

Crammond DJ and Kalaska JF. Neuronal activity in primate parietal cortex area 5 varies with intended movement direction during an instructed-delay period. *Exp Brain Res* 76: 2: 458-462, 1989.

Crawford JD, Henriques DY and Medendorp WP. Three-dimensional transformations for goal-directed action. *Annu Rev Neurosci* 34: 309-331, 2011.

Crawford JD, Medendorp WP and Marotta JJ. Spatial transformations for eye-hand coordination. *J Neurophysiol* 92: 1: 10-19, 2004.

Csicsvari J, Jamieson B, Wise KD and Buzsaki G. Mechanisms of gamma oscillations in the hippocampus of the behaving rat. *Neuron* 37: 2: 311-322, 2003.

Culham JC, Cavina-Pratesi C and Singhal A. The role of parietal cortex in visuomotor control: what have we learned from neuroimaging? *Neuropsychologia* 44: 13: 2668-2684, 2006.

Culham JC and Kanwisher NG. Neuroimaging of cognitive functions in human parietal cortex. *Curr Opin Neurobiol* 11: 2: 157-163, 2001.

Culham JC and Valyear KF. Human parietal cortex in action. *Curr Opin Neurobiol* 16: 2: 205-212, 2006.

Davis PA. Electroencephalographic Studies on three cases of Frontal Lobotomy. *Psychosomatic Medicine* 3: 1: 38-50, 1941.

Denker M, Roux S, Linden H, Diesmann M, Riehle A and Grun S. The local field potential reflects surplus spike synchrony. *Cereb Cortex* 21: 12: 2681-2695, 2011.

DENNY-BROWN D and CHAMBERS RA. The parietal lobe and behavior. *Res Publ Assoc Res Nerv Ment Dis* 36: 35-117, 1958.

Desmurget M, Epstein CM, Turner RS, Prablanc C, Alexander GE and Grafton ST. Role of the posterior parietal cortex in updating reaching movements to a visual target. *Nat Neurosci* 2: 6: 563, 1999.

Desmurget M and Grafton S. Forward modeling allows feedback control for fast reaching movements. *Trends Cogn Sci* 4: 11: 423-431, 2000.

di Pellegrino G and Wise SP. Visuospatial versus visuomotor activity in the premotor and prefrontal cortex of a primate. *J Neurosci* 13: 3: 1227-1243, 1993.

Donner TH and Siegel M. A framework for local cortical oscillation patterns. *Trends Cogn Sci* 15: 5: 191-199, 2011.

Donoghue JP, Sanes JN, Hatsopoulos NG and Gaal G. Neural discharge and local field potential oscillations in primate motor cortex during voluntary movements. *J Neurophysiol* 79: 1: 159-173, 1998.

Engel AK and Fries P. Beta-band oscillations--signalling the status quo? *Curr Opin Neurobiol* 20: 2: 156-165, 2010.

Engel AK, Konig P, Gray CM and Singer W. Stimulus-Dependent Neuronal Oscillations in Cat Visual Cortex: Inter-Columnar Interaction as Determined by Cross-Correlation Analysis. *Eur J Neurosci* 2: 7: 588-606, 1990.

Engel KC, Flanders M and Soechting JF. Oculocentric frames of reference for limb movement. *Arch Ital Biol* 140: 3: 211-219, 2002.

Epelboim J, Steinman RM, Kowler E, Pizlo Z, Erkelens CJ and Collewijn H. Gaze-shift dynamics in two kinds of sequential looking tasks. *Vision Res* 37: 18: 2597-2607, 1997.

Eskandar EN and Assad JA. Dissociation of visual, motor and predictive signals in parietal cortex during visual guidance. *Nat Neurosci* 2: 1: 88-93, 1999.

Everling S, Dorris MC, Klein RM and Munoz DP. Role of primate superior colliculus in preparation and execution of anti-saccades and pro-saccades. *J Neurosci* 19: 7: 2740-2754, 1999.

Fattori P, Breveglieri R, Amoroso K and Galletti C. Evidence for both reaching and grasping activity in the medial parieto-occipital cortex of the macaque. *Eur J Neurosci* 20: 9: 2457-2466, 2004.

Felleman DJ and Van Essen DC. Distributed hierarchical processing in the primate cerebral cortex. *Cereb Cortex* 1: 1: 1-47, 1991.

Ferrier D. *West Riding Lunatic Asylum Medical Reports* 3: 30-96, 1873.

Filimon F, Nelson JD, Huang RS and Sereno MI. Multiple parietal reach regions in humans: cortical representations for visual and proprioceptive feedback during on-line reaching. *J Neurosci* 29: 9: 2961-2971, 2009.

Flanders M, Helms-Tillery SI and Soechting JF. Early stages in the sensorimotor transformation. *Behav Brain Sci* 15: 309-362, 1992.

Flint RD, Lindberg EW, Jordan LR, Miller LE and Slutzky MW. Accurate decoding of reaching movements from field potentials in the absence of spikes. *J Neural Eng* 9: 4: 046006-2560/9/4/046006. Epub 2012 Jun 25, 2012.

Fries P. A mechanism for cognitive dynamics: neuronal communication through neuronal coherence. *Trends Cogn Sci* 9: 10: 474-480, 2005.

Fries P, Reynolds JH, Rorie AE and Desimone R. Modulation of oscillatory neuronal synchronization by selective visual attention. *Science* 291: 5508: 1560-1563, 2001.

Fritsch G and Hitzig E.
On the electrical excitability of the cerebrum. *Arch f Anat , Physiol und wissenschaftl Mediz , Leipzig,* 37: 300-332, 1870.

Frohlich F and McCormick DA. Endogenous electric fields may guide neocortical network activity. *Neuron* 67: 1: 129-143, 2010.

Fujii N, Mushiake H and Tanji J. Rostrocaudal distinction of the dorsal premotor area based on oculomotor involvement. *J Neurophysiol* 83: 3: 1764-1769, 2000.

Gail A, Klaes C and Westendorff S. Implementation of spatial transformation rules for goal-directed reaching via gain modulation in monkey parietal and premotor cortex. *J Neurosci* 29: 30: 9490-9499, 2009.

Galambos R. Cochlear Potentials from the Bat. *Science* 93: 2409: 215, 1941.

Galletti C, Battaglini PP and Fattori P. Parietal neurons encoding spatial locations in craniotopic coordinates. *Exp Brain Res* 96: 2: 221-229, 1993.

Galletti C, Battaglini PP and Fattori P. Functional Properties of Neurons in the Anterior Bank of the Parieto-occipital Sulcus of the Macaque Monkey. *Eur J Neurosci* 3: 5: 452-461, 1991.

Galletti C, Fattori P, Gamberini M and Kutz DF. The cortical visual area V6: brain location and visual topography. *Eur J Neurosci* 11: 11: 3922-3936, 1999.

Galletti C, Fattori P, Kutz DF and Battaglini PP. Arm movement-related neurons in the visual area V6A of the macaque superior parietal lobule. *Eur J Neurosci* 9: 2: 410-413, 1997.

Galletti C, Fattori P, Kutz DF and Gamberini M. Brain location and visual topography of cortical area V6A in the macaque monkey. *Eur J Neurosci* 11: 2: 575-582, 1999.

Galletti C, Gamberini M, Kutz DF, Fattori P, Luppino G and Matelli M. The cortical connections of area V6: an occipito-parietal network processing visual information. *Eur J Neurosci* 13: 8: 1572-1588, 2001.

Galletti C, Kutz DF, Gamberini M, Breveglieri R and Fattori P. Role of the medial parieto-occipital cortex in the control of reaching and grasping movements. *Exp Brain Res* 153: 2: 158-170, 2003.

Gamberini M, Passarelli L, Fattori P, Zucchelli M, Bakola S, Luppino G and Galletti C. Cortical connections of the visuomotor parietooccipital area V6Ad of the macaque monkey. *J Comp Neurol* 513: 6: 622-642, 2009.

Gauthier GM and Hofferer JM. Eye tracking of self-moved targets in the absence of vision. *Exp Brain Res* 26: 2: 121-139, 1976.

Gauthier GM and Mussa Ivaldi F. Oculo-manual tracking of visual targets in monkey: role of the arm afferent information in the control of arm and eye movements. *Exp Brain Res* 73: 1: 138-154, 1988.

Gaveau V, Pelisson D, Blangero A, Urquizar C, Prablanc C, Vighetto A and Pisella L. Saccade control and eye-hand coordination in optic ataxia. *Neuropsychologia* 46: 2: 475-486, 2008.

Georgopoulos AP, Kalaska JF, Caminiti R and Massey JT. On the relations between the direction of two-dimensional arm movements and cell discharge in primate motor cortex. *J Neurosci* 2: 11: 1527-1537, 1982.

Georgopoulos AP and Massey JT. Cognitive spatial-motor processes. 2. Information transmitted by the direction of two-dimensional arm movements and by neuronal populations in primate motor cortex and area 5. *Exp Brain Res* 69: 2: 315-326, 1988.

Geyer S, Matelli M, Luppino G and Zilles K. Functional neuroanatomy of the primate isocortical motor system. *Anat Embryol* 202: 6: 443-474, 2000.

Ghilardi MF, Alberoni M, Marelli S, Rossi M, Franceschi M, Ghez C and Fazio F. Impaired movement control in Alzheimer's disease. *Neurosci Lett* 260: 1: 45-48, 1999.

Gielen CC, van den Heuvel PJ and van Gisbergen JA. Coordination of fast eye and arm movements in a tracking task. *Exp Brain Res* 56: 1: 154-161, 1984.

Godschalk M, Lemon RN, Nijs HG and Kuypers HG. Behaviour of neurons in monkey peri-arcuate and precentral cortex before and during visually guided arm and hand movements. *Exp Brain Res* 44: 1: 113-116, 1981.

Goense JB and Logothetis NK. Neurophysiology of the BOLD fMRI signal in awake monkeys. *Curr Biol* 18: 9: 631-640, 2008.

Goodale MA. Visual pathways supporting perception and action in the primate cerebral cortex. *Curr Opin Neurobiol* 3: 4: 578-585, 1993.

Goodale MA and Milner AD. Separate visual pathways for perception and action. *Trends Neurosci* 15: 1: 20-25, 1992.

Goodbody SJ and Wolpert DM. The effect of visuomotor displacements on arm movement paths. *Exp Brain Res* 127: 2: 213-223, 1999.

Gorbet DJ and Staines WR. Inhibition of contralateral premotor cortex delays visually guided reaching movements in men
but not women. *Exp Brain Res* In Press: 2010.

Gorbet DJ and Sergio LE. The behavioural consequences of dissociating the spatial directions of eye and arm movements. *Brain Res* 1284: 77-88, 2009.

Gorbet DJ and Sergio LE. Preliminary sex differences in human cortical BOLD fMRI activity during the preparation of increasingly complex visually guided movements. *Eur J Neurosci* 25: 4: 1228-1239, 2007.

Gorbet DJ, Staines WR and Sergio LE. Brain mechanisms for preparing increasingly complex sensory to motor transformations. *Neuroimage* 23(3): 1100-1111, 2004.

Gordon J, Ghilardi MF, Cooper SE and Ghez C. Accuracy of planar reaching movements. II. Systematic extent errors resulting from inertial anisotropy. *Exp Brain Res* 99: 1: 112-130, 1994.

Grafton ST, Fagg AH and Arbib MA. Dorsal premotor cortex and conditional movement selection: A PET functional mapping study. *J Neurophysiol* 79: 2: 1092-1097, 1998.

Grafton ST, Fagg AH, Woods RP and Arbib MA. Functional anatomy of pointing and grasping in humans. *Cereb Cortex* 6: 2: 226-237, 1996.

Grafton ST, Hazeltine E and Ivry RB. Abstract and effector-specific representations of motor sequences identified with PET. *J Neurosci* 18: 22: 9420-9428, 1998.

Granek JA, Gorbet DJ and Sergio LE. The effects of video-game experience on the cortical networks for increasingly complex visuomotor tasks. *Soc Neurosci Abstr* 618.24: 2007.

Granek JA and Sergio LE. Evidence for distinct brain networks in the control of rule-based motor behavior. . *Journal of Neurophysiology* In Revision: 2014.

Granek JA and Sergio LE. Different brain pathways for strategic control versus sensorimotor recalibration: Evidence from a dual task reach paradigm. *NCM annual meeting* 2012.

Granek JA, Gorbet DJ and Sergio LE. Extensive video-game experience alters cortical networks for complex visuomotor transformations. *Cortex* 46: 9: 1165-1177, 2010.

Granek JA, Pisella L, Blangero A, Rossetti Y and Sergio LE. The role of the caudal superior parietal lobule in updating hand location in peripheral vision: further evidence from optic ataxia. *PLoS One* 7: 10: e46619, 2012.

Granek JA, Pisella L, Stemberger J, Vighetto A, Rossetti Y and Sergio LE. Decoupled Visually-Guided Reaching in Optic Ataxia: Differences in Motor Control between Canonical and Non-Canonical Orientations in Space. *PLoS One* 8: 12: e86138, 2013.

Graziano MS, Cooke DF and Taylor CS. Coding the location of the arm by sight. *Science* 290: 5497: 1782-1786, 2000.

Grea H, Pisella L, Rossetti Y, Desmurget M, Tilikete C, Grafton S, Prablanc C and Vighetto A. A lesion of the posterior parietal cortex disrupts on-line adjustments during aiming movements. *Neuropsychologia* 40: 13: 2471-2480, 2002.

Grefkes C, Ritzl A, Zilles K and Fink GR. Human medial intraparietal cortex subserves visuomotor coordinate transformation. *Neuroimage* 23: 4: 1494-1506, 2004.

Grol MJ, Majdandzic J, Stephan KE, Verhagen L, Dijkerman HC, Bekkering H, Verstraten FA and Toni I. Parieto-frontal connectivity during visually guided grasping. *J Neurosci* 27: 44: 11877-11887, 2007.

Halsband U and Freund HJ. Premotor cortex and conditional motor learning in man. *Brain* 113 (Pt 1): Pt 1: 207-222, 1990.

Halsband U, Matsuzaka Y and Tanji J. Neuronal activity in the primate supplementary, pre-supplementary and premotor cortex during externally and internally instructed sequential movements. *Neurosci Res* 20: 2: 149-155, 1994.

Halsband U and Passingham R. The role of premotor and parietal cortex in the direction of action. *Brain Res* 240: 2: 368-372, 1982.

Halsband U and Passingham RE. Premotor cortex and the conditions for movement in monkeys (Macaca fascicularis). *Behav Brain Res* 18: 3: 269-277, 1985.

Hanakawa T, Honda M, Zito G, Dimyan MA and Hallett M. Brain activity during visuomotor behavior triggered by arbitrary and spatially constrained cues: an fMRI study in humans. *Exp Brain Res* 172: 2: 275-282, 2006.

Harris KD, Csicsvari J, Hirase H, Dragoi G and Buzsaki G. Organization of cell assemblies in the hippocampus. *Nature* 424: 6948: 552-556, 2003.

Hawkins KM, Sayegh P, Yan X, Crawford JD and Sergio LE. Neural activity in superior parietal cortex during rule-based visual-motor transformations. *J Cog Neurosci* (in press): 2012.

Hawkins KM, Sayegh P, Yan X, Crawford JD and Sergio LE. Neural activity in superior parietal cortex during rule-based visual-motor transformations. *J Cogn Neurosci* 25: 3: 436-454, 2013.

Henriques DY, Klier EM, Smith MA, Lowy D and Crawford JD. Gaze-centered remapping of remembered visual space in an open-loop pointing task. *J Neurosci* 18: 4: 1583-1594, 1998.

Hocherman S and Wise SP. Effects of hand movement path on motor cortical activity in awake, behaving rhesus monkeys. *Exp Brain Res* 83: 2: 285-302, 1991.

Hoshi E. Functional specialization within the dorsolateral prefrontal cortex: A review of anatomical and physiological studies of non-human primates. *Neuroscience Research* 54: 73, 2006.

Hoshi E and Tanji J. Integration of target and body-part information in the premotor cortex when planning action. *Nature* 408: 6811: 466-470, 2000.

Hughes JR. Gamma, fast, and ultrafast waves of the brain: their relationship with epilepsy and behaviour. *Epilepsy & Behaviour* 13: 25-31, 2008.

Hughlings Jackson J. Observation of the localisation of movements in the cerebral hemisphere, as revealed by cases of convulsion, chorea, and "aphasia". *West Riding Lunatic Asylum Medical Reports* 3: 175-195, 1873.

Hwang EJ, Hauschild M, Wilke M and Andersen RA. Inactivation of the parietal reach region causes optic ataxia, impairing reaches but not saccades. *Neuron* 76: 5: 1021-1029, 2012.

Iacoboni M. Visuo-motor integration and control in the human posterior parietal cortex: evidence from TMS and fMRI. *Neuropsychologia* 44: 13: 2691-2699, 2006.

Jackson SR, Newport R, Husain M, Fowlie JE, O'Donoghue M and Bajaj N. There may be more to reaching than meets the eye: re-thinking optic ataxia. *Neuropsychologia* 47: 6: 1397-1408, 2009.

Jackson SR, Newport R, Husain M, Harvey M and Hindle JV. Reaching movements may reveal the distorted topography of spatial representations after neglect. *Neuropsychologia* 38: 4: 500-507, 2000.

Jackson SR, Newport R, Mort D and Husain M. Where the eye looks, the hand follows; limb-dependent magnetic misreaching in optic ataxia. *Curr Biol* 15: 1: 42-46, 2005.

Jaffard M, Longcamp M, Velay JL, Anton JL, Roth M, Nazarian B and Boulinguez P. Proactive inhibitory control of movement assessed by event-related fMRI. *Neuroimage* 42: 3: 1196-1206, 2008.

Jarvis MR and Mitra PP. Sampling properties of the spectrum and coherency of sequences of action potentials. *Neural Comput* 13: 4: 717-749, 2001.

Jensen O, Gelfand J, Kounios J and Lisman JE. Oscillations in the alpha band (9-12 Hz) increase with memory load during retention in a short-term memory task. *Cereb Cortex* 12: 8: 877-882, 2002.

Jensen O, Kaiser J and Lachaux JP. Human gamma-frequency oscillations associated with attention and memory. *Trends Neurosci* 30: 7: 317-324, 2007.

Johnson PB, Ferraina S, Bianchi L and Caminiti R. Cortical networks for visual reaching: physiological and anatomical organization of frontal and parietal lobe arm regions. *Cereb Cortex* 6: 2: 102-119, 1996.

Johnson PB, Ferraina S and Caminiti R. Cortical networks for visual reaching. *Exp Brain Res* 97: 2: 361-365, 1993.

Jones EG and Powell TP. An anatomical study of converging sensory pathways within the cerebral cortex of the monkey. *Brain* 93: 4: 793-820, 1970.

Kajikawa Y and Schroeder CE. How local is the local field potential? *Neuron* 72: 5: 847-858, 2011.

Kalaska JF. Parietal cortex area 5 and visuomotor behavior. *Can J Physiol Pharmacol* 74: 4: 483-498, 1996.

Kalaska JF, Caminiti R and Georgopoulos AP. Cortical mechanisms related to the direction of two-dimensional arm movements: relations in parietal area 5 and comparison with motor cortex. *Exp Brain Res* 51: 2: 247-260, 1983.

Kalaska JF, Cohen DA, Hyde ML and Prud'homme M. A comparison of movement direction-related versus load direction-related activity in primate motor cortex, using a two-dimensional reaching task. *J Neurosci* 9: 6: 2080-2102, 1989.

Kalaska JF, Cohen DA, Prud'homme M and Hyde ML. Parietal area 5 neuronal activity encodes movement kinematics, not movement dynamics. *Exp Brain Res* 80: 2: 351-364, 1990.

Kalaska JF and Crammond DJ. Deciding not to GO: neuronal correlates of response selection in a GO/NOGO task in primate premotor and parietal cortex. *Cereb Cortex* 5: 5: 410-428, 1995a.

Kalaska JF and Crammond DJ. Deciding not to GO: neuronal correlates of response selection in a GO/NOGO task in primate premotor and parietal cortex. *Cereb Cortex* 5: 5: 410-428, 1995b.

Kalaska JF, Scott SH, Cisek P and Sergio LE. Cortical control of reaching movements. *Curr Opin Neurobiol* 7: 6: 849-859, 1997.

Kalaska JF, Sergio LE and Cisek P. Cortical control of whole-arm motor tasks. *Novartis Found Symp* 218: 176-90; discussion 190-201, 1998.

Karnath HO and Perenin MT. Cortical control of visually guided reaching: evidence from patients with optic ataxia. *Cereb Cortex* 15: 10: 1561-1569, 2005.

Katzner S, Nauhaus I, Benucci A, Bonin V, Ringach DL and Carandini M. Local Origin of Field Potentials in Visual Cortex. 61: 1: 35-41, 2009.

Kertzman C, Schwarz U, Zeffiro TA and Hallett M. The role of posterior parietal cortex in visually guided reaching movements in humans. *Exp Brain Res* 114: 1: 170-183, 1997.

Knight RT, Scabini D and Woods DL. Prefrontal cortex gating of auditory transmission in humans. *Brain Res* 504: 2: 338-342, 1989.

Koralek AC, Costa RM and Carmena JM. Temporally precise cell-specific coherence develops in corticostriatal networks during learning. *Neuron* 79: 5: 865-872, 2013.

Kurata K. Information processing for motor control in primate premotor cortex. *Behav Brain Res* 61: 2: 135-142, 1994.

Kurata K. Premotor cortex of monkeys: set- and movement-related activity reflecting amplitude and direction of wrist movements. *J Neurophysiol* 69: 1: 187-200, 1993.

Kurata K. Corticocortical inputs to the dorsal and ventral aspects of the premotor cortex of macaque monkeys. *Neurosci Res* 12: 1: 263-280, 1991.

Kurata K. Motor programming in the premotor cortex of monkeys. In: Anonymous 1989, p. 39-47.

Kurata K and Hoffman DS. Differential effects of muscimol microinjection into dorsal and ventral aspects of the premotor cortex of monkeys. *J Neurophysiol* 71: 3: 1151-1164, 1994.

Lackner JR and Dizio P. Rapid adaptation to Coriolis force perturbations of arm trajectory. *J Neurophysiol* 72: 299-313, 1994.

Lakatos P, Shah AS, Knuth KH, Ulbert I, Karmos G and Schroeder CE. An oscillatory hierarchy controlling neuronal excitability and stimulus processing in the auditory cortex. *J Neurophysiol* 94: 3: 1904-1911, 2005.

Lamar M and Resnick SM. Aging and prefrontal functions: dissociating orbitofrontal and dorsolateral abilities. 25: 4: 553-558, 2004.

Lampl I, Reichova I and Ferster D. Synchronous membrane potential fluctuations in neurons of the cat visual cortex. *Neuron* 22: 2: 361-374, 1999.

Lee JH and van Donkelaar P. The human dorsal premotor cortex generates on-line error corrections during sensorimotor adaptation. *J Neurosci* 26: 12: 3330-3334, 2006.

Lloyd DM, Shore DI, Spence C and Calvert GA. Multisensory representation of limb position in human premotor cortex. *Nat Neurosci* 6: 1: 17-18, 2003.

Logothetis NK, Pauls J, Augath M, Trinath T and Oeltermann A. Neurophysiological investigation of the basis of the fMRI signal. *Nature* 412: 6843: 150-157, 2001.

Lu MT, Preston JB and Strick PL. Interconnections between the prefrontal cortex and the premotor areas in the frontal lobe. *J Comp Neurol* 341: 3: 375-392, 1994.

Luppino G. 12 Organizations of the Posterior Parietal Lobe and of Parietofrontal Connections. In: *From Monkey Brain to Human Brain*, edited by Dehaene S, Duhamel JR, Hauser MD and Rizzolatti G. Cambridge, MA: MIT Press, 2005, p. 235.

Luppino G, Hamed SB, Gamberini M, Matelli M and Galletti C. Occipital (V6) and parietal (V6A) areas in the anterior wall of the parieto-occipital sulcus of the macaque: a cytoarchitectonic study. *Eur J Neurosci* 21: 11: 3056-3076, 2005.

Luppino G, Matelli M and Rizzolatti G. Cortico-cortical connections of two electrophysiologically identified arm representations in the mesial agranular frontal cortex. *Exp Brain Res* 82: 1: 214-218, 1990.

Luppino G and Rizzolatti G. The Organization of the Frontal Motor Cortex. *News Physiol Sci* 15: 219-224, 2000.

Luppino G, Rozzi S, Calzavara R and Matelli M. Prefrontal and agranular cingulate projections to the dorsal premotor areas F2 and F7 in the macaque monkey. *Eur J Neurosci* 17: 3: 559-578, 2003.

Lynch JC. The functional organization of the posterior parietal association cortex. *Behav Brain Sci* 3: 485, 1980.

Lynch JC, Mountcastle VB, Talbot WH and Yin TC. Parietal lobe mechanisms for directed visual attention. *J Neurophysiol* 40: 2: 362-389, 1977.

MacKay WA. Properties of reach-related neuronal activity in cortical area 7A. *J Neurophysiol* 67: 5: 1335-1345, 1992.

Maier A, Adams GK, Aura C and Leopold DA. Distinct superficial and deep laminar domains of activity in the visual cortex during rest and stimulation. *Front Sys Neruosci* 4: 31: 2010.

Malmivuo J and Plonsey R:.
Bioelectromagnetism, Principles and Applications of Bioelectric and Biomagnetic Fields. Oxford University Press, 1995.

Marconi B, Genovesio A, Battaglia-Mayer A, Ferraina S, Squatrito S, Molinari M, Lacquaniti F and Caminiti R. Eye-hand coordination during reaching. I. Anatomical relationships between parietal and frontal cortex. *Cereb Cortex* 11: 6: 513-527, 2001.

Marshall WH, Woolsey CN and Bard P. Cortical Representation of Tactile Sensibility as Indicated by Cortical Potentials. *Science* 85: 2207: 388-390, 1937.

Marzocchi N, Breveglieri R, Galletti C and Fattori P. Reaching activity in parietal area V6A of macaque: eye influence on arm activity or retinocentric coding of reaching movements? *Eur J Neurosci* 27: 3: 775-789, 2008.

Matelli M, Govoni P, Galletti C, Kutz DF and Luppino G. Superior area 6 afferents from the superior parietal lobule in the macaque monkey. *J Comp Neurol* 402: 3: 327-352, 1998.

Matelli M and Luppino G. Parietofrontal circuits for action and space perception in the macaque monkey. *Neuroimage* 14: 1 Pt 2: S27-32, 2001.

Matelli M, Luppino G and Rizzolatti G. Patterns of cytochrome oxidase activity in the frontal agranular cortex of the macaque monkey. *Behav Brain Res* 18: 2: 125-136, 1985.

Mazzoni P, Andersen RA and Jordan MI. A more biologically plausible learning rule than backpropagation applied to a network model of cortical area 7a. *Cereb Cortex* 1: 4: 293-307, 1991.

Mehring C, Rickert J, Vaadia E, Cardosa de Oliveira S, Aertsen A and Rotter S. Inference of hand movements from local field potentials in monkey motor cortex. *Nat Neurosci* 6: 12: 1253-1254, 2003.

Messier J and Kalaska JF. Comparison of variability of initial kinematics and endpoints of reaching movements. *Exp Brain Res* 125: 2: 139-152, 1999.

Messier J and Kalaska JF. Differential effect of task conditions on errors of direction and extent of reaching movements. *Exp Brain Res* 115: 3: 469-478, 1997.

Mesulam MM. Large-scale neurocognitive networks and distributed processing for attention, language, and memory. *Ann Neurol* 28: 5: 597-613, 1990.

Mesulam MM, Nobre AC, Kim YH, Parrish TB and Gitelman DR. Heterogeneity of cingulate contributions to spatial attention. *Neuroimage* 13: 6 Pt 1: 1065-1072, 2001.

Milner AD and Goodale MA, eds. ***The visual brain*** *in* ***action****,* 1995.

Milner AD and Harvey M. Visuomotor control of spatially directed action. In: *Imagery and spatial cognition: Methods, models and cognitive assessment.*, edited by Vecchi T and Bottini G. Amsterdam, Netherlands: John Benjamins Publishing Company, 2006, p. 299-324.

Mitzdorf U. Current source-density method and application in cat cerebral cortex: investigation of evoked potentials and EEG phenomena. *Physiol Rev* 65: 1: 37-100, 1985.

Moore GP, Perkel DH and Segundo JP. Statistical analysis and functional interpretation of neuronal spike data. *Annu Rev Physiol* 28: 493-522, 1966.

Morasso P. Spatial control of arm movements. *Exp Brain Res* 42: 2: 223-227, 1981.

Morecraft RJ, Cipolloni PB, Stilwell-Morecraft KS, Gedney MT and Pandya DN. Cytoarchitecture and cortical connections of the posterior cingulate and adjacent somatosensory fields in the rhesus monkey. *J Comp Neurol* 469: 1: 37-69, 2004.

Moscovitch C, Kapur S, Kohler S and Houle S. Distinct neural correlates of visual long-term memory for spatial location and object identity: a positron emission tomography study in humans. *Proc Natl Acad Sci U S A* 92: 9: 3721-3725, 1995.

Mountcastle VB. The parietal system and some higher brain functions. *Cereb Cortex* 5: 5: 377-390, 1995.

Mountcastle VB, Lynch JC, Georgopoulos A, Sakata H and Acuna C. Posterior parietal association cortex of the monkey: command functions for operations within extrapersonal space. *J Neurophysiol* 38: 4: 871-908, 1975.

Murray EA, Bussey TJ and Wise SP. Role of prefrontal cortex in a network for arbitrary visuomotor mapping. *Exp Brain Res* 133: 1: 114-129, 2000.

Murray SO, Kersten D, Olshausen BA, Schrater P and Woods DL. Shape perception reduces activity in human primary visual cortex. *Proc Natl Acad Sci U S A* 99: 23: 15164-15169, 2002.

Neggers SF and Bekkering H. Gaze anchoring to a pointing target is present during the entire pointing movement and is driven by a non-visual signal. *J Neurophysiol* 86: 2: 961-970, 2001.

Neggers SF and Bekkering H. Ocular gaze is anchored to the target of an ongoing pointing movement. *J Neurophysiol* 83: 2: 639-651, 2000.

Newport R, Brown L, Husain M, Mort D and Jackson SR. The role of the posterior parietal lobe in prism adaptation: Failure to adapt to optical prisms in a patient with bilateral damage to posterior parietal cortex. *Cortex* 42: 5: 720-729, 2006.

Nir Y, Fisch L, Mukamel R, Gelbard-Sagiv H, Arieli A, Fried I and Malach R. Coupling between neuronal firing rate, gamma LFP, and BOLD fMRI is related to interneuronal correlations. *Curr Biol* 17: 15: 1275-1285, 2007.

Nixon PD, Burbaud P and Passingham RE. Control of arm movement after bilateral lesions of area 5 in the monkey (Macaca mulatta). *Exp Brain Res* 90: 1: 229-232, 1992.

O'Leary JG and Hatsopoulos NG. Early visuomotor representations revealed from evoked local field potentials in motor and premotor cortical areas. *J Neurophysiol* 96: 3: 1492-1506, 2006.

Olsen SR, Bortone DS, Adesnik H and Scanziani M. Gain control by layer six in cortical circuits of vision. *Nature* 483: 7387: 47-52, 2012.

Pandya DN and Kuypers HG. Cortico-cortical connections in the rhesus monkey. *Brain Res* 13: 1: 13-36, 1969.

Pandya DN and Seltzer B. Intrinsic connections and architectonics of posterior parietal cortex in the rhesus monkey. *J Comp Neurol* 204: 2: 196-210, 1982.

Pandya DN and Yeterian EH. Proposed neural circuitry for spatial memory in the primate brain. *Neuropsychologia* 22: 2: 109-122, 1984.

Passarelli L, Rosa MG, Gamberini M, Bakola S, Burman KJ, Fattori P and Galletti C. Cortical connections of area V6Av in the macaque: a visual-input node to the eye/hand coordination system. *J Neurosci* 31: 5: 1790-1801, 2011.

Passingham RE. Premotor cortex and preparation for movement. *Exp Brain Res* 70: 3: 590-596, 1988.

Paxinos G, Huang XF and Toga AW. *The Rhesus Monkey Brain in Stereotaxic Coordinates.* San Diego, USA: Academic Press, 2000.

Pellijeff A, Bonilha L, Morgan PS, McKenzie K and Jackson SR. Parietal updating of limb posture: an event-related fMRI study. *Neuropsychologia* 44: 13: 2685-2690, 2006.

Perenin MT and Vighetto A. Optic ataxia: a specific disruption in visuomotor mechanisms. I. Different aspects of the deficit in reaching for objects. *Brain* 111 (Pt 3): 643-674, 1988.

Pesaran B, Nelson MJ and Andersen RA. A relative position code for saccades in dorsal premotor cortex. *J Neurosci* 30: 19: 6527-6537, 2010.

Pesaran B, Nelson MJ and Andersen RA. Free choice activates a decision circuit between frontal and parietal cortex. *Nature* 453: 7193: 406-409, 2008.

Pesaran B, Nelson MJ and Andersen RA. Dorsal premotor neurons encode the relative position of the hand, eye, and goal during reach planning. *Neuron* 51: 1: 125-134, 2006.

Pesaran B, Pezaris JS, Sahani M, Mitra PP and Andersen RA. Temporal structure in neuronal activity during working memory in macaque parietal cortex. *Nat Neurosci* 5: 8: 805-811, 2002.

Petrides M. Visuo-motor conditional associative learning after frontal and temporal lesions in the human brain. *Neuropsychologia* 35: 7: 989-997, 1997.

Petrides M. Deficits on conditional associative-learning tasks after frontal- and temporal-lobe lesions in man. *Neuropsychologia* 23: 5: 601-614, 1985.

Petrides M. Motor conditional associative-learning after selective prefrontal lesions in the monkey. *Behav Brain Res* 5: 4: 407-413, 1982.

Petrides M and Pandya DN. Projections to the frontal cortex from the posterior parietal region in the rhesus monkey. *J Comp Neurol* 228: 1: 105-116, 1984.

Piaget J. *The Construction of Reality in the Child.* New York: Basic Books, Inc, 1965.

Picard N and Strick PL. Imaging the premotor areas. *Curr Opin Neurobiol* 11: 6: 663-672, 2001.

Pisella L, Andre V, Gavault E, Le Flem A, Luc-Pupat E, Glissoux C, Barriere A, Vindras P, Rossetti Y and Gonzalez-Monge S. A test revealing the slow acquisition and the dorsal stream substrate of visuo-spatial perception. *Neuropsychologia* 51: 1: 106-113, 2013.

Pisella L, Grea H, Tilikete C, Vighetto A, Desmurget M, Rode G, Boisson D and Rossetti Y. An 'automatic pilot' for the hand in human posterior parietal cortex: toward reinterpreting optic ataxia. *Nat Neurosci* 3: 7: 729-736, 2000.

Pisella L, Sergio L, Blangero A, Torchin H, Vighetto A and Rossetti Y. Optic ataxia and the function of the dorsal stream: Contributions to perception and action. *Neuropsychologia* 2009.

Pogosyan A, Gaynor LD, Eusebio A and Brown P. Boosting cortical activity at Beta-band frequencies slows movement in humans. *Curr Biol* 19: 19: 1637-1641, 2009.

Prablanc C, Echallier JF, Komilis E and Jeannerod M. Optimal response of eye and hand motor systems in pointing at a visual target. I. Spatio-temporal characteristics of eye and hand movements and their relationships when varying the amount of visual information. *Biol Cybern* 35: 2: 113-124, 1979.

Prado J, Clavagnier S, Otzenberger H, Scheiber C, Kennedy H and Perenin MT. Two cortical systems for reaching in central and peripheral vision. *Neuron* 48: 5: 849-858, 2005.

Raos V, Umilta MA, Gallese V and Fogassi L. Functional properties of grasping-related neurons in the dorsal premotor area F2 of the macaque monkey. *J Neurophysiol* 92: 4: 1990-2002, 2004.

Ray S and Maunsell JHR. Different Origins of Gamma Rhythm and High-Gamma Activity in Macaque Visual Cortex. *PLoS Biol* 9: 4: e1000610, 2011.

Redding GM, Rossetti Y and Wallace B. Applications of prism adaptation: a tutorial in theory and method. *Neurosci Biobehav Rev* 29: 3: 431-444, 2005.

Redding GM and Wallace B. Adaptive spatial alignment and strategic perceptual-motor control. *J Exp Psychol Hum Percept Perform* 22: 2: 379-394, 1996.

Rickert J, Oliveira SC, Vaadia E, Aertsen A, Rotter S and Mehring C. Encoding of movement direction in different frequency ranges of motor cortical local field potentials. *J Neurosci* 25: 39: 8815-8824, 2005.

Riehle A, Grun S, Diesmann M and Aertsen A. Spike synchronization and rate modulation differentially involved in motor cortical function. *Science* 278: 5345: 1950-1953, 1997.

Rizzolatti G, Fogassi L and Gallese V. Parietal cortex: from sight to action. *Curr Opin Neurobiol* 7: 4: 562-567, 1997.

Rizzolatti G, Luppino G and Matelli M. The organization of the cortical motor system: new concepts. *Electroencephalogr Clin Neurophysiol* 106: 4: 283-296, 1998.

Rizzolatti G and Matelli M. Two different streams form the dorsal visual system: anatomy and functions. *Exp Brain Res* 153: 2: 146-157, 2003.

Roberts MJ, Lowet E, Brunet NM, Ter Wal M, Tiesinga P, Fries P and De Weerd P. Robust gamma coherence between macaque V1 and V2 by dynamic frequency matching. *Neuron* 78: 3: 523-536, 2013.

Rockland KS and Pandya DN. Laminar origins and terminations of cortical connections of the occipital lobe in the rhesus monkey. *Brain Res* 179: 1: 3-20, 1979.

Roland PE, Larsen B, Lassen NA and Skinhoj E. Supplementary motor area and other cortical areas in organization of voluntary movements in man. *J Neurophysiol* 43: 1: 118-136, 1980.

Roopun AK, Middleton SJ, Cunningham MO, LeBeau FE, Bibbig A, Whittington MA and Traub RD. A beta2-frequency (20-30 Hz) oscillation in nonsynaptic networks of somatosensory cortex. *Proc Natl Acad Sci U S A* 103: 42: 15646-15650, 2006.

Rossetti Y, Revol P, McIntosh R, Pisella L, Rode G, Danckert J, Tilikete C, Dijkerman HC, Boisson D, Vighetto A, Michel F and Milner AD. Visually guided reaching: bilateral posterior parietal lesions cause a switch from fast visuomotor to slow cognitive control. *Neuropsychologia* 43: 2: 162-177, 2005.

Rushworth MF, Nixon PD and Passingham RE. Parietal cortex and movement. I. Movement selection and reaching. *Exp Brain Res* 117: 2: 292-310, 1997a.

Rushworth MF, Nixon PD and Passingham RE. Parietal cortex and movement. II. Spatial representation. *Exp Brain Res* 117: 2: 311-323, 1997b.

Sabes PN. The planning and control of reaching movements. *Curr Opin Neurobiol* 10: 6: 740-746, 2000.

Sakata H, Takaoka Y, Kawarasaki A and Shibutani H. Somatosensory properties of neurons in the superior parietal cortex (area 5) of the rhesus monkey. *Brain Res* 64: 85-102, 1973.

Salek Y, Anderson ND and Sergio L. Mild cognitive impairment is associated with impaired visual-motor planning when visual stimuli and actions are incongruent. *Eur Neurol* 66: 5: 283-293, 2011.

Sanes JN and Donoghue JP. Oscillations in local field potentials of the primate motor cortex during voluntary movement. *Proc Natl Acad Sci U S A* 90: 10: 4470-4474, 1993.

Sauve K. Gamma-band synchronous oscillations: recent evidence regarding their functional significance. *Conscious Cogn* 8: 2: 213-224, 1999.

Sayegh PF, Hawkins KM, Hoffman KL and Sergio LE. Differences in spectral profiles between rostral and caudal premotor cortex when eye-hand actions are decoupled. *J Neurophysiol* 2013.

Sayegh PF, Hawkins KM, Neagu B, Crawford JD, Hoffman KL and Sergio LE. Decoupling the actions of the eyes from the hand alters beta and gamma synchrony within SPL. *J Neurophysiol* 2014.

Scherberger H, Jarvis MR and Andersen RA. Cortical local field potential encodes movement intentions in the posterior parietal cortex. *Neuron* 46: 2: 347-354, 2005.

Schlag-Rey M, Amador N, Sanchez H and Schlag J. Antisaccade performance predicted by neuronal activity in the supplementary eye field. *Nature* 390: 6658: 398-401, 1997.

Schnitzler A and Gross J. Normal and pathological oscillatory communication in the brain. *Nat Rev Neurosci* 6: 4: 285-296, 2005.

Schroeder CE, Tenke CE, Givre SJ, Arezzo JC and Vaughan HG,Jr. Striate cortical contribution to the surface-recorded pattern-reversal VEP in the alert monkey. *Vision Res* 31: 7-8: 1143-1157, 1991.

Scott SH and Kalaska JF. Reaching movements with similar hand paths but different arm orientations. I. Activity of individual cells in motor cortex. *J Neurophysiol* 77: 2: 826-852, 1997.

Scott SH, Sergio LE and Kalaska JF. Reaching movements with similar hand paths but different arm orientations. II. Activity of individual cells in dorsal premotor cortex and parietal area 5. *J Neurophysiol* 78: 5: 2413-2426, 1997.

Sergio LE, Gorbet DJ, Tippett WJ, Yan X and Neagu B. Cortical mechanisms of vision for complex action. In: *Cortical mechanisms of vision*, edited by Jenkins M and Harris L. Cambridge: Cambridge University Press, 2009.

Sergio LE and Kalaska JF. Systematic changes in motor cortex cell activity with arm posture during directional isometric force generation. *J Neurophysiol* 89: 1: 212-228, 2003.

Sergio LE and Scott SH. Hand and joint paths during reaching movements with and without vision. *Exp Brain Res* 122: 2: 157-164, 1998.

Shadmehr R and Wise SP. *The computational neurobiology of pointing and reaching.* Cambridge, MA, USA: MIT press, 2005.

Shen L and Alexander GE. Neural correlates of a spatial sensory-to-motor transformation in primary motor cortex. *J Neurophysiol* 77: 3: 1171-1194, 1997a.

Shen L and Alexander GE. Preferential representation of instructed target location versus limb trajectory in dorsal premotor area. *J Neurophysiol* 77: 3: 1195-1212, 1997b.

Shipp S, Blanton M and Zeki S. A visuo-somatomotor pathway through superior parietal cortex in the macaque monkey: cortical connections of areas V6 and V6A. *Eur J Neurosci* 10: 10: 3171-3193, 1998.

Siegel M, Donner TH and Engel AK. Spectral fingerprints of large-scale neuronal interactions. *Nat Rev Neurosci* 13: 2: 121-134, 2012.

Snedecor GW and Cochrane WG. *Statistical methods.* 2121 State Avenue, Ames, Iowa: Blackwell Publishing Professional, 1989.

Snodderly DM and Gur M. Organization of striate cortex of alert, trained monkeys (Macaca fascicularis): ongoing activity, stimulus selectivity, and widths of receptive field activating regions. *J Neurophysiol* 74: 5: 2100-2125, 1995.

Sober SJ and Sabes PN. Flexible strategies for sensory integration during motor planning. *Nat Neurosci* 8: 4: 490-497, 2005.

Soechting JF and Flanders M. Moving in three-dimensional space: frames of reference, vectors, and coordinate systems. *Annu Rev Neurosci* 15: 167-191, 1992.

Spaak E, Bonnefond M, Maier A, Leopold DA and Jensen O. Layer-specific entrainment of gamma-band neural activity by the alpha rhythm in monkey visual cortex. *Curr Biol* 22: 24: 2313-2318, 2012.

Tachibana Y, Nambu A, Hatanaka N, Miyachi S and Takada M. Input–output organization of the rostral part of the dorsal premotor cortex, with special reference to its corticostriatal projection. 48: 1: 45-57, 2004.

Takada M, Nambu A, Hatanaka N, Tachibana Y, Miyachi S, Taira M and Inase M. Organization of prefrontal outflow toward frontal motor-related areas in macaque monkeys. *Eur J Neurosci* 19: 12: 3328-3342, 2004.

Tanne-Gariepy J, Rouiller EM and Boussaoud D. Parietal inputs to dorsal versus ventral premotor areas in the macaque monkey: evidence for largely segregated visuomotor pathways. *Exp Brain Res* 145: 1: 91-103, 2002.

Taylor CS and Gross CG. Twitches versus movements: a story of motor cortex. *Neuroscientist* 9: 5: 332-342, 2003.

Terao Y, Andersson NE, Flanagan JR and Johansson RS. Engagement of gaze in capturing targets for future sequential manual actions. *J Neurophysiol* 88: 4: 1716-1725, 2002.

Tillery SI and Taylor DM. Signal acquisition and analysis for cortical control of neuroprosthetics. *Curr Opin Neurobiol* 14: 6: 758-762, 2004.

Tippett WJ, Krajewski A and Sergio LE. Visuomotor integration is compromised in Alzheimer's disease patients reaching for remembered targets. *Eur Neurol* 58: 1: 1-11, 2007.

Tippett WJ and Sergio LE. Visuomotor integration is impaired in early stage Alzheimer's disease. *Brain Res* 1102: 1: 92-102, 2006.

Tippett WJ, Sergio LE and Black SE. Compromised visually guided motor control in individuals with Alzheimer's disease: can reliable distinctions be observed? *J Clin Neurosci* 19: 5: 655-660, 2012.

Tomassini V, Jbabdi S, Klein JC, Behrens TE, Pozzilli C, Matthews PM, Rushworth MF and Johansen-Berg H. Diffusion-weighted imaging tractography-based parcellation of the human lateral premotor cortex identifies dorsal and ventral subregions with anatomical and functional specializations. *J Neurosci* 27: 38: 10259-10269, 2007.

Toni I, Rushworth MF and Passingham RE. Neural correlates of visuomotor associations. Spatial rules compared with arbitrary rules. *Exp Brain Res* 141: 3: 359-369, 2001.

Traub RD, Bibbig A, LeBeau FE, Buhl EH and Whittington MA. Cellular mechanisms of neuronal population oscillations in the hippocampus in vitro. *Annu Rev Neurosci* 27: 247-278, 2004.

Ungerleider LG and Haxby JV. 'What' and 'where' in the human brain. *Curr Opin Neurobiol* 4: 2: 157-165, 1994.

Ungerleider LG and Mishkin M. Two cortical visual systems. In: *Analysis of visual behaviour*, edited by Ingle DJ, Goodale MA and Mansfield RJW. Cambridge, MA: MIT Press, 1982, p. 549-586.

Vercher JL, Magenes G, Prablanc C and Gauthier GM. Eye-head-hand coordination in pointing at visual targets: spatial and temporal analysis. *Exp Brain Res* 99: 3: 507-523, 1994.

Vesia M and Crawford JD. Specialization of reach function in human posterior parietal cortex. *Exp Brain Res* 221: 1: 1-18, 2012.

Vesia M, Prime SL, Yan X, Sergio LE and Crawford JD. Specificity of human parietal saccade and reach regions during transcranial magnetic stimulation. *J Neurosci* 30: 39: 13053-13065, 2010.

von Stein A and Sarnthein J. Different frequencies for different scales of cortical integration: from local gamma to long range alpha/theta synchronization. *Int J Psychophysiol* 38: 3: 301-313, 2000.

Weinrich M and Wise SP. The premotor cortex of the monkey. *J Neurosci* 2: 9: 1329-1345, 1982.

Weinrich M, Wise SP and Mauritz KH. A neurophysiological study of the premotor cortex in the rhesus monkey. *Brain* 107 (Pt 2): Pt 2: 385-414, 1984.

White IM and Wise SP. Rule-dependent neuronal activity in the prefrontal cortex. *Exp Brain Res* 126: 3: 315-335, 1999.

Wiedemann HR. Hans Berger (1873-1941). *Eur J Pediatr* 153: 10: 705, 1994.

Wise SP, Boussaoud D, Johnson PB and Caminiti R. Premotor and parietal cortex: corticocortical connectivity and combinatorial computations. *Annu Rev Neurosci* 20: 25-42, 1997.

Wise SP, di Pellegrino G and Boussaoud D. The premotor cortex and nonstandard sensorimotor mapping. *Can J Physiol Pharmacol* 74: 4: 469-482, 1996.

Wise SP and Mauritz KH. Set-related neuronal activity in the premotor cortex of rhesus monkeys: effects of changes in motor set. *Proc R Soc Lond B Biol Sci* 223: 1232: 331-354, 1985.

Witham CL, Wang M and Baker SN. Cells in somatosensory areas show synchrony with beta oscillations in monkey motor cortex. *Eur J Neurosci* 26: 9: 2677-2686, 2007.

Wolpert DM, Goodbody SJ and Husain M. Maintaining internal representations: the role of the human superior parietal lobe. *Nat Neurosci* 1: 6: 529-533, 1998.

Womelsdorf T and Fries P. Neuronal coherence during selective attentional processing and sensory-motor integration. *J Physiol Paris* 100: 4: 182-193, 2006.

Zanos S, Zanos TP, Marmarelis VZ, Ojemann GA and Fetz EE. Relationships between spike-free local field potentials and spike timing in human temporal cortex. *J Neurophysiol* 107: 7: 1808-1821, 2012.

Zanos TP, Mineault PJ and Pack CC. Removal of spurious correlations between spikes and local field potentials. *J Neurophysiol* 105: 1: 474-486, 2011.

Zeitler M, Fries P and Gielen S. Biased competition through variations in amplitude of gamma-oscillations. *J Comput Neurosci* 25: 1: 89-107, 2008.

Zeki SM. The cortical projections of foveal striate cortex in the rhesus monkey. *J Physiol* 277: 227-244, 1978.